Macrophage MicroRNA-155 Promotes Cardiac Hypertrophy and Failure

Stephane Heymans, Maarten F. Corsten, Wouter Verhesen, Paolo Carai, Rick E. W. van Leeuwen, Kevin Custers, Tim Peters, Mark Hazebroek, Lauran Stöger, Erwin Wijnands, Ben J. Janssen, Esther E. Creemers, Yigal M. Pinto, Dirk Grimm, Nina Schürmann, Elena Vigorito, Thomas Thum, Frank Stassen, Xiaoke Yin, Manuel Mayr, Leon J. De Windt, Esther Lutgens, Kristiaan Wouters, Menno P. J. de Winther, Serena Zacchigna, Mauro Giacca, Marc van Bilsen, Anna-Pia Papageorgiou and Blanche Schroen

Circulation. published online August 16, 2013;
Circulation is published by the American Heart Association, 7272 Greenville Avenue, Dallas, TX 75231

Print ISSN: 0009-7322. Online ISSN: 1524-4539

DOI: 10.1161/CIRCULATIONAHA.112.001357

Macrophage MicroRNA-155 Promotes Cardiac Hypertrophy and Failure

Running title: *Heymans et al.; Macrophage miR-155 promotes heart failure*

Stephane Heymans, MD, PhD[1,2,3]*; Maarten F. Corsten, MD, PhD[1]*; Wouter Verhesen, BSc[1]; Paolo Carai, MSc[1,3];Rick E.W. van Leeuwen, BSc[1]; Kevin Custers, BSc[1]; Tim Peters, MSc[1]; Mark Hazebroek, MD, MSc[1]; Lauran Stöger, MD, PhD[4,5]; Erwin Wijnands, BSc[6]; Ben J. Janssen, PhD[7]; Esther E. Creemers, PhD[8]; Yigal M. Pinto, MD, PhD[8]; Dirk Grimm, PhD[9]; Nina Schürmann, MSc[9]; Elena Vigorito, PhD[10]; Thomas Thum, MD, PhD[11]; Frank Stassen, PhD[12]; Xiaoke Yin, PhD[13]; Manuel Mayr, MD, PhD[13]; Leon J. de Windt, PhD[14]; Esther Lutgens, PhD[5,6,15]; Kristiaan Wouters, PhD[16]; Menno P.J. de Winther, PhD[4,5]; Serena Zacchigna, MD, PhD[17]; Mauro Giacca, MD, PhD[17]; Marc van Bilsen, PhD[1]; Anna-Pia Papageorgiou, PhD[1,3]; Blanche Schroen, PhD[1]

[1]Center for Heart Failure Research, Dept of Cardiology; [4]Dept of Molecular Genetics; [6]Dept of Pathology; [7]Dept of Pharmacology; [14]Dept of Cardiology; [16]Dept of Internal Medicine, Cardiovascular Research Institute Maastricht (CARIM), Maastricht University, Maastricht, The Netherlands; [2]Interuniversity Cardiology Institute of the Netherlands (ICIN), Utrecht, The Netherlands; [3]Center for Molecular and Cardiovascular Biology (CMVB), Dept of Cardiovascular Sciences, University of Leuven, Leuven, Belgium; [5]Dept of Medical Biochemistry; [8]Heart Failure Research Center, Academic Medical Center Amsterdam, Amsterdam, The Netherlands; [9]Cluster of Excellence CellNetworks, Dept of Infectious Diseases/Virology, Virus Host Interactions, Heidelberg University, Heidelberg, Germany; [10]Laboratory of Lymphocyte Signaling and Development, Babraham Institute, Cambridge, UK; [11]Institute for Molecular and Translational Therapeutic Strategies (IMTTS), Hannover Medical School, Hannover, Germany; [12]Medical Microbiology, Maastricht University, Maastricht, The Netherlands; [13]King's BHF Centre, King's College London, London, UK; [15]Institute for Cardiovascular Prevention (IPEK), Ludwig Maximilians University, Munich, Germany; [17]Molecular Medicine Laboratory, International Centre for Genetic Engineering and Biotechnology (ICGEB), Trieste, Italy
*contributed equally

Address for Correspondence:
Blanche Schroen, PhD
Center for Heart Failure Research, Department of Cardiology
Cardiovascular Research Institute Maastricht (CARIM), Maastricht University
Universiteitssingel 50
6229 ER Maastricht, The Netherlands
Tel: +31 43 3882949
Fax: +31 43 3882952
E-mail: b.schroen@maastrichtuniversity.nl

Journal Subject Codes: Hypertension:[15] Hypertrophy, Myocardial biology:[108] Other myocardial biology

DOI: 10.1161/CIRCULATIONAHA.112.001357

Abstract:

***Background*—**Cardiac hypertrophy and subsequent heart failure triggered by chronic hypertension represent major challenges for cardiovascular research. Beyond neurohormonal and myocyte signaling pathways, growing evidence suggests inflammatory signaling pathways as therapeutically targetable contributors to this process. We recently reported that microRNA-155 is a key mediator of cardiac inflammation and injury in infectious myocarditis. Here we investigated the impact of miRNA-155 manipulation in hypertensive heart disease.

***Methods and Results*—**Genetic loss or pharmacological inhibition of the leukocyte-expressed microRNA-155 in mice markedly reduced cardiac inflammation, hypertrophy and dysfunction upon pressure overload. These alterations were macrophage-dependent, as *in vivo* cardiomyocyte-specific microRNA-155 manipulation did not affect cardiac hypertrophy or dysfunction, whereas bone marrow transplantation from wild type into microRNA-155 knockout animals rescued the cardiomyocytes' hypertrophic response and vice versa. *In vitro*, media from microRNA-155 knockout macrophages blocked the hypertrophic growth of stimulated cardiomyocytes, confirming that macrophages influence myocyte growth in a *miR-155*-dependent paracrine manner. These effects were at least partly mediated by the direct microRNA-155 target Suppressor of Cytokine Signaling 1 (Socs1), as Socs1 knockdown in microRNA-155 knockout macrophages largely restored their hypertrophy-stimulating potency.

***Conclusions*—**Our findings reveal that microRNA-155 expression in macrophages promotes cardiac inflammation, hypertrophy and failure in response to pressure overload. These data support the causative significance of inflammatory signaling in hypertrophic heart disease and demonstrate the feasibility of therapeutic microRNA targeting of inflammation in heart failure.

Key words: microRNA, inflammation, left ventricular hypertrophy, heart failure

DOI: 10.1161/CIRCULATIONAHA.112.001357

Introduction

Cardiac hypertrophy and consequent heart failure in response to chronic hypertension represent one of the major health challenges in Western societies[1]. Over the past decade, growing evidence has indicated the causative contribution of the immune system in hypertrophy and heart failure[2-4]. Angiotensin II (AngII), one of the major mediators of hypertension-induced target organ damage and hypertrophy, is a potent promoter of inflammation[5]. The signaling mechanisms that mediate these effects, however, remain largely obscure. In this study, we show that *microRNA-155* (*miR-155*) expression by macrophages is a powerful mediator of cardiac hypertrophy and failure, through the up-regulation of pro-inflammatory paracrine signaling.

MicroRNAs are small non-coding RNAs that inhibit gene expression of complementary target genes at the post-transcriptional level[6]. Whereas others have studied the implication of cardiomyocyte- or fibroblast-derived microRNAs[7-9], inflammatory microRNAs have hitherto remained unaddressed in pressure overload-induced heart disease. *MiR-155* expression is upregulated in a multitude of inflammatory diseases, including rheumatoid arthritis and multiple sclerosis[10, 11]. *MiR-155* knockout mice generate normal leukocyte populations under steady-state conditions, but display defective B-cell responses upon immunization and resistance to T cell-dependent experimental autoimmune encephalomyelitis[12-14]. In macrophages, *miR-155* is induced by pro-inflammatory M1-type stimuli including LPS, TNFa, and IFNj[15] and plays a central role in macrophage activation[16].

miR-155 promotes cardiac inflammation and injury in viral heart disease[17], suggesting that macrophage *miR-155* may also promote failure in other cardiac diseases, such as hypertensive heart disease. Here, we demonstrate that macrophages promote hypertension-induced cardiac hypertrophy and failure in a paracrine, *miR-155*-dependent manner. This effect

involves suppression of its target Suppressor of cytokine signaling 1 (Socs1)[18], which promotes pro-inflammatory and pro-hypertrophic cytokine signaling that is lost in the absence of *miR-155*. Our data demonstrate that local inflammation in the myocardium is driven by *miR-155* and mediates cardiac remodeling and function.

Methods

An expanded Methods section is available in the online Supplement.

Animal studies

All mouse experiments were performed according to the local relevant guidelines and group sizes are summarized in **Table 1**. Male *miR-155* KO and WT C57Bl/6J mice (10-12 weeks-old)[13] were subcutaneously infused with AngII (2.5 µg/g/day)[19] or subjected to TAC[20]. After 7 and/or 28 days, mice were sacrificed and blood and/or hearts were taken for histological, protein and RNA analyses and for flow cytometry as described[21].

Bone marrow transplantations were performed on 8 weeks-old male *miR-155* KO and WT mice as described[22]. After 8 weeks, mice were treated with AngII for 28 days as described above.

For antimiR experiments, eight weeks-old male WT C57Bl/6J mice were tail vein-injected on 3 consecutive days with a total of 10mg/kg LNA-modified anti*miR-155* or control antimiR (Ribotask, Denmark), followed by AngII administration as described above.

For AAV experiments, eight weeks-old male WT C57Bl/6J mice were tail vein-injected with $2.5x10^{11}$ viral genome particles of AAV9. AAV9-mediated gene transfer and expression was allowed for 3 weeks before AngII treatment as described above.

In vitro experiments

Rat ventricular cardiomyocytes (RCMs)[23] were transfected with 35nM *miR-155* antagomiR or scrambled control (Ambion) and treated with 100nM Et-1 (Sigma, St. Louis, MO) or sham for 24 hours.

BMMs from *miR-155* KO and WT mice were stimulated 1μM AngII or 10ng/ml LPS (from *E. coli* 055.B5; Sigma) for 0, 1, 6 and 24 hours, or transfected with siSocs1 or siControl (Ambion) by electroporation as described[24]. Media were subjected to mass spectroscopic proteomics analyses as described[25] or used for RCM culturing after dialysis in low serum RCM media using slide-a-lyzer dialysis cassettes (1/100, 3.5kDa, Thermo Fisher Scientific, Waltham, MA).

Statistical analyses

Data are presented as average +/- SEM. Comparisons between 2 groups were performed with two-tailed Student's t testing for Gaussian data or Mann-Whitney tests for non-Gaussian data. For comparisons of more than 2 groups, one-way ANOVA was used, followed by post hoc testing using Bonferroni correction for more groups. $P<0.05$ was considered statistically significant.

Supplemental Information

Supplemental Information includes a full methods section, 5 figures, and 5 tables.

Results

Pressure overload triggers cardiac infiltration of miR-155-expressing monocytes/macrophages in mice

To assess the dynamics of inflammatory cell infiltration in the pressure-overloaded heart, we analyzed cardiac leukocyte isolates from mice subjected to AngII using flow cytometry at

baseline, 1 and 4 weeks. We observed a peak of CD45-positive leukocytes at 1 week after start of AngII infusion, predominantly consisting of CD11b+ monocytes/ F4/80+ macrophages (**Fig. 1a**) consistent with previous data on transverse aortic constriction (TAC), another model of pressure overload[26]. The amount of cardiac granulocytes, T and B cells in both sham and AngII-treated hearts was low to negligible (**Fig. 1a**). *In situ* hybridization showed cardiac *miR-155* expression following AngII-infusion in infiltrating patches of interstitial leukocytes (**Fig. 1b**). In bone marrow-derived macrophages (BMMs), *miR-155* expression was induced by AngII, as well as by LPS as described before (**Fig. 1c**)[27]. Based on these results, we hypothesized that *miR-155* may modulate macrophage function in the pressure overloaded heart.

MiR-155 governs the macrophage secretome

We used proteomics analyses of the macrophage secretome to study *miR-155*-dependent macrophage functions and observed a broadly reduced activation status in LPS-activated *miR-155* KO macrophages as compared to WT macrophages (**Fig. 1d**). Levels of proteins indicative of macrophage activation or important for tissue infiltration, including the macrophage receptor Mac1, the adhesion-mediating integrins LFA1 and VLA4a, and the inflammatory cytokines TNFa, IL1B and IL12, were significantly less abundant in the *miR-155* KO macrophage secretome, suggesting compromised macrophage function upon activation in the absence of *miR-155* (**Fig. 1d**, **Table S1-2**). Using ELISA, we also found decreased levels of IL6 following LPS in *miR-155* KO BMMs (**Fig. 1e**). Both AngII- and LPS-induced expression of a subset of these genes, including *Il6*, *Tnfa, Il1b LFA1*, *VLA4a* and *Icam1*, was significantly blunted in *miR-155* KO macrophages at the mRNA level (**Fig. 1f**). Finally, AngII induces a predominantly pro-inflammatory M1-type response in WT but not *miR-155* KO macrophages. This was evidenced on the gene expression level by the induction of M1 marker *iNos* and the reduction of M2 marker

Arginase 1 (*Arg1*) following AngII in WT but not *miR-155* KO macrophages (**Fig. 1g**). In the absence of *miR-155*, macrophages seem skewed towards an M2-type phenotype with high baseline expression of *Arg1* (**Fig. 1g**). The presence of an anti-inflammatory phenotype in the absence of *miR-155* was further substantiated by increased secretion of the anti-inflammatory IL10 by *miR-155* KO as compared to WT macrophages, both at baseline and after AngII and LPS stimulation (**Fig. 1h**). Secreted pro-inflammatory IL12 p70 was around the detection limit.

Absence of miR-155 inhibits cardiac monocyte/macrophage infiltration, hypertrophy and failure

To investigate whether the absence of *miR-155* influences pressure overload-induced cardiac monocyte/macrophage influx and cardiac remodeling, we subjected *miR-155* KO and WT mice to AngII infusion for 1 and 4 weeks. The absence of *miR-155* prevented the increase in circulating leukocyte numbers - including monocytes - in response to AngII as seen in WT mice, while baseline numbers of circulating leukocytes were higher in *miR-155* KO as compared to WT mice (**Fig. 2a**, **Fig. S1a**, **Table S3**). This was paralleled at the tissue level by decreased infiltration of CD45+ leukocytes and of either CD68+ or CD11b+ F4/80+ monocytes/macrophages into the hearts of *miR-155* KO mice at 1 and 4 weeks after start of AngII, as determined by both immunohistochemistry and FACS (**Fig. 2a,b**, **Table S3**). Leukocyte numbers in sham-treated *miR-155* KO and WT hearts were similar. The total numbers of cardiac CD3+ T cells and Nimp1+ neutrophils were relatively small and unresponsive to AngII (**Fig. S1b,c**).

In addition to reduced inflammation, the hearts of *miR-155* KO mice showed a preserved contractile function and heart weight after 4 weeks of AngII, whereas WT mice exhibited a significant decrease in fractional shortening associated with development of significant cardiac

hypertrophy over the course of AngII treatment (**Fig. 2c-e**, **Table 1**). Protection from hypertrophy and heart failure in *miR-155* KO hearts was confirmed by quantification of individual cardiomyocyte cross-sectional area (**Fig. 2e**), the echocardiographically determined average wall thickness (**Table 1**), expression levels of cardiac hypertrophy markers alpha skeletal actin (*Acta1*), atrial natriuretic peptide (*Nppa*) and brain natriuretic factor (*Nppb*) (**Fig. 2f**), and desmin staining as a marker of cardiomyocyte stress[19] (**Fig. S2a**)[19]. Both *miR-155* KO and WT mice developed a similarly moderate hypertension upon AngII (**Fig. 2g**), paralleled by a similar cardiac interstitial fibrotic response (**Fig. S2b**). As expected, cardiac vascularization increased along with hypertrophy in WT mice yet capillary density was comparable in untreated *miR-155* KO and WT sham hearts (**Fig. S2c**), and could therefore not explain differences in hypertrophy. Finally, cardiac protein levels of the angiotensin II type 1 receptor (Agtr1), which has been reported to be a *miR-155* target in humans[28] though not conserved in mice, were not different between WT and KO mice (**Fig. S2d**). In conclusion, *miR-155* KO mice are protected against AngII-induced cardiac hypertrophy, inflammation and dysfunction by a mechanism that is independent of blood pressure, vascularization, cardiac fibrosis, and its target Agtr1.

Cardiac protection by miR-155 deficiency is independent of the model of pressure overload or miR-targeting strategy

To validate these findings in another model of pressure overload, we subjected *miR-155* KO and WT mice to 4 weeks of TAC. Again, *miR-155* KO mice were protected from cardiac CD45+ leukocyte influx, hypertrophy and heart failure (**Fig. 3a-c**, **Table 1**, **Fig. S3a**), and the induction of hypertrophic markers *Acta1*, *Nppa* and *Nppb* was blunted (**Fig. 3d**). Interstitial fibrosis was not different between WT and KO mice after TAC (**Fig. S3b**).

To ensure that the observed protection against macrophage influx and heart failure was

not due to differences inherent to embryologic development between *miR-155* KO and WT mice, we injected LNA-modified antimiRs against *miR-155* (antimiR-155) into adult WT mice followed by AngII treatment for 4 weeks. We obtained a cardiac knockdown of 81±4% in antimiR-155-treated mice as compared to mice treated with LNA-control (**Fig. S3c**). Similar to the *miR-155* KO mice, antimiR-155-treated mice showed a decreased cardiac infiltration of CD45+ leukocytes following AngII (**Fig. 3e**), as well as a significant reduction in hypertrophy and heart failure (**Fig. 3f,g**, **Fig. S3d**). Again, this was supported by decreased induction of *Acta1*, *Nppa* and *Nppb* in antimiR-155 AngII hearts compared to LNA-control AngII hearts (**Fig. 3h**), while interstitial fibrosis induced by AngII did not significantly differ in both groups (**Fig. S3e**).

In conclusion, *miR-155* is crucial for pressure overload-induced cardiac monocyte/macrophage influx. Blunted cardiac monocyte/macrophage responses to pressure overload in the absence of *miR-155* are associated with protection from cardiac hypertrophy and failure. We therefore hypothesized that cardiac monocyte/macrophage presence and activity may contribute to the early pathogenesis of cardiac hypertrophy and the progression to heart failure.

miR-155 expression is increased in human cardiac hypertrophy and correlates with decreased cardiac function and increased wall thickness

To translate our findings to human cardiac hypertrophy and failure, we determined cardiac *miR-155* expression in hypertrophic patients with aortic stenosis (AOS) and in non-hypertrophic control patients with preserved function undergoing coronary bypass artery ligation (CABG). Here, *miR-155* expression was increased in AOS as compared to control (**Fig. 3i**). Moreover, *miR-155* levels correlated significantly negatively with cardiac function and significantly positively with averaged wall thickness (**Fig. 3j**). Finally, also in a human hypertrophic heart

section, *miR-155* localized to interstitial cells rather than cardiomyocytes (**Fig. S4**).

Monocyte/macrophage expression of miR-155 mediates cardiac hypertrophy

To study the contribution of macrophage *miR-155* to cardiac hypertrophy and failure, we performed bone marrow transplantation of WT bone marrow into *miR-155* KO mice (WT to KO) and vice versa (KO to WT), and infused AngII for 4 weeks. WT to WT and KO to KO mice served as controls. WT donor macrophages were capable of cardiac infiltration in both WT and *miR-155* KO recipients, as shown by increased numbers of CD45+ leukocytes in WT to KO AngII hearts (**Fig. 4a**). In contrast, both WT and *miR-155* KO recipients of *miR-155* KO macrophages showed a blunted cardiac leukocyte infiltration. In agreement, the presence of WT donor macrophages in either WT or KO recipients was sufficient to cause cardiac hypertrophy and failure by AngII, while presence of KO macrophages - and concomitant decreased cardiac macrophage numbers - protected from cardiac hypertrophy and dysfunction (**Fig. 4b,c**, **Fig. S5a**). Therefore, the macrophage genotype determined the susceptibility to heart failure, and not the genotype of the host. These findings suggest that *miR-155* promotes cardiac pro-hypertrophic signaling by macrophages, predisposing to heart failure.

To independently confirm this mechanism *in vitro*, we grew neonatal rat cardiomyocytes in the presence of conditioned culture media from LPS-activated WT and KO BMMs. In line with our *in vivo* data, cardiomyocytes cultured in *miR-155* KO macrophage media displayed a limited hypertrophic response to endothelin-1 (Et-1) as compared to WT macrophage media-cultured cardiomyocytes, demonstrated by myocyte size and hypertrophic gene expression (**Fig. 4d,e**).

Though the expression of *miR-155* by cardiomyocytes is low, a contribution of cardiomyocyte *miR-155* to hypertrophy is conceivable. To rule out this mechanism, we

introduced hsa-pre-*miR-155* in WT mice *in vivo* specifically into cardiomyocytes using an adeno-associated virus serotype 9 (AAV9)-vector (**Fig. S5b**) and observed no difference in cardiac hypertrophy neither at baseline nor following AngII (**Fig. 4f**, **Fig. S5c**). Vice versa, efficient inhibition of cardiomyocyte *miR-155* function using AAV9-introduced *miR-155* sponges in WT mice (**Fig. S5d,e**) did not affect cardiac mass and hypertrophic marker responses following AngII infusion as compared to control sponges (**Fig. 4g**, **Fig. S5f**). Finally, we knocked down *miR-155 in vitro* in cardiomyocytes and induced hypertrophy with Et-1, and did not observe differences in induction of hypertrophic markers (**Fig. S5g,h**). Together, these data show that macrophage - but not myocyte - expression of *miR-155* regulates hypertrophic cardiomyocyte growth in a paracrine fashion.

Macrophage miR-155 promotes cardiomyocyte hypertrophic growth by inhibiting Socs1/Stat3 signaling

We next addressed how *miR-155* expression in macrophages influences macrophage paracrine activity. Direct anti-inflammatory *miR-155* targets include Socs1[18] and Src homology 2-containing inositol phosphatase-1 (Ship-1)[29]. We found that in the absence of *miR-155*, Socs1 protein expression is elevated (i.e. de-repressed) in LPS- as well as AngII-activated macrophages as compared to WT macrophages, while Ship1 was found mildly de-repressed only in unstimulated macrophages (**Fig. 5a-c**). Therefore, we focused on Socs1, which suppresses macrophage inflammatory responses by inhibiting the Jak/Stat axis[30, 31]. Increased Socs1 levels in LPS-treated *miR-155*-deficient macrophages were associated with diminished Stat3 phosphorylation at baseline and following LPS (**Fig. 5a,b**). In cardiomyocytes conditioned with *miR-155*-deficient macrophage media and subjected to pro-hypertrophic Et-1, Stat3 activation was hampered (**Fig. 5d**). Similarly, *in vivo*, *miR-155*-deficient hearts showed dramatically

reduced Stat3 activities upon pressure overload (**Fig. 5e**). Together, these data support a central role for Socs1/Stat3 signaling in *miR-155*-driven cardiac inflammation, hypertrophy and failure.

To confirm that macrophage-expressed *miR-155* mediates cardiac hypertrophy via Socs1, we prevented the de-repression of Socs1 in *miR-155* KO macrophages with siRNAs (**Fig. 6a**). Socs1 knockdown in macrophages largely rescued the limited hypertrophic response of myocytes grown in *miR-155* KO macrophage-conditioned media both at the level of myocyte growth and gene expression (**Fig. 6b-e**). Therefore, we conclude that the paracrine effects of *miR-155* on myocyte hypertrophy are mediated at least in part by the *miR-155* direct target Socs1 in macrophages.

Discussion

In this study, we address the inflammatory response during cardiac pressure-overload and identify *miR-155* expressed by macrophages as a potent contributor to cardiac hypertrophy and failure in response to pressure overload through paracrine signaling. Both genetic inactivation and pharmacological inhibition of *miR-155* significantly reduced cardiac inflammation and hypertrophic growth and prevented systolic dysfunction in pressure-overloaded hearts, indicating both robustness of the observed phenotype and theoretical feasibility of therapeutic intervention.

We demonstrate that the protected *miR-155* KO phenotype is macrophage- and not myocyte-autonomous in several ways: 1) bone marrow transplantation experiments demonstrate that mouse susceptibility to hypertrophy and heart failure is determined by bone marrow genotype and not cardiac genotype; 2) cardiomyocyte-specific AAV9-mediated overexpression and knockdown do not affect heart failure susceptibility; 3) *in vitro* cardiomyocyte hypertrophy is inhibited in the presence of KO macrophage conditioned media, but not WT macrophage media; 4) *in vitro* knockdown of miR-155 in cardiomyocytes does not affect their response to

hypertrophic signaling. In line with these findings, *miR-155* expression co-localized with the areas of interstitial inflammation in pressure overloaded WT hearts. In addition, we translated our findings to human cardiac hypertrophy and failure by measuring *miR-155* in biopsies from human hypertrophic and control CABG hearts and found that increased *miR-155* levels significantly correlated with depressed cardiac function and increased wall thickness.

We applied two distinct models for pressure overload to exclude model specificity of the protected phenotype. Our data suggest that both trigger a pro-inflammatory response in the heart. While AngII is a known powerful direct promoter of inflammation[5], TAC is primarily a hemodynamic intervention and the exact nature of its pro-inflammatory effects (e.g. through an induction of local and/or circulating AngII) remains speculative. However, the shared phenotype strengthens the concept that inflammation is a general feature of hypertensive heart disease with targetable components such as *miR-155* signaling. Indeed, our finding that macrophages contribute to cardiac hypertrophy is in line with previous studies revealing a role for leukocyte-derived galectin-3 and PI3 kinase in cardiac hypertrophic remodeling[5, 32, 33]. Also, adoptive transfer of anti-inflammatory regulatory T cells in mice during AngII-mediated pressure overload reduces cardiac monocyte infiltration and prevents cardiac hypertrophy and damage[34]. These studies and the current work imply that macrophage inflammatory signaling may be necessary for hypertrophic remodeling during pressure overload. Importantly, our data show that the cardiac influx of macrophages upon pressure overload precedes signs of hypertrophy and heart failure, suggesting a direct contribution to cardiac pathophysiology.

Whereas in the absence of *miR-155,* baseline cardiac leukocyte numbers were similar, baseline circulating leukocyte numbers were high, possibly reflecting both a hampered activation and extravasation potential of *miR-155*-deficient leukocytes. Importantly, in an earlier study

using LNA-antimiR-155 to inhibit miR-155, we did not see these baseline hematological differences[17], implying that they are the result of embryological loss of *miR-155* and keeping the road open for antimiR-155 therapy in heart disease. The latter is interesting, since in response to AngII, both circulating and cardiac *miR-155*-deficient leukocytes fail to increase numbers. These data imply that *miR-155* is crucial for monocytes/macrophages to infiltrate the pressure-overloaded heart.

In addition, we found that the *in vitro* M1-polarized pro-inflammatory macrophage response to AngII in the presence of *miR-155* is abrogated and even reversed to M2-polarisation in the absence of *miR-155*. The M1/M2 polarization status of macrophages can affect disease severity[35], and our data may imply that M2-polarised macrophages are cardioprotective.

Cardioprotection of *miR-155* KO mice was mediated at least in part by de-repression of the translational *miR-155* target Socs1, as blocking Socs1 upregulation by LPS in miR-155 KO macrophages *in vitro* rescued the blunted pro-hypertrophic potential of their conditioned media. Socs1 de-repression was associated with reduced Stat3 activation in cardiomyocytes as well as macrophages. Socs1 is an endogenous inhibitor of Stat3 activation, as well as a potent inhibitor of production and release of cytokines that can activate Stat3 in adjacent cells[36]. Since Stat3 signaling has both pro-hypertrophic and pro-inflammatory effects[37, 38], we propose that increased Socs1 levels and chronically suppressed Stat3 signaling reduce cytokine production in *miR-155*-deficient cardiac macrophages during pressure overload. Along this line, chronic activation of Stat3 signaling during pressure overload[39] was shown to be detrimental and cause increased cardiac inflammation and failure[40], even though rapid Stat3 activation in acute heart failure is cardio-protective[40-42]. Here, we show by both *in vivo* bone marrow transplantation and *in vitro* conditioned macrophage media approaches that the altered milieu of macrophage secreted

factors - as determined by proteomics and including many cytokines with documented pro-hypertrophic effects[43] - in the absence of *miR-155* blunts the hypertrophic response of cardiomyocytes and prevents contractile dysfunction. As such, *miR-155* links hypertension-induced interstitial cardiac inflammation to myocyte hypertrophy and function. A diagram of the proposed signaling pathway is provided in **Fig. 6e**.

While absence of *miR-155* blunted pressure overload-induced cardiac hypertrophy and inflammation, the cardiac fibrotic response remained intact, indicating that pressure overload-induced fibrotic remodeling was independent of macrophage *miR-155* function. Possible explanations include that *miR-155* deficient macrophages can still secrete pro-fibrotic factors, or fibrotic remodeling in the heart is not solely dependent on macrophage signaling as was previously suggested[26]. Interestingly, it was recently shown that leukocyte *PI3Kγ* influences cardiac fibrotic responses to TAC, but, in agreement with our findings, cardiac function was found to be independent of this leukocyte-mediated fibrotic remodeling[32]. The mechanisms driving cardiac fibrotic remodeling in response to pressure overload, and the relation between fibrosis and cardiac function, therefore need further scientific attention.

In conclusion, inflammatory signaling through macrophage *miR-155* modulates cardiac hypertrophy and failure during pressure overload. Both genetic deficiency and pharmacological inhibition of *miR-155* prevent cardiac hypertrophy and failure, an effect that is independent from *miR-155* expression by cardiomyocytes. While signaling in pressure overload-induced cardiac hypertrophy and consequent failure is a highly complex process involving many cell types and signaling molecules, our data uncover the existence of a macrophage-cardiomyocyte crosstalk that contributes to cardiac responses to pressure overload, and identify *miR-155* as a potential therapeutic target in heart failure.

Acknowledgements: We thank Laura de Rijck, Georg Summer, Dr Hamid El Azzouzi, Nicole Bitsch, Paul Veulemans, Sylvia Jochems, Mathijs van de Vrie, Dr Jan D'Hooge, Dr Jack P Cleutjens, Ermira Samara, Janka Matrai, Dr Giulia Ruozi, Gregorio Fazzi and Linda Beckers for technical assistance and expertise; Dr Marinee Chuah and Dr Thierry VandenDriessche for control AAV9 vectors.

Funding Sources: This work was supported by research grants to BS (Veni 016.096.126 from Netherlands Organization for Scientific Research (NWO), Horizon 93519017 from Netherlands Genomics Initiative, and 2009B025 from Netherlands Heart Foundation (NHS)). Additional support was from NWO Vidi 91796338 (SH), Research Foundation – Flanders 1183211N, 1167610N, G074009N (SH), European Union, FP7-HEALTH-2010 MEDIA (BS and SH), FP7-HEALTH-2011 EU-Mascara (SH), and NWO 40-00506-98-10016 (BJJ). MdW is an Established Investigator of the Netherlands Heart Foundation (2007T067). NS and DG thank the Cluster of Excellence CellNetworks and the CHS foundation for funding.

Conflict of Interest Disclosures: None.

References:

1. Jessup M, Brozena S. Heart failure. *N Engl J Med.* 2003;348:2007-2018.

2. Heymans S, Hirsch E, Anker SD, Aukrust P, Balligand JL, Cohen-Tervaert JW, Drexler H, Filippatos G, Felix SB, Gullestad L, Hilfiker-Kleiner D, Janssens S, Latini R, Neubauer G, Paulus WJ, Pieske B, Ponikowski P, Schroen B, Schultheiss HP, Tschope C, Van Bilsen M, Zannad F, McMurray J, Shah AM. Inflammation as a therapeutic target in heart failure? A scientific statement from the Translational Research Committee of the Heart Failure Association of the European Society of Cardiology. *Eur J Heart Fail.* 2009;11:119-129.

3. Mann DL. Inflammatory mediators and the failing heart: past, present, and the foreseeable future. *Circ Res.* 2002;91:988-998.

4. Marchant DJ, Boyd JH, Lin DC, Granville DJ, Garmaroudi FS, McManus BM. Inflammation in myocardial diseases. *Circ Res.* 2012;110:126-144.

5. Kvakan H, Luft FC, Muller DN. Role of the immune system in hypertensive target organ damage. *Trends Cardiovasc Med.* 2009;19:242-246.

6. Lee RC, Ambros V. An extensive class of small RNAs in Caenorhabditis elegans. *Science.*

2001;294:862-864.

7. Duisters RF, Tijsen AJ, Schroen B, Leenders JJ, Lentink V, van der Made I, Herias V, van Leeuwen RE, Schellings MW, Barenbrug P, Maessen JG, Heymans S, Pinto YM, Creemers EE. miR-133 and miR-30 regulate connective tissue growth factor: implications for a role of microRNAs in myocardial matrix remodeling. *Circ Res.* 2009;104:170-178, 176p following 178.

8. Thum T, Gross C, Fiedler J, Fischer T, Kissler S, Bussen M, Galuppo P, Just S, Rottbauer W, Frantz S, Castoldi M, Soutschek J, Koteliansky V, Rosenwald A, Basson MA, Licht JD, Pena JT, Rouhanifard SH, Muckenthaler MU, Tuschl T, Martin GR, Bauersachs J, Engelhardt S. MicroRNA-21 contributes to myocardial disease by stimulating MAP kinase signalling in fibroblasts. *Nature.* 2008;456:980-984.

9. van Rooij E, Sutherland LB, Qi X, Richardson JA, Hill J, Olson EN. Control of stress-dependent cardiac growth and gene expression by a microRNA. *Science.* 2007;316:575-579.

10. Junker A, Krumbholz M, Eisele S, Mohan H, Augstein F, Bittner R, Lassmann H, Wekerle H, Hohlfeld R, Meinl E. MicroRNA profiling of multiple sclerosis lesions identifies modulators of the regulatory protein CD47. *Brain.* 2009;132:3342-3352.

11. Stanczyk J, Pedrioli DM, Brentano F, Sanchez-Pernaute O, Kolling C, Gay RE, Detmar M, Gay S, Kyburz D. Altered expression of MicroRNA in synovial fibroblasts and synovial tissue in rheumatoid arthritis. *Arthritis Rheum.* 2008;58:1001-1009.

12. O'Connell RM, Kahn D, Gibson WS, Round JL, Scholz RL, Chaudhuri AA, Kahn ME, Rao DS, Baltimore D. MicroRNA-155 promotes autoimmune inflammation by enhancing inflammatory T cell development. *Immunity.* 2010;33:607-619.

13. Rodriguez A, Vigorito E, Clare S, Warren MV, Couttet P, Soond DR, van Dongen S, Grocock RJ, Das PP, Miska EA, Vetrie D, Okkenhaug K, Enright AJ, Dougan G, Turner M, Bradley A. Requirement of bic/microRNA-155 for normal immune function. *Science.* 2007;316:608-611.

14. Thai TH, Calado DP, Casola S, Ansel KM, Xiao C, Xue Y, Murphy A, Frendewey D, Valenzuela D, Kutok JL, Schmidt-Supprian M, Rajewsky N, Yancopoulos G, Rao A, Rajewsky K. Regulation of the germinal center response by microRNA-155. *Science.* 2007;316:604-608.

15. O'Connell RM, Taganov KD, Boldin MP, Cheng G, Baltimore D. MicroRNA-155 is induced during the macrophage inflammatory response. *Proc Natl Acad Sci U S A.* 2007;104:1604-1609.

16. Tili E, Michaille JJ, Cimino A, Costinean S, Dumitru CD, Adair B, Fabbri M, Alder H, Liu CG, Calin GA, Croce CM. Modulation of miR-155 and miR-125b levels following lipopolysaccharide/TNF-alpha stimulation and their possible roles in regulating the response to endotoxin shock. *J Immunol.* 2007;179:5082-5089.

17. Corsten MF, Papageorgiou A, Verhesen W, Carai P, Lindow M, Obad S, Summer G, Coort

SL, Hazebroek M, van Leeuwen R, Gijbels MJ, Wijnands E, Biessen EA, De Winther MP, Stassen FR, Carmeliet P, Kauppinen S, Schroen B, Heymans S. MicroRNA profiling identifies microRNA-155 as an adverse mediator of cardiac injury and dysfunction during acute viral myocarditis. *Circ Res.* 2012;111:415-425.

18. Lu LF, Thai TH, Calado DP, Chaudhry A, Kubo M, Tanaka K, Loeb GB, Lee H, Yoshimura A, Rajewsky K, Rudensky AY. Foxp3-dependent microRNA155 confers competitive fitness to regulatory T cells by targeting SOCS1 protein. *Immunity.* 2009;30:80-91.

19. Schroen B, Leenders JJ, van Erk A, Bertrand AT, van Loon M, van Leeuwen RE, Kubben N, Duisters RF, Schellings MW, Janssen BJ, Debets JJ, Schwake M, Hoydal MA, Heymans S, Saftig P, Pinto YM. Lysosomal integral membrane protein 2 is a novel component of the cardiac intercalated disc and vital for load-induced cardiac myocyte hypertrophy. *J Exp Med.* 2007;204:1227-1235.

20. da Costa Martins PA, Salic K, Gladka MM, Armand AS, Leptidis S, el Azzouzi H, Hansen A, Coenen-de Roo CJ, Bierhuizen MF, van der Nagel R, van Kuik J, de Weger R, de Bruin A, Condorelli G, Arbones ML, Eschenhagen T, De Windt LJ. MicroRNA-199b targets the nuclear kinase Dyrk1a in an auto-amplification loop promoting calcineurin/NFAT signalling. *Nat Cell Biol.* 2010;12:1220-1227.

21. Bai L, Beckers L, Wijnands E, Lutgens SP, Herias MV, Saftig P, Daemen MJ, Cleutjens K, Lutgens E, Biessen EA, Heeneman S. Cathepsin K gene disruption does not affect murine aneurysm formation. *Atherosclerosis.* 2010;209:96-103.

22. Goossens P, Gijbels MJ, Zernecke A, Eijgelaar W, Vergouwe MN, van der Made I, Vanderlocht J, Beckers L, Buurman WA, Daemen MJ, Kalinke U, Weber C, Lutgens E, de Winther MP. Myeloid type I interferon signaling promotes atherosclerosis by stimulating macrophage recruitment to lesions. *Cell Metab.* 2010;12:142-153.

23. De Windt LJ, Willemsen PH, Popping S, Van der Vusse GJ, Reneman RS, Van Bilsen M. Cloning and cellular distribution of a group II phospholipase A2 expressed in the heart. *J Mol Cell Cardiol.* 1997;29:2095-2106.

24. Wiese M, Castiglione K, Hensel M, Schleicher U, Bogdan C, Jantsch J. Small interfering RNA (siRNA) delivery into murine bone marrow-derived macrophages by electroporation. *J Immunol Methods.* 2010;353:102-110.

25. Yin X, Cuello F, Mayr U, Hao Z, Hornshaw M, Ehler E, Avkiran M, Mayr M. Proteomics analysis of the cardiac myofilament subproteome reveals dynamic alterations in phosphatase subunit distribution. *Mol Cell Proteomics.* 2010;9:497-509.

26. Xia Y, Lee K, Li N, Corbett D, Mendoza L, Frangogiannis NG. Characterization of the inflammatory and fibrotic response in a mouse model of cardiac pressure overload. *Histochem Cell Biol.* 2009;131:471-481.

27. Baltimore D, Boldin MP, O'Connell RM, Rao DS, Taganov KD. MicroRNAs: new regulators of immune cell development and function. *Nat Immunol.* 2008;9:839-845.

28. Martin MM, Buckenberger JA, Jiang J, Malana GE, Nuovo GJ, Chotani M, Feldman DS, Schmittgen TD, Elton TS. The human angiotensin II type 1 receptor +1166 A/C polymorphism attenuates microrna-155 binding. *J Biol Chem.* 2007;282:24262-24269.

29. Kurowska-Stolarska M, Alivernini S, Ballantine LE, Asquith DL, Millar NL, Gilchrist DS, Reilly J, Ierna M, Fraser AR, Stolarski B, McSharry C, Hueber AJ, Baxter D, Hunter J, Gay S, Liew FY, McInnes IB. MicroRNA-155 as a proinflammatory regulator in clinical and experimental arthritis. *Proc Natl Acad Sci U S A.* 2011;108:11193-11198.

30. Boengler K, Hilfiker-Kleiner D, Drexler H, Heusch G, Schulz R. The myocardial JAK/STAT pathway: from protection to failure. *Pharmacol Ther.* 2008;120:172-185.

31. Dimitriou ID, Clemenza L, Scotter AJ, Chen G, Guerra FM, Rottapel R. Putting out the fire: coordinated suppression of the innate and adaptive immune systems by SOCS1 and SOCS3 proteins. *Immunol Rev.* 2008;224:265-283.

32. Damilano F, Franco I, Perrino C, Schaefer K, Azzolino O, Carnevale D, Cifelli G, Carullo P, Ragona R, Ghigo A, Perino A, Lembo G, Hirsch E. Distinct effects of leukocyte and cardiac phosphoinositide 3-kinase gamma activity in pressure overload-induced cardiac failure. *Circulation.* 2011;123:391-399.

33. Sharma UC, Pokharel S, van Brakel TJ, van Berlo JH, Cleutjens JP, Schroen B, Andre S, Crijns HJ, Gabius HJ, Maessen J, Pinto YM. Galectin-3 marks activated macrophages in failure-prone hypertrophied hearts and contributes to cardiac dysfunction. *Circulation.* 2004;110:3121-3128.

34. Kvakan H, Kleinewietfeld M, Qadri F, Park JK, Fischer R, Schwarz I, Rahn HP, Plehm R, Wellner M, Elitok S, Gratze P, Dechend R, Luft FC, Muller DN. Regulatory T cells ameliorate angiotensin II-induced cardiac damage. *Circulation.* 2009;119:2904-2912.

35. Hunter MM, Wang A, Parhar KS, Johnston MJ, Van Rooijen N, Beck PL, McKay DM. In vitro-derived alternatively activated macrophages reduce colonic inflammation in mice. *Gastroenterology.* 2010;138:1395-1405.

36. Heinrich PC, Behrmann I, Haan S, Hermanns HM, Muller-Newen G, Schaper F. Principles of interleukin (IL)-6-type cytokine signalling and its regulation. *Biochem J.* 2003;374:1-20.

37. Hirota H, Yoshida K, Kishimoto T, Taga T. Continuous activation of gp130, a signal-transducing receptor component for interleukin 6-related cytokines, causes myocardial hypertrophy in mice. *Proc Natl Acad Sci U S A.* 1995;92:4862-4866.

38. Rebouissou S, Amessou M, Couchy G, Poussin K, Imbeaud S, Pilati C, Izard T, Balabaud C, Bioulac-Sage P, Zucman-Rossi J. Frequent in-frame somatic deletions activate gp130 in

inflammatory hepatocellular tumours. *Nature.* 2009;457:200-204.

39. Gao XM, Wong G, Wang B, Kiriazis H, Moore XL, Su YD, Dart A, Du XJ. Inhibition of mTOR reduces chronic pressure-overload cardiac hypertrophy and fibrosis. *J Hypertens.* 2006;24:1663-1670.

40. Hilfiker-Kleiner D, Shukla P, Klein G, Schaefer A, Stapel B, Hoch M, Muller W, Scherr M, Theilmeier G, Ernst M, Hilfiker A, Drexler H. Continuous glycoprotein-130-mediated signal transducer and activator of transcription-3 activation promotes inflammation, left ventricular rupture, and adverse outcome in subacute myocardial infarction. *Circulation.* 2010;122:145-155.

41. Kunisada K, Negoro S, Tone E, Funamoto M, Osugi T, Yamada S, Okabe M, Kishimoto T, Yamauchi-Takihara K. Signal transducer and activator of transcription 3 in the heart transduces not only a hypertrophic signal but a protective signal against doxorubicin-induced cardiomyopathy. *Proc Natl Acad Sci U S A.* 2000;97:315-319.

42. Oshima Y, Fujio Y, Nakanishi T, Itoh N, Yamamoto Y, Negoro S, Tanaka K, Kishimoto T, Kawase I, Azuma J. STAT3 mediates cardioprotection against ischemia/reperfusion injury through metallothionein induction in the heart. *Cardiovasc Res.* 2005;65:428-435.

43. Gullestad L, Ueland T, Vinge LE, Finsen A, Yndestad A, Aukrust P. Inflammatory cytokines in heart failure: mediators and markers. *Cardiology.* 2012;122:23-35.

DOI: 10.1161/CIRCULATIONAHA.112.001357

Table 1. Biometric data.

	n	BW (g)	HW/BW (mg/g)	LW/BW (mg/g)	LVWd (mm)	LVIDd (mm)	LVIDs (mm)	FS (%)	Heart rate (bpm)
WT sham	13	26.4±0.7	5.53±0.20	6.12±0.19	0.75±0.01	3.76±0.05	2.60±0.06	27.8±2.9	449±9
WT AngII	11	24.9±0.4	6.94±0.26*	8.00±0.56*	0.92±0.04*	4.33±0.19*	3.70±0.22*	13.5±2.5*	525±26
miR-155 KO sham	11	24.9±0.2	4.87±0.13	5.89±0.11	0.72±0.01	3.74±0.05	2.66±0.07	29.2±2.3	396±13
miR-155 KO AngII	14	25.0±0.5	5.22±0.20*$	6.17±0.22$	0.80±0.04*$	3.62±0.08$	2.56±0.14$	35.5±1.9$	547±8
WT sham	5	22.5±0.5	5.00±0.15	7.35±0.12	0.70±0.03	4.03±0.10	3.10±0.09	23.4±1.6	520±38
WT TAC	6	22.1±0.2	7.00±0.16*	8.21±0.43	0.99±0.06*	4.01±0.11	3.40±0.13	15.5±1.1*	554±21
miR-155 KO sham	11	24.1±0.7	4.84±0.09	6.63±0.21	0.70±0.03	3.99±0.09	3.11±0.10	23.6±1.2	477±25
miR-155 KO TAC	11	23.9±0.4	5.90±0.28*$	7.30±0.19*	0.93±0.05*	4.22±0.05	3.19±0.06	24.2±1.7$	543±27
WT scrambled sham	6	22.5±0.3	4.81±0.09	7.72±0.11	0.69±0.01	3.94±0.16	2.96±0.11	26.6±2.7	473±65
WT scrambled AngII	8	23.2±0.7	6.47±0.15*	9.57±0.32	1.00±0.02*	3.74±0.30	3.01±0.12	19.6±1.7*	542±55
Anti-miR-155 sham	6	22.0±0.4	4.53±0.04	7.49±0.32	0.70±0.01	3.98±0.17	3.04±0.10	25.1±1.6	477±37
Anti-miR-155 AngII	6	22.4±0.6	5.84±0.29*$	8.89±0.47	0.85±0.04*$	3.68±0.25	2.68±0.10*	27.1±2.0$	485±59
WT to WT sham	7	25.4±0.7	5.10±0.07	6.92±0.18	0.83±0.03	3.75±0.08	2.62±0.09	30.2±1.7	420±24
WT to WT AngII	13	23.5±1.9	6.39±0.17*	8.38±1.23*	1.17±0.04*	3.68±0.10	3.08±0.11*	16.4±1.4*	494±15*
WT to KO sham	7	25.9±0.7	4.91±0.12	7.18±0.78	0.87±0.03	4.12±0.17	2.69±0.07	34.6±1.3	503±9
WT to KO AngII	11	23.1±2.1	6.15±0.11*	8.54±1.71	1.09±0.04*	3.97±0.15	3.17±0.17	20.1±1.8*	487±21
KO to WT sham	5	24.4±0.6	4.89±0.16	6.38±0.61	0.87±0.02	3.71±0.08	2.51±0.08	32.3±1.9	443±9
KO to WT AngII	12	25.5±1.4	5.50±0.17*$	8.29±1.06*	0.93±0.03*$	3.50±0.09	2.26±0.14$	35.8±2.6$	588±16*
KO to KO sham	7	27.4±3.0	4.85±0.17	6.37±1.11	0.93±0.02	4.19±0.09	2.85±0.09	32.0±1.4	544±8
KO to KO AngII	7	22.5±1.6*	5.84±0.08*$#	8.56±0.36*	0.86±0.01$#	4.06±0.18	2.83±0.22	30.6±2.6$#	513±23

AngII, angiotensin II treatment for 4 weeks; n, number of animals per group (also for Fig. 2-4); BW (g), body weight in grams; HW/BW (mg/g), heart weight corrected for body weight in milligram per gram; LVWd (mm), left ventricular wall in diastole in millimeters (average of distal and septal walls); LVIDd (mm), left ventricular inner diameter in millimeter; bpm, beats per minute; % fibrosis, percentage interstitial left ventricular fibrosis; LW/BW (mg/g), lung weight corrected for body weight in milligram per gram. *P<0.05 versus sham; $P<0.05 versus WT (to WT); #P<0.05 versus WT to KO.

DOI: 10.1161/CIRCULATIONAHA.112.001357

Figure Legends:

Figure 1. *MiR-155* localizes to cardiac macrophages following pressure overload and controls macrophage activity. (**a**) Flow cytometry of cardiac inflammatory cells reveals that predominantly monocytes/macrophages respond to AngII after 1 and 4 weeks, with a peak at 1 week (n=6/group). Please note that the markers used for monocytes (CD11b) and macrophages (CD11b and F4/80) overlap and therefore their added numbers exceed the total leukocyte numbers. (**b**) *In situ* hybridization of *miR-155* in cardiac sections. While *miR-155* expression is hardly detected in myocytes and interstitium of sham hearts, *miR-155* signal is readily detected in patchy infiltrates of inflammatory cells after AngII treatment. No signal was observed in KO hearts (scale bars: 50μm). (c) *miR-155* expression is induced by both LPS and AngII in macrophages. (**d**) Fold changes (FC) of the secreted abundance of of significantly changed (P<0.05) selected macrophage proteins in *miR-155* KO over WT LPS BMM media (n=3/group). (**e**) Levels of Il6 are higher in WT versus KO macrophages in response to LPS. (f) Induction of gene expression of cytokines and adhesion molecules by AngII and LPS is repressed in *miR-155* KO macrophages. (g) Induction of the macrophage M1 marker iNOS by AngII is repressed in *miR-155* KO macrophages, while these cells have higher baseline and post-AngII levels of the M2 marker Arg1. (h) While secreted levels of the pro-inflammatory Il12 p70 by macrophages following AngII and LPS are low, secreted levels of the anti-inflammatory Il10 are significantly higher in unstimulated and AngII- and LPS-stimulated *miR-155* KO versus WT macrophages. Data are represented by mean +/- SEM. All quantitative *in vitro* data were generated from a minimum of three replicates. *P < 0.05, **P < 0.01, ***P < 0.005.

Figure 2. *MiR-155* KO mice are protected from AngII-induced cardiac inflammation, hypertrophy and failure. (**a**) Flow cytometry of circulating monocytes shows impaired monocyte mobilization by 1 week AngII in KO animals, while absolute circulating baseline numbers are higher (P=0.06). Flow cytometry of cardiac macrophages shows similar baseline numbers, which are significantly increased by AngII only in WT hearts (n=3-6/group). (**b**) Quantification and representative images of cardiac sections (scale bars: 100μm) of CD45 and CD68 immunoreactive cells (n=4/group) substantiate the cardiac flow cytometry results. Macrophages have infiltrated the heart after 1 and 4 weeks of AngII in WT mice, but this is significantly depressed in *miR-155* KO hearts. (**c**) Fractional shortening as a measure of cardiac function shows no significant differences between *miR-155* WT and KO mice at baseline. WT mice develop systolic dysfunction with cardiac dilatation as evidenced by increased left ventricular inner diameter in diastole (LVIDd) after 4 weeks of AngII, while KO mice are protected. (**d**) Heart weight to body weight ratios of *miR-155* WT and KO mice are not significantly different at baseline. WT mice but not KO mice develop cardiac hypertrophy following AngII, already apparent at week 1 and pronounced after 4 weeks. (**e**) Representative images of whole hearts (top panels, scale bar: 5mm) and HE-stained sections of the left ventricles (lower panels, scale bar: 50μm) of *miR-155* WT and KO mice. Quantifications of myocyte cross-sectional area (**e**) and cardiac expression of the fetal hypertrophy markers *Acta1*, *Nppa* and *Nppb* (**f**) show an increase in AngII-treated *miR-155* WT mice, but to a significantly lesser extent in KO mice. (**g**) Tail cuff measurements of arterial blood pressure in WT and KO mice after 3 weeks of AngII reveal a comparable development of hypertension in both genotypes measured under similar heart rates. Data are represented by mean +/- SEM. WT AngII 1w, n=4; KO AngII 1w, n=5; $*P < 0.05$, $**P < 0.01$, $***P < 0.005$.

Figure 3. Absence of *miR-155* protects against TAC- and AngII-induced cardiac inflammation, hypertrophy and failure. (**a**) Quantification and representative images of cardiac sections (scale bars: 100μm) of CD45+ immunoreactive cells in TAC- or sham-operated mice show diminished cardiac leukocyte infiltration in the absence of *miR-155*. (**b**) Echocardiographic analysis shows that *miR-155* KO but not WT mice are protected from systolic dysfunction following 4 weeks of TAC. (**c**) Both WT and KO mice develop cardiac hypertrophy following TAC, but this response is significantly blunted in KO mice. (**d**) Induction of cardiac *Acta1*, *Nppa* and *Nppb* is significantly blunted in KO mice following TAC. (**e**) Quantification and representative images of cardiac sections (scale bars: 100μm) of CD45+ immunoreactive cells in AngII- or sham-treated mice show diminished cardiac leukocyte infiltration upon *miR-155* inhibition. (**f,g**) AntimiR-mediated *miR-155* inhibition protects WT mice from AngII-induced systolic dysfunction (**f**) and cardiac hypertrophy (**g**). (**h**) Induction of cardiac hypertrophic markers *Acta1* and *Nppa* is significantly reduced in anti*miR-155* treated mice following AngII, while *Nppb* induction does not differ significantly. (i-j) Expression of *miR-155* in cardiac biopsies of AOS patients (n=15) is 1.9-fold higher than in control (n=11) (i) and correlates negatively with ejection fraction and positively with averaged wall thickness (***j***). Data are represented by mean +/- SEM. **P* < 0.05, ***P* < 0.01, ****P* < 0.005.

Figure 4. Macrophages influence hypertrophic growth of cardiomyocytes via *miR-155*. (**a**) Quantification and representative images of cardiac sections (scale bars: 100μm) of CD45+ immunoreactive cells in AngII- or sham-treated mice following adoptive bone marrow transfer between *miR-155* WT and KO mice. Absence of *miR-155* in bone marrow-derived cells (the "KO to"-groups) diminishes their cardiac leukocyte infiltration upon AngII (**a**), and rescues

hearts from hypertrophy (**c**) and failure (**b**). Vice versa, KO mice reconstituted with WT bone marrow ("WT to KO" group) have re-enabled cardiac leukocyte infiltration (**a**), show partial rescue of the hypertrophic response (**c**), and develop heart failure after 4 weeks AngII (**b**). (**d**) Representative images and quantification of phalloidin staining (red) of actin filaments in cultured RCMs (scale bar: 50μm). The hypertrophic growth (**d**) and *Acta1* and *Nppa* gene expression response (**e**) of RCMs to Et-1 are significantly blunted by addition of culture media from *miR-155* KO BMMs. (**f**) *In vivo* cardiomyocyte *miR-155* overexpression using AAV9-hsa-*miR-155* leads to similar induction of cardiac hypertrophy by AngII as compared to both PBS and AAV9-scrambled treatment. *In vivo* cardiomyocyte *miR-155* inhibition using AAV9-sponge-*miR-155* also allows induction of similar levels of cardiac hypertrophy following AngII (**g**). Data are represented by mean +/- SEM. All quantitative *in vitro* data were generated from a minimum of three replicates. PBS AngII, n=8; AAV-scram sham, n=8; AAV-scram AngII, n=12; AAV-155 sham, n=6; AAV-155 AngII, n=8; AAV-sponge control sham, n=5; AAV-sponge control AngII, n=10; AAV-sponge-*miR-155* sham, n=5; AAV-sponge-*miR-155* AngII, n=10; * $P < 0.05$, ** $P < 0.01$, *** $P < 0.005$.

Figure 5. *MiR-155* controls inflammatory signaling through its target Socs1 and downstream Stat3. Representative Western blot images (**a**) and quantification (**b**) of Socs1, Ship1, and total and phosphorylated Stat3 (P-Stat3) in BMMs from *miR-155* WT or KO mice stimulated with LPS. GAPDH is used as loading control. *MiR-155* KO macrophages show higher Socs1 levels and lower Stat3 activation (P-Stat3/Stat3 levels) in response to LPS as compared to WT macrophages. (c) Socs1 and Ship1 protein expression are both induced by AngII in WT macrophages, and absence of *miR-155* exaggerates this response only for Socs1. (**d**) Adding

culture media from KO macrophages to RCMs inhibits their Stat3 activation in response to Et-1 stimulation. (**e**) Stat3 activation is significantly lower in KO versus WT mouse hearts after 1 and 4 weeks of AngII infusion (Representative western blot images are shown; quantification based on WT sham, n=5; WT AngII 1w, n=4; WT AngII 4w, n=6; KO sham, n=6; KO AngII 1w, n=4; KO AngII 4w, n=4). Data are represented by mean +/- SEM. Western blot images are representative. All quantitative *in vitro* data were generated from a minimum of three replicates.*$P < 0.05$, **$P < 0.01$, ***$P < 0.005$.

Figure 6. Socs1 knockdown in macrophages rescues paracrine hypertrophic stimulation to myocytes**.** (**a**) Knockdown of Socs1 transcripts in BMMs from *miR-155* WT and KO mice. (**b**) Phalloidin staining (red) of actin filaments in RCMs stimulated with Et-1 and grown in culture media from WT or KO BMMs that were treated with siRNAs against Socs1 or control (scale bar: 50μm). Quantification of cross-sectional myocyte areas (**c**) and expression of hypertrophic markers *Acta1*, *Nppa* and *Nppb* (**d**) show that the blunting of hypertrophy by media from KO macrophages is rescued by Socs1 knockdown in macrophages. (**e**) Schematic representation of the cardiac *miR-155* signaling pathway. *MiR-155* inhibits macrophage Socs1, relieving Socs1-mediated repression of macrophage Stat3 activity and of pro-hypertrophic paracrine signaling to cardiomyocytes to induce Stat3 activity, leading both to inflammatory activation and cardiomyocyte hypertrophy. Data are represented by mean +/- SEM. All quantitative *in vitro* data were generated from a minimum of three replicates. *$P < 0.05$, **$P < 0.01$, ***$P < 0.005$.

Figure 1

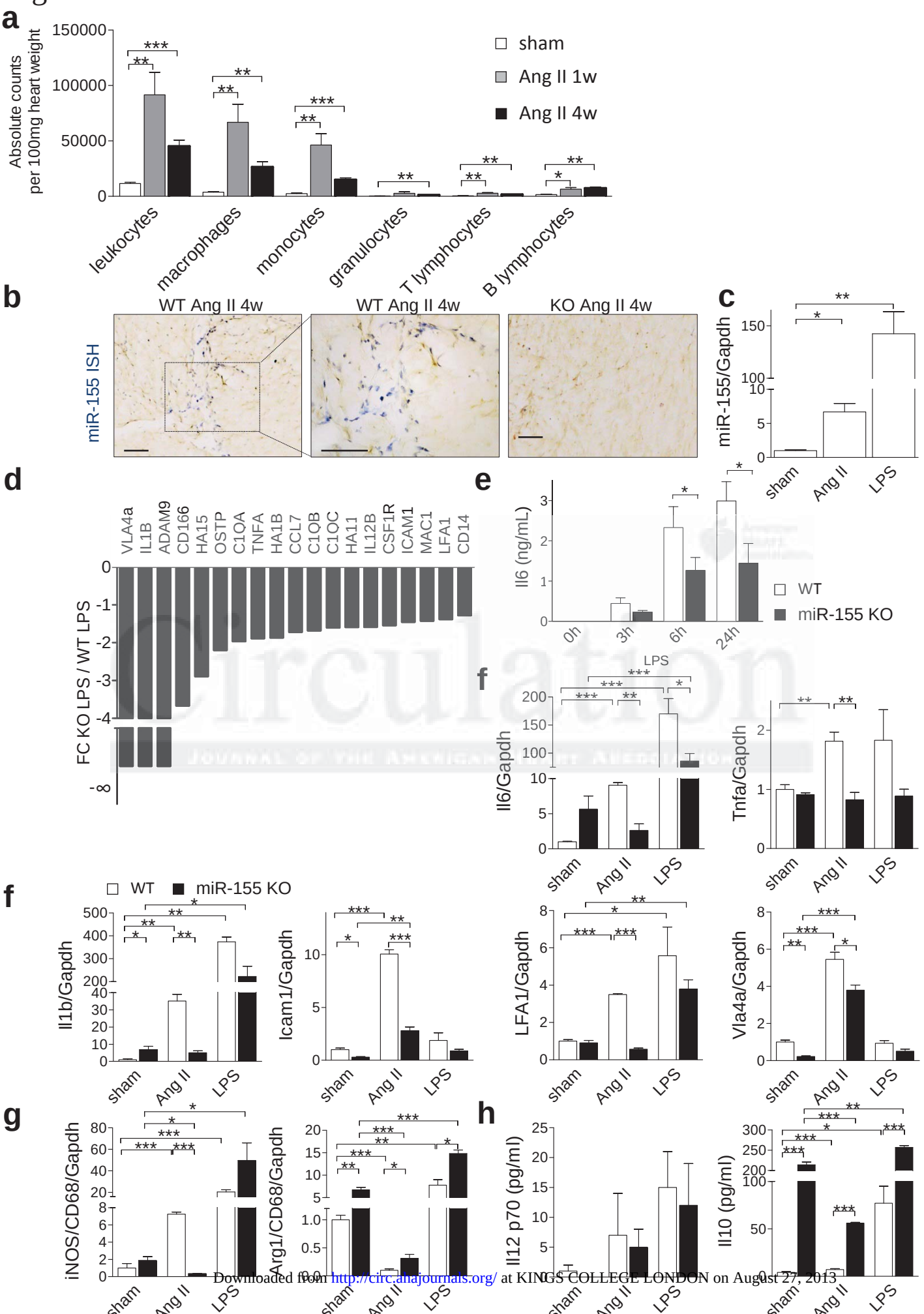

Figure 2

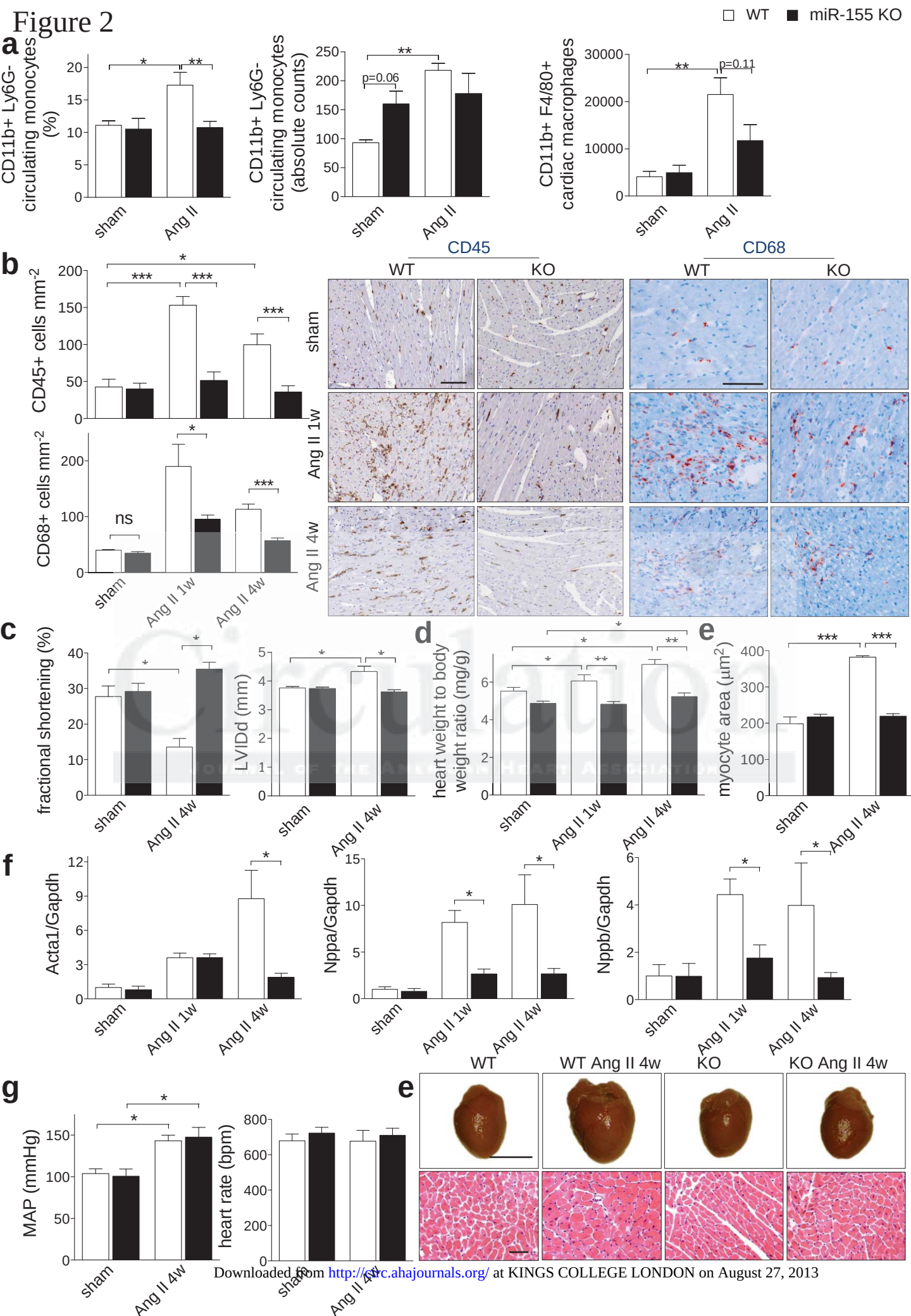

Figure 3

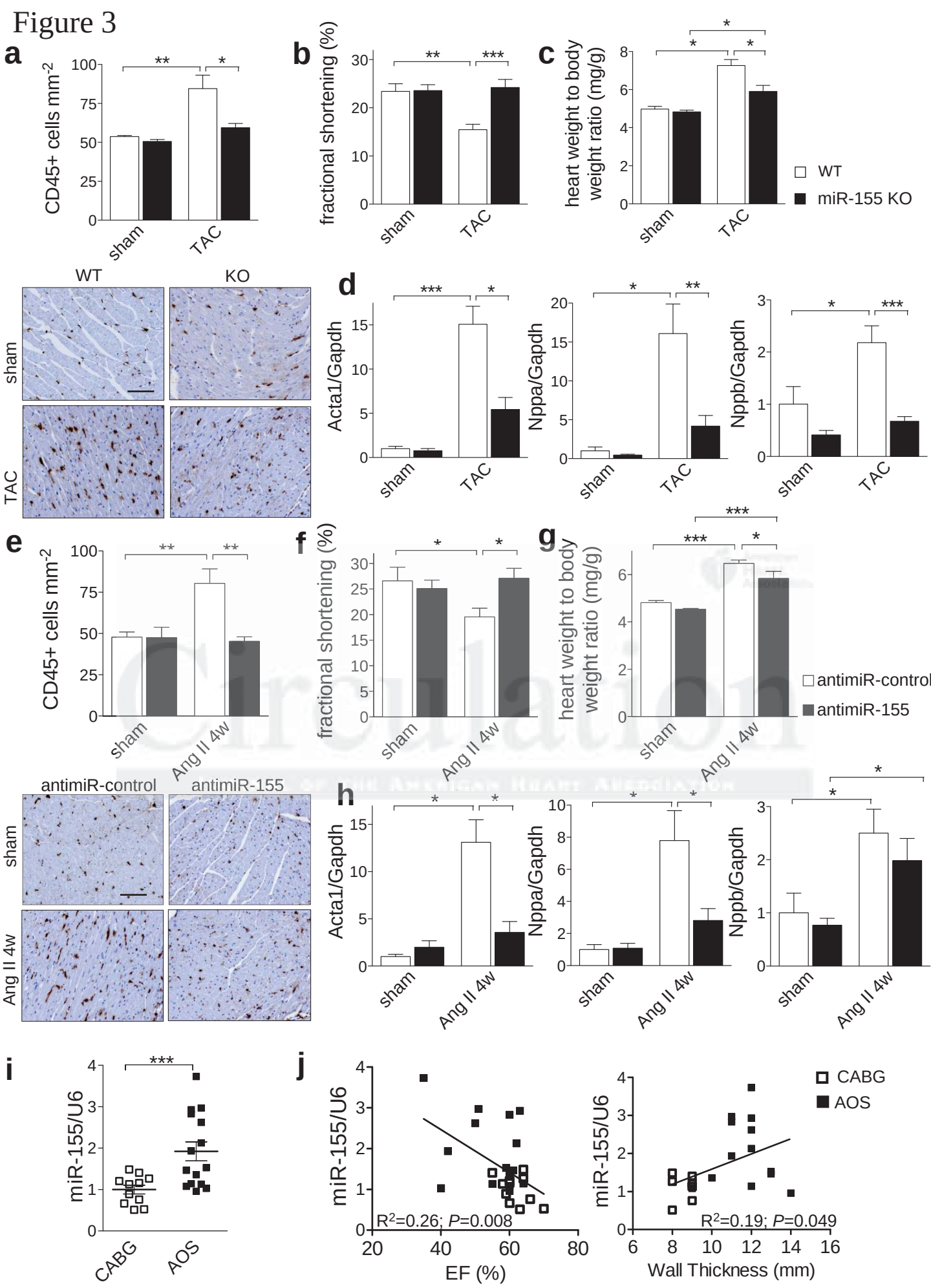

Figure 4

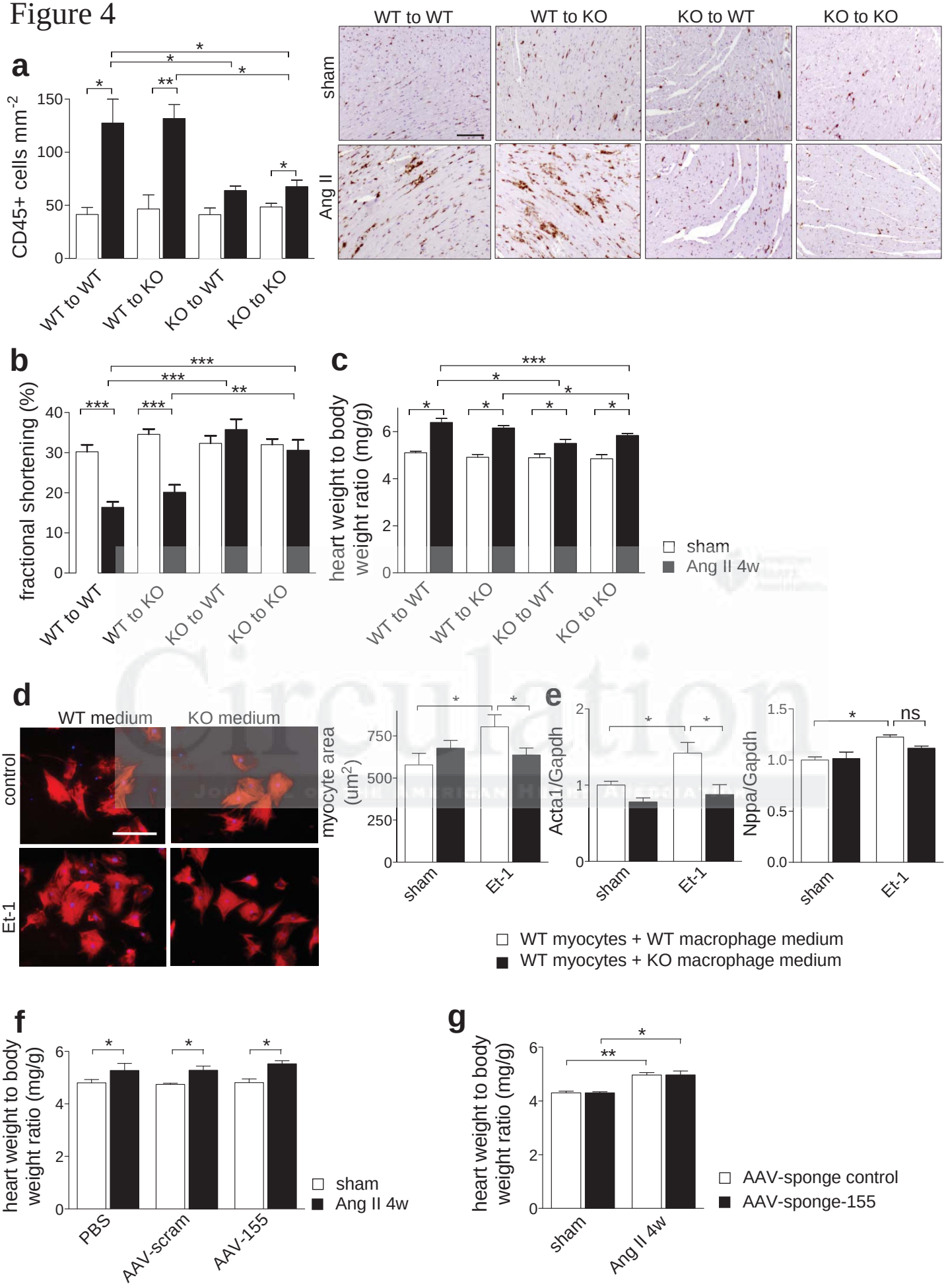

Figure 5

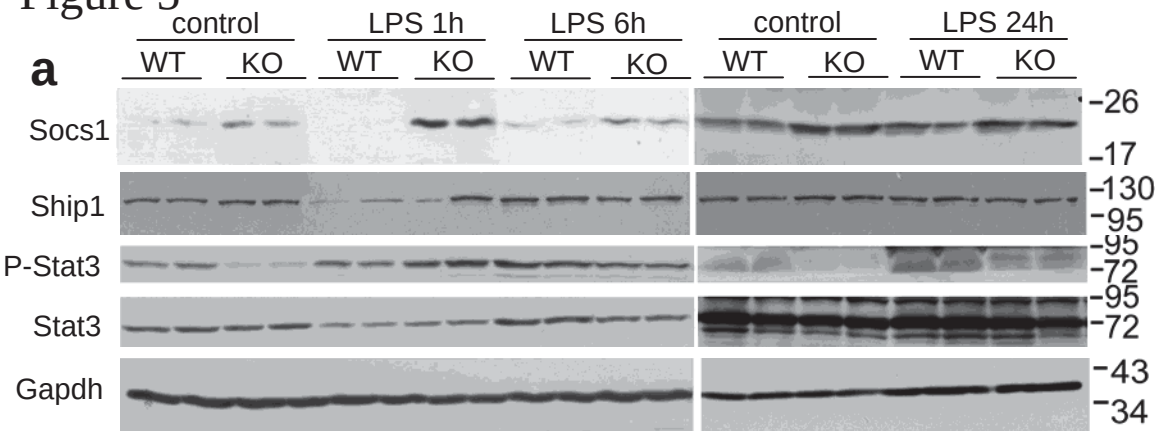

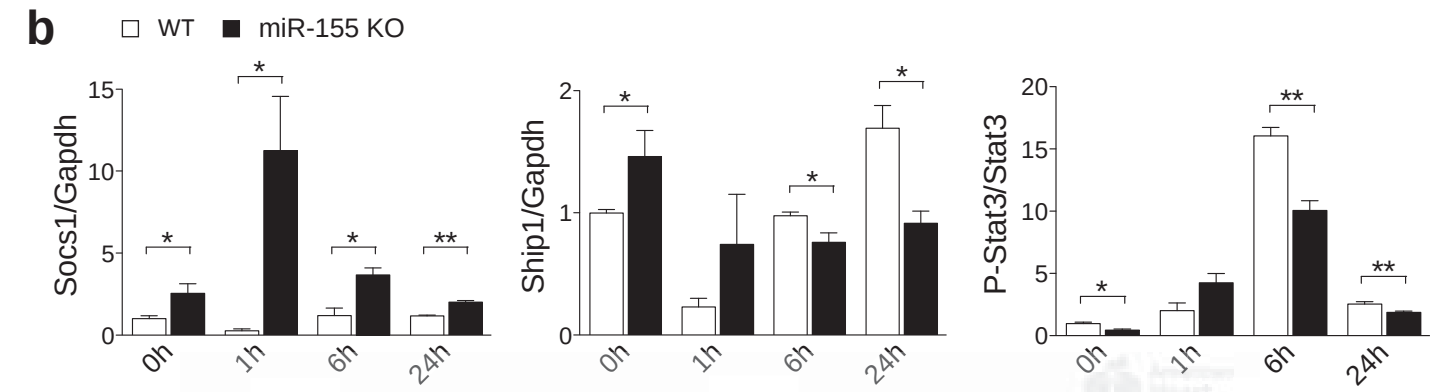

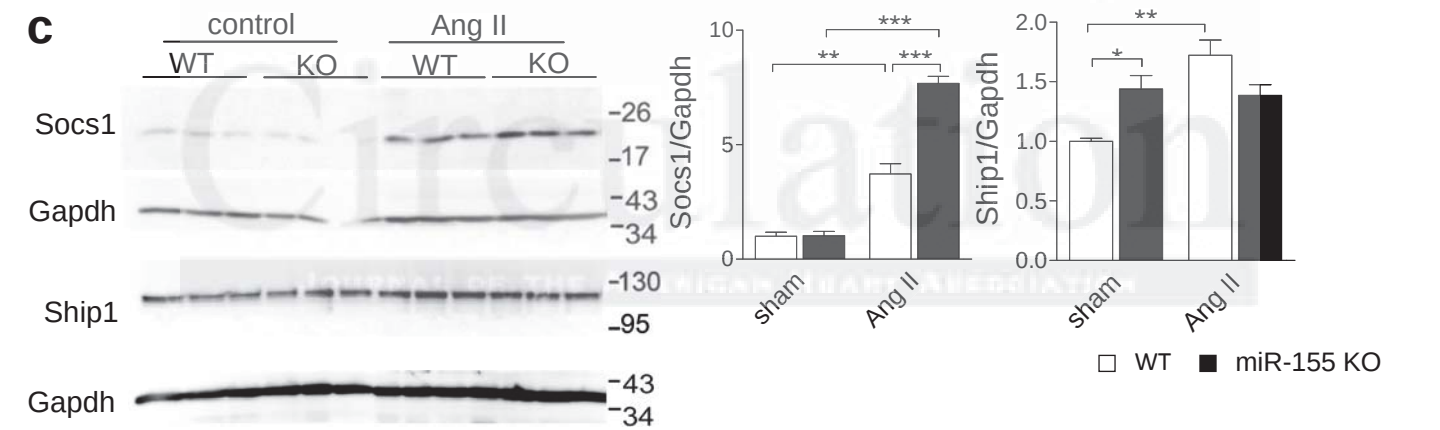

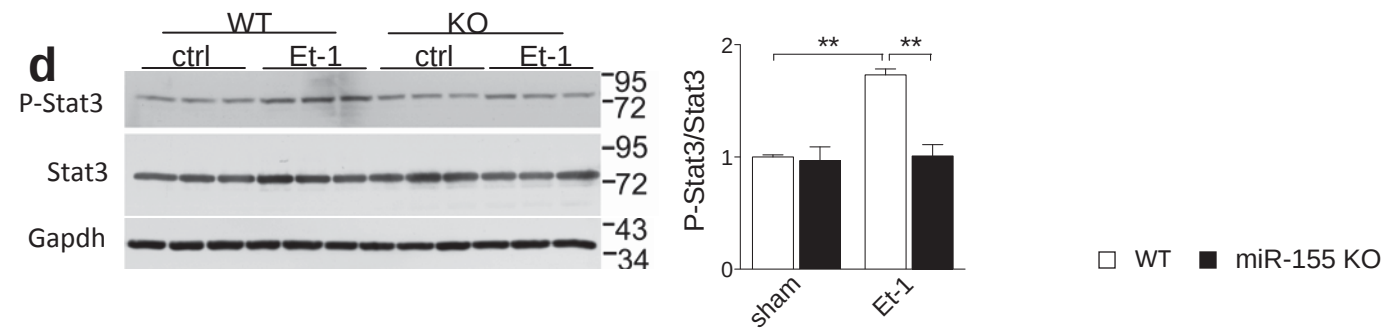

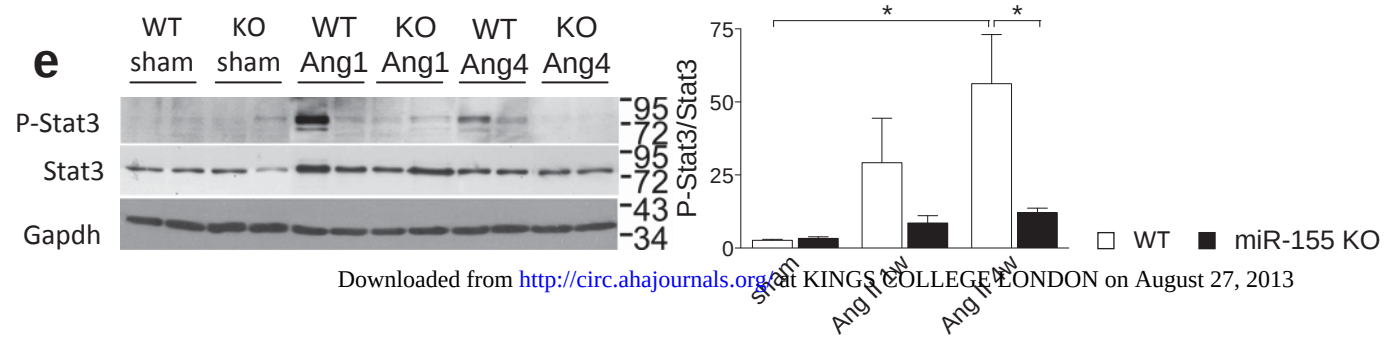

Figure 6

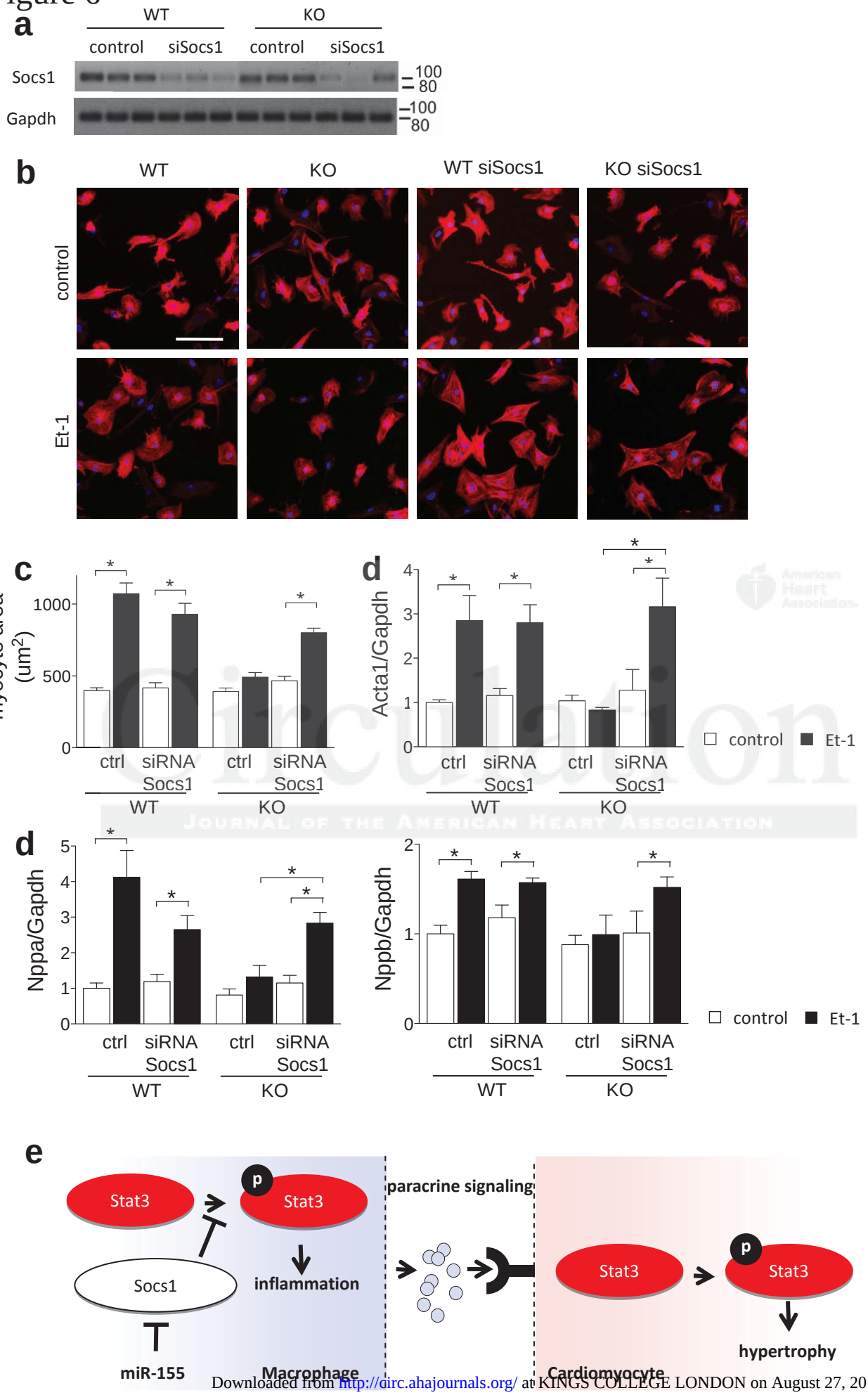

SUPPLEMENTAL MATERIAL

Supplemental Methods

Mice

Male *miR-155* KO and WT C57Bl/6J mice (10-12 weeks-old)[1] were subcutaneously infused with Angiotensin II (AngII, 2.5 µg/g/day; Bachem, Switserland) by Alzet osmotic minipump 2004 (Cupertino, CA) for 7 and 28 days. Echocardiography was performed with the Vevo770 (Visualsonics, Toronto, Canada) and probe RMV707B (15-45 MHz) at days 0 and 28 under light isoflurane anesthesia (mean 1% in oxygen). At day 21, blood pressure was monitored with tail cuff (CODA, Kent Scientific, Torrington, CT). At day 7 or 28, mice were sacrificed and blood and/or hearts were taken for flow cytometry and histological and molecular analyses. Total RNA was isolated with RNeasy mini kit (Qiagen, Valencia, CA) and SYBR Green quantitative PCR was performed on a Bio-Rad iCycler (Hercules, CA) to determine *Acta1*, *Nppa*, *Nppb* and *Gapdh* levels (primers in **Table S4**). Cardiac protein extracts (50µg) were immunoblotted with antibodies to Agtr1 (Abcam, Cambridge, UK), Stat3 (C-20 Santa Cruz Biotechnology, Santa Cruz, CA), P-Stat3 (Tyr705, Cell Signaling Technology, Danvers, MA) and Gapdh (Fitzgerald, Acton, MA). At day 7, peripheral blood was taken for flow cytometry analysis as described[2].

Transverse aortic constriction or sham surgery was performed in 2-month-old male *miR-155* WT and KO mice by subjecting the aorta to a defined 27-gauge constriction between the first and second truncus of the aortic arch, as described previously[3, 4]. Echocardiography was performed as above and Doppler was used to calculate the pressure gradient between the proximal and distal sites of the transverse aortic constriction; only mice with a pressure gradient >50 mm Hg were included.

Bone marrow transplantations were performed on 8 weeks-old male *miR-155* KO and WT mice as described[5]. After 8 weeks, mice were treated with AngII for 28 days as described above.

Eight weeks-old male WT C57Bl/6J mice were tail vein-injected on 3 consecutive days with a total of 10mg/kg LNA-modified antimiR-155 or control antimiR (Ribotask, Denmark). On the last day of injection, AngII administration started as described above. Total RNA was isolated from hearts with the miRVana microRNA isolation kit (Ambion, Austin, TX) and the miScript PCR system (Qiagen) was used with highly specific LNA-modified primers to determine *miR-155* expression.

Eight weeks-old male WT C57Bl/6J mice were tail vein-injected with $2.5x10^{11}$ viral genome particles of AAV9 in 100µl PBS. AAV9-pre-hsa-miR-155 and -scrambled vectors, and AAV9-sponge-miR-155 and sponge-control vectors were produced at high-titer as described[6, 7]. The AAV9-sponge-miR-155 vector contained 4 imperfect binding sites (in bold) for mmu-miR-155 (acccctatcac**gtca**agcattaa), while the AAV9-sponge-control vector contained 3 mutated binding sites (in bold) for miR-122 (acaaacaccattgtca**g**a**t**tc**g**a). Rescue efficiency of the sponge-miR-155 construct was determined by co-transfection of HEK293T cells with 1) sponge-miR-155 or sponge-control vector, 2) psiCheck2 luciferase vector (Promega) containing the sponge's imperfect *miR-155* target sequence in the Renilla luciferase 3'UTR, and 3) either mmu-pre-miR-155 in pCDM vector (System Biosciences, Mountain View, CA) or pBluescriptII control vector (Stratagene, Santa Clara, CA). *In vivo* AAV9-mediated gene transfer and CMV-driven expression of pre-*miR-155*, scrambled, sponge-miR-155 and sponge-control was allowed for 3 weeks. Then, mice were treated with AngII as described above.

All animal experiments were approved by the Committees for Animal Welfare of Maastricht and Leuven Universities, and performed adhering to Dutch and Belgian law.

Histology

Paraffin-embedded 4µm left ventricular sections were stained with hematoxylin-eosin (HE) and Picro Sirious red (SR) as described before[8], or with monoclonal rat anti-mouse CD45 Leukocyte Common Antigen Ly-5 (BD-Biosciences Pharmingen, San Diego, CA) and monoclonal mouse anti-human desmin (Dako Cytomation, Denmark) using HRP/DAB. Left ventricular cryo-sections of 7µm were stained using AP/Fast Red with polyclonal rat anti-mouse antibodies against CD68, CD3 and Nimp1 as described[5]. Morphometric analyses were performed using a microscope (Leica DM2000; Leica, Wetzlar, Germany), camera (Leica DFC295 3Mpix CMOS color), and LAS Image Analysis and QWin morphometry software (Leica).

In situ hybridization was preformed as described[9, 10]. In brief, 12µm cryo-sections were prepared from 4% paraformaldehyde-fixed hearts, air-dried for 30', incubated in 1.3mg/ml Pepsin/0.1mM HCl solution for 20', and incubated overnight at 37ºC in 1x hybridization buffer (ENZO Life sciences, Farmingdale, NY) with 40nM mmu-*miR-155* double DIG-labeled probe (Exiqon, Vedbaek, Denmark). DIG signal from anti-DIG-AP (Roche, Basel, Switzerland) was detected with NBT/BCIP tablets (Roche) for 4hrs at 30ºC in darkness.

Cardiac fractionation and flow cytometry

Animals were euthanized and the whole heart was flushed and placed in PBS for isolation of the immune cell fraction as described before[11]. Peripheral blood and the cardiac immune cell fraction were analyzed using FACS CantoII flow cytometer (Becton Dickenson (BD), San Diego, CA). Erythrocytes were removed by hypotonic lysis with NH_4Cl. Cells were first incubated with anti-CD16/32 (eBioscience, San Diego, CA) to block Fc receptor binding. CD45+ leukocytes subpopulations were defined as follows: T lymphocytes (CD3+), Regulatory T lymphocytes, (CD3+, CD4+, CD25+, Foxp3+), B lymphocytes (B220+), Granulocytes (CD11b+ Ly6G+), Monocytes (CD11b+ F4/80-), Pro-inflammatory monocytes (CD11b+, F4/80-, Ly6C+), Macrophages (CD11b+, F4/80+), with the following antibodies; CD45 (Biolegend clone 30-F11), F4/80 (Biolegend, clone BM8), CD3 (eBioscience, clone 145-C11), CD45R/B220 (eBioscience, clone RA3-6B2), Ly6G (BD, clone 1A8), CD11b (BD, clone M1/70), Ly6C (Miltenyi, 1G7.G10), CD4 (BD, clone RM4-5), CD8 (BD, clone 53-6.7), CD25 (eBiosciencs, clone PC61.5), FoxP3 (eBiosciences, clone FJK-16s) and NK1.1PerCp (BD). Absolute counts for cardiac and blood samples were determined with BD Trucount™ tubes according to the manufacturers instructions and normalized for weight of tissue.

In vitro experiments

Rat ventricular cardiomyocytes (RCMs) were isolated and cultured in 6 well plates as described[12]. Per well, $5*10^5$ RCMs were grown on low serum media and transfected with 35nM *miR-155* antagomiR or scrambled control (Ambion). After 24 hours, cells were treated with 100nM Et-1 (Sigma, St. Louis, MO) or sham for 24 hours, after which RNA was isolated with miRVana (Ambion) and quantitative PCR was performed as described above.

BMMs were obtained and cultured from *miR-155* KO and WT mice as described[13, 14]. Cells were stimulated with 10ng/ml LPS (from *E. coli* 055.B5; Sigma) for 0, 1, 6 and 24 hours, or transfected with siSocs1 or siControl (Ambion) by electroporation as described[15]. Alternatively, cells were stimulated during their differentiation to macrophages with 1μM AngII (Bachem) on days 3, 6, 7 and 8 after isolation, plated in 6-wells plates on day 8 and harvested on day 9. Media were stored after residual cell removal by centrifugation. BMMs were harvested for protein extraction or RNA isolation with miRVana RNA isolation kit. *Socs1* knockdown was assessed by RT-PCR, with *Gapdh* as a loading control (primers in **Table S4**). BMM proteins were blotted for Socs1

and Ship1 (both from Cell Signaling Technology). Media were subjected to Il6 ELISA (kindly provided by Dr. Frank Stassen), and to Multi-array electrochemiluminescence platform of MesoScaleDiscovery (K15012A-5, detection range 2.4 pg/ml to 10 000 pg/ml from MesoScaleDiscovery, Gaithersburg, MD, USA, www.mesoscale.com) as described before.

KO and WT BMM-conditioned media were dialyzed in low serum RCM media using slide-a-lyzer dialysis cassettes (1/100, 3.5kDa, Thermo Fisher Scientific, Waltham, MA). RCMs were incubated with dialyzed conditioned media for 24 hours, treated with Et-1 or PBS for 24 hours, and either stained with rhodamin-phalloidin (Molecular probes, Invitrogen, Paisley, UK) or processed for RNA extraction (RNeasy) and qPCR as described above.

Proteomics

BMM media were subjected to mass spectroscopic proteomics analyses as described[16]. Then, the MS/MS data were matched to SwissProt mouse database (version 57.15, 16230 protein entries) using Mascot version 2.3.0 (Proteome Discoverer 1.1, Thermo Scientific). Carboxyamidomethylation of cysteine was used as a fixed modification, and oxidation of methionine was used as a variable modification. The mass tolerance was set at 10 ppm for the precursor ions and 0.8 Da for fragment ions. Two missed cleavage were allowed. Search results were loaded into Scaffold software (version 3.0.8, Proteome Software). Assignments were accepted with >99.0% protein probability, >95.0% peptide probability, and a minimum of two peptides.

Human subjects

Cardiac biopsies were taken from AOS (n=15) and CABG (n=11) patients during valve replacement and bypass surgery, respectively (**Table S5**). Expression levels of mature *miR-155* and of *U6* were determined by qRT-PCR as described above. All human material was obtained for research purposes in accordance with the Declaration of Helsinki and the ethical committee at Maastricht University Medical Center.

Statistical analyses

Data are presented as average +/- SEM. Comparisons between 2 groups were performed with two-tailed Student's t testing for Gaussian data or Mann-Whitney tests for non-Gaussian data. For comparisons of more than 2 groups, one-way ANOVA was

used, followed by post hoc testing using Bonferroni correction for more groups. $P<0.05$ was considered statistically significant.

Supplemental Tables

Table S1. Secretome of miR-155 WT and KO bone marrow-derived macrophages

Protein Name	Uniprot ID	Secretome	KO LPS / WT LPS P-value	FC	KO / WT P-value	FC	WT / WT LPS P-value	FC	KO / KO LPS p-value	FC	avg spectral count WT	KO	WT LPS	KO LPS
Disintegrin and metalloproteinase domain-containing protein 9	**ADAM9_MOUSE**	**YES**	**8,90E-07**	**NA**	**3,70E-01**	**NA**	**6,40E-02**	**3,00**	**1,00E+00**	**NA**	**2**	**0**	**6**	**0**
N-acetyl-D-glucosamine kinase	NAGK_MOUSE	NO	3,80E-06	0,00	3,60E-01	0,74	5,80E-02	0,00	9,30E-03	0,47	5	6	0	3
Dihydropyrimidinase-related protein 2	DPYL2_MOUSE	NO	3,60E-05	0,38	3,80E-01	1,19	2,70E-03	0,18	1,30E-05	0,57	83	70	15	40
Heme-binding protein 1	HEBP1_MOUSE	NO	1,30E-04	0,00	1,40E-01	0,00	1,00E+00	NA	5,50E-01	1,25	0	3	0	3
Complement C1q subcomponent subunit C	**C1QC_MOUSE**	**YES**	**2,10E-04**	**1,60**	**6,50E-01**	**1,10**	**1,50E-05**	**2,16**	**1,50E-02**	**1,48**	**43**	**39**	**92**	**57**
EH domain-containing protein 1	EHD1_MOUSE	YES	2,90E-04	0,30	8,00E-01	0,85	9,60E-01	0,82	4,30E-02	2,31	7	9	6	20
Ubiquitin-conjugating enzyme E2 D2	UB2D2_MOUSE	NO	3,00E-04	0,00	8,30E-01	1,30	1,40E-01	0,00	3,10E-01	1,70	4	3	0	6
Abhydrolase domain-containing protein 14B	ABHEB_MOUSE	NO	4,60E-04	0,00	2,10E-02	7,00	5,70E-03	0,00	6,90E-03	6,50	5	1	0	4
Neutral alpha-glucosidase AB	GANAB_MOUSE	NO	4,70E-04	7,88	5,40E-01	0,50	6,90E-04	10,50	7,20E-01	0,67	2	4	21	3
Interleukin-1 beta	**IL1B_MOUSE**	**YES**	**5,40E-04**	**NA**	**1,00E+00**	**NA**	**5,40E-04**	**NA**	**1,00E+00**	**NA**	**0**	**0**	**4**	**0**
Protein FAM3C	FAM3C_MOUSE	YES	9,10E-04	2,41	1,00E+00	NA	3,50E-05	NA	1,90E-03	NA	0	0	14	6
Alpha-N-acetylgalactosaminidase	NAGAB_MOUSE	NO	1,00E-03	0,00	2,30E-01	2,33	2,30E-02	0,00	3,00E-01	1,67	5	2	0	3
Keratin, type I cytoskeletal 10	K1C10_MOUSE	NO	1,40E-03	NA	1,00E+00	NA	1,40E-03	NA	1,00E+00	NA	0	0	4	0
LIM and SH3 domain protein 1	LASP1_MOUSE	YES	1,80E-03	0,00	7,80E-01	1,00	3,60E-03	0,00	5,30E-02	0,57	10	10	0	6
ADP-ribosylation factor 6	ARF6_MOUSE	YES	1,90E-03	0,00	1,00E+00	NA	1,00E+00	NA	1,90E-03	NA	0	0	0	5
Importin subunit beta-1	IMB1_MOUSE	NO	1,90E-03	0,56	6,90E-02	0,65	2,50E-02	0,42	1,40E-02	0,48	18	27	7	13
Tyrosine-protein phosphatase non-receptor type 6	PTN6_MOUSE	YES	2,00E-03	0,38	4,40E-02	1,39	2,20E-04	0,16	9,60E-03	0,57	41	29	6	17
H-2 class I histocompatibility antigen, K-B alpha chain	**HA1B_MOUSE**	**YES**	**2,20E-03**	**1,70**	**4,50E-01**	**1,19**	**2,50E-07**	**10,43**	**2,10E-03**	**7,32**	**12**	**10**	**129**	**76**
Tubulin beta-2C chain	TBB2C_MOUSE	NO	2,20E-03	0,00	9,20E-02	1,19	6,20E-05	0,00	4,50E-01	0,34	23	19	0	7
Coatomer subunit zeta-1	COPZ1_MOUSE	NO	2,30E-03	0,00	6,30E-01	0,95	6,70E-04	0,00	2,40E-01	0,68	6	6	0	4
V-type proton ATPase catalytic subunit A	VATA_MOUSE	YES	2,40E-03	0,24	6,30E-01	1,13	9,10E-03	0,32	2,80E-02	1,51	15	13	5	20
cAMP-dependent protein kinase type I-alpha regulatory subunit	KAP0_MOUSE	NO	2,60E-03	0,00	8,10E-01	0,80	2,00E-01	0,00	7,50E-01	1,10	3	3	0	4
Collagenase 3	MMP13_MOUSE	NO	2,60E-03	2,00	1,00E+00	NA	1,90E-07	NA	4,60E-03	NA	0	0	103	52
Clathrin light chain A	CLCA_MOUSE	YES	2,70E-03	0,00	3,30E-01	0,50	3,70E-01	0,00	9,20E-01	1,00	2	4	0	4
Intercellular adhesion molecule 1	**ICAM1_MOUSE**	**YES**	**2,70E-03**	**1,46**	**1,00E+00**	**NA**	**1,20E-05**	**NA**	**1,30E-04**	**NA**	**0**	**0**	**28**	**19**
Sequestosome-1	SQSTM_MOUSE	NO	2,80E-03	0,05	1,00E+00	NA	3,70E-01	NA	1,50E-03	NA	0	0	1	19
Complement C1q subcomponent subunit B	**C1QB_MOUSE**	**YES**	**3,30E-03**	**1,68**	**2,40E-01**	**1,72**	**8,30E-04**	**3,55**	**1,50E-03**	**3,64**	**21**	**12**	**73**	**44**
Omega-amidase NIT2	NIT2_MOUSE	NO	3,30E-03	0,00	9,00E-01	1,00	2,80E-03	0,00	4,90E-01	1,17	4	4	0	5
GTP-binding nuclear protein Ran	RAN_MOUSE	NO	3,30E-03	0,48	7,70E-01	1,03	3,80E-04	0,31	2,50E-03	0,67	23	22	7	15
Acidic leucine-rich nuclear phosphoprotein 32 family member A	AN32A_MOUSE	NO	3,90E-03	0,07	1,00E+00	NA	3,70E-01	NA	1,50E-03	NA	0	0	1	9
N(4)-(beta-N-acetylglucosaminyl)-L-asparaginase	ASPG_MOUSE	NO	4,10E-03	1,47	7,70E-01	1,63	2,00E-01	2,15	7,10E-02	2,38	4	3	9	6
Protein disulfide-isomerase A3	PDIA3_MOUSE	NO	4,30E-03	1,58	7,40E-01	0,99	3,70E-01	0,95	8,50E-02	0,60	63	64	60	38
Agrin	AGRIN_MOUSE	YES	5,30E-03	NA	1,00E+00	NA	5,30E-03	NA	1,00E+00	NA	0	0	7	0
Integrin beta-2	**ITB2_MOUSE**	**YES**	**5,30E-03**	**1,38**	**4,10E-01**	**1,14**	**3,20E-05**	**3,44**	**1,40E-03**	**2,83**	**41**	**36**	**141**	**102**
Chloride intracellular channel protein 1	CLIC1_MOUSE	YES	5,50E-03	0,56	3,60E-01	0,89	2,90E-02	0,46	8,70E-02	0,74	37	41	17	30
Integrin alpha-M	**ITAM_MOUSE**	**YES**	**5,60E-03**	**1,42**	**1,40E-01**	**1,57**	**3,30E-05**	**4,17**	**1,60E-03**	**4,59**	**42**	**27**	**177**	**124**
Interferon-alpha/beta receptor beta chain	INAR2_MOUSE	YES	5,70E-03	0,00	5,10E-01	0,63	1,30E-01	0,00	1,80E-01	2,00	3	5	0	11
Carbonyl reductase [NADPH] 1	CBR1_MOUSE	NO	5,80E-03	0,13	7,30E-01	1,16	4,40E-02	0,18	8,30E-02	1,58	7	6	1	10
T-complex protein 1 subunit eta	TCPH_MOUSE	NO	6,50E-03	0,00	4,90E-01	1,25	4,50E-03	0,00	4,00E-01	0,75	8	7	0	5
Alpha-1,6-mannosylglycoprotein 6-beta-N-acetylglucosaminyltransferase A	MGT5A_MOUSE	NO	6,80E-03	5,67	3,70E-01	2,75	1,80E-01	1,55	8,60E-01	0,75	4	1	6	1
Heterogeneous nuclear ribonucleoprotein A3	ROA3_MOUSE	NO	6,90E-03	0,08	8,70E-01	1,07	1,20E-02	0,10	3,20E-01	1,41	10	9	1	13
Peroxiredoxin-1	PRDX1_MOUSE	NO	7,10E-03	0,69	1,80E-01	0,96	1,60E-01	0,89	2,10E-02	1,24	210	218	187	271
ATP-citrate synthase	ACLY_MOUSE	NO	7,40E-03	2,00	4,40E-01	0,83	6,70E-01	0,74	8,60E-03	0,31	12	14	9	4
Complement C1q subcomponent subunit A	**C1QA_MOUSE**	**YES**	**7,40E-03**	**1,96**	**9,80E-01**	**1,00**	**3,40E-03**	**3,98**	**7,00E-02**	**2,02**	**14**	**14**	**56**	**28**
Ubiquitin-like modifier-activating enzyme 1	UBA1_MOUSE	NO	7,80E-03	0,43	3,90E-01	1,16	3,00E-04	0,25	5,80E-02	0,66	84	73	21	48
N-acetylgalactosaminyltransferase 7	GALT7_MOUSE	NO	7,90E-03	NA	1,00E+00	NA	7,90E-03	NA	1,00E+00	NA	0	0	7	0
Farnesyl pyrophosphate synthetase	FPPS_MOUSE	NO	8,10E-03	0,70	8,80E-01	1,10	7,60E-02	0,53	2,00E-01	0,83	19	17	10	14
Cytosolic acyl coenzyme A thioester hydrolase	BACH_MOUSE	NO	8,80E-03	0,00	3,40E-01	2,33	2,40E-02	0,00	9,00E-01	1,07	12	5	0	5
Ras-related protein Rap-1b	RAP1B_MOUSE	YES	9,40E-03	0,23	8,30E-01	1,00	6,40E-02	0,37	3,80E-02	1,58	6	6	2	10
Endoplasmin	ENPL_MOUSE	YES	9,80E-03	2,36	8,40E-01	1,07	4,50E-03	3,03	3,30E-03	1,37	21	20	64	27
Growth arrest-specific protein 6	GAS6_MOUSE	YES	1,00E-02	2,53	1,40E-01	0,72	4,20E-04	5,85	2,70E-01	1,67	4	6	25	10
Xanthine dehydrogenase/oxidase	XDH_MOUSE	YES	1,00E-02	0,00	4,10E-01	0,83	2,90E-02	0,00	1,70E-04	0,17	13	15	0	3
T-complex protein 1 subunit alpha B	TCPA2_MOUSE	NO	1,10E-02	0,07	7,70E-01	1,14	5,60E-03	0,03	1,80E-01	0,47	22	19	1	9
Vacuolar protein sorting-associated protein 29	VPS29_MOUSE	NO	1,10E-02	1,27	3,20E-01	1,33	3,30E-01	1,00	6,70E-01	1,05	9	7	9	7
H-2 class I histocompatibility antigen, D-B alpha chain	**HA11_MOUSE**	**YES**	**1,20E-02**	**1,45**	**2,30E-01**	**1,91**	**2,90E-05**	**5,57**	**2,80E-03**	**7,34**	**22**	**12**	**124**	**86**
Creatine kinase B-type	KCRB_MOUSE	NO	1,20E-02	0,61	5,10E-01	1,25	7,00E-02	0,38	3,50E-02	0,77	75	60	28	46
Serine/threonine-protein phosphatase 2A catalytic subunit alpha isoform	PP2AA_MOUSE	YES	1,20E-02	0,16	7,70E-01	1,13	1,40E-01	0,28	2,20E-02	2,00	6	5	2	11
Transketolase	TKT_MOUSE	NO	1,20E-02	0,65	3,70E-01	0,96	8,90E-04	0,33	1,80E-03	0,49	164	171	54	83
Twinfilin-2	TWF2_MOUSE	NO	1,20E-02	2,45	2,00E-01	1,54	2,40E-01	0,68	1,30E-01	0,42	13	9	9	4
Filamin-A	FLNA_MOUSE	YES	1,30E-02	0,64	2,90E-01	0,92	6,20E-03	0,46	1,20E-02	0,66	329	357	151	236
Hypoxanthine-guanine phosphoribosyltransferase	HPRT_MOUSE	NO	1,30E-02	1,90	7,90E-01	1,11	3,30E-01	0,68	5,70E-02	0,40	20	18	13	7
Tumor necrosis factor	**TNFA_MOUSE**	**YES**	**1,30E-02**	**1,89**	**1,00E+00**	**NA**	**9,00E-04**	**NA**	**4,10E-04**	**NA**	**0**	**0**	**102**	**54**
Coagulation factor XIII A chain	F13A_MOUSE	YES	1,40E-02	1,95	1,60E-01	1,59	3,90E-01	1,04	2,60E-01	0,85	24	15	25	13
Platelet-activating factor acetylhydrolase IB subunit gamma	PA1B3_MOUSE	NO	1,40E-02	0,17	1,00E+00	NA	3,70E-01	NA	3,80E-06	NA	0	0	1	6
Fibronectin	FINC_MOUSE	YES	1,50E-02	3,90	1,00E+00	NA	1,20E-03	NA	1,90E-01	NA	0	0	13	3
Heterogeneous nuclear ribonucleoprotein L	HNRPL_MOUSE	NO	1,50E-02	0,00	6,00E-01	1,13	8,30E-04	0,00	8,20E-02	0,58	14	13	0	7
Macrophage-expressed gene 1 protein	MPEG1_MOUSE	NO	1,50E-02	8,00	1,00E+00	NA	5,60E-03	NA	3,70E-01	NA	0	0	5	1
Neuropilin-2	NRP2_MOUSE	YES	1,70E-02	1,98	3,70E-01	NA	7,40E-04	28,75	7,80E-03	NA	1	0	38	19
Plasminogen activator inhibitor 1	PAI1_MOUSE	YES	1,70E-02	2,58	1,00E+00	NA	2,90E-03	NA	2,70E-03	NA	0	0	10	4
Serglycin	SRGN_MOUSE	YES	1,70E-02	2,41	1,00E+00	NA	2,30E-03	NA	5,30E-03	NA	0	0	14	6
Vimentin	VIME_MOUSE	NO	1,70E-02	0,62	7,90E-01	1,02	5,20E-03	0,34	7,10E-03	0,55	327	322	110	178
Elongation factor 2	EF2_MOUSE	NO	1,80E-02	0,64	7,50E-02	0,89	1,30E-03	0,49	1,20E-02	0,68	129	144	63	99
Tropomyosin alpha-4 chain	TPM4_MOUSE	NO	1,80E-02	0,51	1,90E-01	0,83	1,20E-02	0,46	1,60E-01	0,74	30	36	14	27
Ubiquitin carboxyl-terminal hydrolase isozyme L3	UCHL3_MOUSE	NO	1,80E-02	0,13	3,20E-01	0,78	3,30E-02	0,17	9,60E-01	1,00	6	8	1	8
Chloride intracellular channel protein 4	CLIC4_MOUSE	NO	1,90E-02	0,52	6,00E-01	1,11	5,60E-01	0,76	9,40E-03	1,63	14	13	11	21
Palmitoyl-protein thioesterase 1	PPT1_MOUSE	YES	1,90E-02	1,50	2,60E-01	1,88	2,10E-03	2,60	2,00E-02	3,25	5	3	13	9
Protein-glutamine gamma-glutamyltransferase 2	TGM2_MOUSE	YES	1,90E-02	0,35	6,10E-02	1,25	9,00E-03	0,34	2,10E-01	1,20	32	25	11	30
Vasodilator-stimulated phosphoprotein	VASP_MOUSE	YES	1,90E-02	0,45	5,20E-01	1,52	5,50E-01	0,71	8,20E-02	2,39	12	8	8	18
6-phosphogluconate dehydrogenase, decarboxylating	6PGD_MOUSE	NO	2,00E-02	0,74	9,70E-01	1,05	2,00E-03	0,34	2,50E-03	0,49	105	100	36	49
Low-density lipoprotein receptor	LDLR_MOUSE	YES	2,00E-02	3,17	1,00E+00	NA	1,00E-03	NA	1,20E-01	NA	0	0	6	2
Prolow-density lipoprotein receptor-related protein 1	LRP1_MOUSE	YES	2,00E-02	1,53	6,60E-01	0,88	2,30E-03	3,04	6,80E-02	1,75	50	56	151	99
Heterogeneous nuclear ribonucleoprotein A/B	ROAA_MOUSE	NO	2,00E-02	0,26	9,70E-01	1,06	3,70E-03	0,15	4,50E-02	0,63	22	21	3	13
F-actin-capping protein subunit alpha-1	CAZA1_MOUSE	NO	2,10E-02	0,55	6,20E-01	1,01	6,20E-04	0,45	2,60E-01	0,84	29	29	13	24
Ran-specific GTPase-activating protein	RANG_MOUSE	NO	2,10E-02	0,23	5,40E-01	0,87	2,60E-02	0,25	8,70E-01	0,96	7	8	2	7
Phosphoglycerate mutase 1	PGAM1_MOUSE	NO	2,20E-02	0,62	5,20E-01	0,94	2,60E-01	0,65	9,90E-01	0,99	70	75	46	74
Prolyl endopeptidase	PPCE_MOUSE	NO	2,20E-02	0,15	2,60E-01	0,66	1,30E-01	0,15	1,10E-01	0,63	9	14	1	9
Alpha-enolase	ENOA_MOUSE	YES	2,30E-02	0,56	5,70E-01	1,02	4,50E-04	0,45	1,10E-01	0,81	244	239	109	193
H-2 class I histocompatibility antigen, D-37 alpha chain	**HA15_MOUSE**	**YES**	**2,30E-02**	**2,17**	**1,00E+00**	**NA**	**3,50E-03**	**NA**	**1,30E-02**	**NA**	**0**	**0**	**17**	**8**
Cathepsin D	CATD_MOUSE	NO	2,40E-02	1,15	3,90E-01	1,14	7,10E-04	1,16	1,90E-01	1,16	274	239	319	277
Osteopontin	**OSTP_MOUSE**	**YES**	**2,50E-02**	**2,00**	**1,00E+00**	**NA**	**2,80E-03**	**NA**	**7,40E-05**	**NA**	**0**	**0**	**17**	**8**
Serine/threonine-protein kinase PAK 2	PAK2_MOUSE	NO	2,50E-02	0,18	6,80E-02	2,71	5,00E-03	0,11	3,90E-01	1,57	6	2	1	4
Annexin A1	ANXA1_MOUSE	YES	2,60E-02	0,59	4,70E-06	0,10	1,00E-03	5,79	9,20E-01	0,96	9	95	54	91
C-C motif chemokine 7	**CCL7_MOUSE**	**YES**	**2,60E-02**	**1,72**	**1,60E-01**	**NA**	**3,60E-03**	**4,78**	**6,80E-03**	**NA**	**3**	**0**	**14**	**8**
Glyceraldehyde-3-phosphate dehydrogenase	G3P_MOUSE	NO	2,60E-02	0,56	6,40E-01	1,00	4,60E-02	0,62	4,50E-01	1,11	133	133	83	148
Transgelin-2	TAGL2_MOUSE	NO	2,60E-02	0,66	9,90E-01	1,05	4,20E-02	0,58	4,40E-01	0,92	52	50	30	46
Gamma-glutamyl hydrolase	GGH_MOUSE	YES	2,70E-02	1,59	3,10E-01	0,86	1,70E-02	1,53	4,20E-01	0,83	10	12	15	10
Granulins	GRN_MOUSE	YES	2,70E-02	1,28	1,30E-01	1,23	4,70E-01	0,82	2,20E-01	0,79	114	93	94	73
40S ribosomal protein S3	RS3_MOUSE	NO	2,70E-02	0,11	4,90E-01	1,56	9,80E-02	0,21	8,30E-02	3,17	9	6	2	19
Small nuclear ribonucleoprotein Sm D3	SMD3_MOUSE	NO	2,70E-02	0,00	2,40E-01	2,00	7,50E-03	0,00	4,00E-01	1,67	6	3	0	5
Dipeptidyl-peptidase 1	CATC_MOUSE	NO	2,80E-02	1,35	4,00E-03	1,67	6,20E-04	3,41	9,70E-04	4,21	27	16	91	67
Heterogeneous nuclear ribonucleoprotein K	HNRPK_MOUSE	NO	2,80E-02	0,23	4,80E-01	1,42	7,00E-02	0,13	3,60E-01	0,80	26	18	3	15
Proteasome subunit alpha type-6	PSA6_MOUSE	NO	2,80E-02	0,62	1,80E-01	1,51	8,20E-01	0,81	5,10E-03	1,98	21	14	17	27
Glucosylceramidase	GLCM_MOUSE	NO	2,90E-02	1,48	3,70E-01	NA	1,60E-04	15,50	4,30E-03	NA	1	0	21	14
Interferon-induced protein with tetratricopeptide repeats 2	IFIT2_MOUSE	NO	2,90E-02	0,00	1,20E-02	NA	1,20E-02	0,00	2,90E-02	NA	4	0	0	3
Nucleobindin-1	NUCB1_MOUSE	NO	2,90E-02	1,21	3,80E-01	0,92	2,90E-05	1,70	1,10E-01	1,30	64	69	109	90
Vacuolar protein sorting-associated protein 35	VPS35_MOUSE	NO	2,90E-02	0,39	2,10E-02	1,23	3,50E-05	0,19	1,90E-02	0,59	51	42	10	25
Actin, cytoplasmic 1	ACTB_MOUSE	NO	3,00E-02	0,61	1,40E-01	0,94	8,30E-04	0,56	3,00E-01	0,87	452	482	254	417
Interleukin-12 subunit beta	**IL12B_MOUSE**	**YES**	**3,00E-02**	**1,59**	**1,00E+00**	**NA**	**1,20E-05**	**NA**	**9,40E-03**	**NA**	**0**	**0**	**117**	**74**

Mps one binder kinase activator-like 1A	MOL1A_MOUSE	NO	3,00E-02	4,00	7,80E-01	1,15	1,30E-02	0,40	2,50E-02	0,12	10	9	4	1
CD166 antigen	**CD166_MOUSE**	**YES**	**3,10E-02**	**3,67**	**1,00E+00**	**NA**	**7,00E-03**	**NA**	**1,20E-01**	**NA**	**0**	**0**	**7**	**2**
Cytosolic non-specific dipeptidase	CNDP2_MOUSE	NO	3,10E-02	0,47	4,80E-02	0,90	9,70E-05	0,20	5,70E-04	0,38	137	152	27	57
Beta-hexosaminidase subunit beta	HEXB_MOUSE	NO	3,20E-02	1,36	4,70E-01	1,34	7,80E-02	1,40	1,00E-01	1,38	25	19	35	26
Tripeptidyl-peptidase 1	TPP1_MOUSE	NO	3,20E-02	1,26	2,20E-02	1,74	2,10E-01	1,00	2,50E-02	1,39	18	10	18	14
Plastin-3	PLST_MOUSE	NO	3,30E-02	0,67	3,80E-01	0,69	4,60E-03	0,32	1,80E-01	0,33	15	21	5	7
Xylosyltransferase 2	XYLT2_MOUSE	NO	3,30E-02	4,80	1,00E+00	NA	3,40E-03	NA	3,70E-01	NA	0	0	8	2
Annexin A2	ANXA2_MOUSE	YES	3,40E-02	1,35	1,00E+00	NA	1,50E-04	NA	7,80E-04	NA	0	0	19	14
Heme oxygenase 1	HMOX1_MOUSE	NO	3,40E-02	0,48	6,80E-01	1,00	2,90E-01	1,12	5,10E-03	2,32	8	8	9	19
Inorganic pyrophosphatase	IPYR_MOUSE	NO	3,40E-02	0,00	3,70E-01	NA	3,70E-01	0,00	3,40E-02	NA	1	0	0	5
Tropomyosin alpha-3 chain	TPM3_MOUSE	NO	3,40E-02	0,40	4,70E-01	0,88	4,30E-03	0,33	3,00E-01	0,72	48	54	16	39
SUMO-conjugating enzyme UBC9	UBC9_MOUSE	NO	3,40E-02	5,00	1,60E-01	0,69	1,00E+00	0,83	2,20E-03	0,11	8	12	7	1
Annexin A4	ANXA4_MOUSE	NO	3,50E-02	0,00	1,00E+00	NA	1,00E+00	NA	3,50E-02	NA	0	0	0	5
Dipeptidase 2	DPEP2_MOUSE	NO	3,50E-02	1,59	7,40E-01	1,12	7,70E-04	2,54	1,00E-01	1,79	22	19	55	35
EF-hand domain-containing protein D2	EFHD2_MOUSE	NO	3,60E-02	0,67	9,10E-02	0,92	6,90E-01	0,81	2,10E-01	1,10	47	51	38	56
Far upstream element-binding protein 2	FUBP2_MOUSE	NO	3,60E-02	0,11	1,80E-01	1,44	4,70E-03	0,04	2,60E-02	0,49	19	13	1	6
Rho GDP-dissociation inhibitor 2	GDIR2_MOUSE	NO	3,60E-02	0,68	3,70E-01	0,98	7,20E-01	0,81	5,20E-02	1,17	21	21	17	25
Pyruvate kinase isozymes M1/M2	KPYM_MOUSE	NO	3,60E-02	0,57	7,00E-02	0,88	7,30E-04	0,44	3,70E-02	0,69	338	385	150	264
26S proteasome non-ATPase regulatory subunit 3	PSMD3_MOUSE	NO	3,60E-02	0,00	8,40E-01	0,95	7,90E-03	0,00	4,50E-01	0,68	7	7	0	5
Elongation factor 1-alpha 1	EF1A1_MOUSE	NO	3,80E-02	0,36	8,40E-02	1,21	2,00E-03	0,52	9,20E-02	1,72	68	57	35	98
Polypeptide N-acetylgalactosaminyltransferase 2	GALT2_MOUSE	YES	3,80E-02	2,04	8,10E-01	1,50	3,00E-03	18,33	2,30E-02	13,50	1	1	18	9
78 kDa glucose-regulated protein	GRP78_MOUSE	YES	3,80E-02	1,27	6,30E-01	1,21	1,20E-02	1,70	2,20E-02	1,62	83	69	142	111
Alpha-mannosidase 2	MA2A1_MOUSE	NO	3,80E-02	1,33	7,80E-01	1,21	2,40E-01	1,27	6,70E-01	1,15	14	11	17	13
Neutrophil gelatinase-associated lipocalin	NGAL_MOUSE	YES	3,80E-02	1,31	1,00E+00	NA	1,60E-05	NA	1,60E-03	NA	0	0	58	44
Neuropilin-1	NRP1_MOUSE	YES	3,90E-02	1,39	6,50E-01	1,20	3,00E-02	1,29	6,50E-01	1,11	22	18	28	20
Phosphatidylinositol transfer protein alpha isoform	PIPNA_MOUSE	NO	3,90E-02	1,63	7,80E-01	1,13	3,30E-01	1,06	2,70E-01	0,73	21	19	22	14
Carbonic anhydrase 13	CAH13_MOUSE	NO	4,10E-02	0,57	4,50E-01	1,56	4,10E-01	1,14	1,70E-03	3,11	5	3	5	9
Endoplasmic reticulum protein ERp29	ERP29_MOUSE	NO	4,10E-02	1,41	6,80E-02	0,78	4,30E-02	1,18	5,90E-02	0,65	13	16	15	11
Macrophage colony-stimulating factor 1 receptor	**CSF1R_MOUSE**	**YES**	**4,20E-02**	**1,41**	**5,10E-01**	**1,11**	**1,40E-04**	**2,27**	**5,90E-02**	**1,78**	**38**	**34**	**85**	**61**
Disabled homolog 2	DAB2_MOUSE	NO	4,20E-02	0,49	1,70E-01	1,42	2,70E-02	0,60	8,10E-02	1,73	31	22	19	38
Metalloproteinase inhibitor 2	TIMP2_MOUSE	YES	4,50E-02	1,30	1,00E-01	1,50	8,40E-02	1,18	4,70E-02	1,36	11	7	13	10
40S ribosomal protein S10	RS10_MOUSE	NO	4,70E-02	0,00	8,80E-02	3,20	3,30E-05	0,00	9,90E-02	5,60	5	2	0	9
Pigment epithelium-derived factor	PEDF_MOUSE	YES	4,80E-02	1,65	1,20E-01	0,00	7,80E-04	NA	2,50E-02	5,20	0	2	14	9
Lysosomal protective protein	PPGB_MOUSE	NO	4,80E-02	1,41	1,10E-02	1,42	3,00E-04	1,62	9,50E-02	1,64	56	39	91	64
Syndecan-4	SDC4_MOUSE	NO	4,80E-02	1,61	1,00E+00	NA	2,60E-07	NA	2,00E-02	NA	0	0	32	20
Exostosin-2	EXT2_MOUSE	NO	4,90E-02	2,80	1,00E+00	NA	3,70E-03	NA	1,30E-01	NA	0	0	5	2
Serum albumin	ALBU_MOUSE	YES	5,00E-02	2,16	9,60E-01	1,25	2,40E-02	3,94	5,10E-01	2,29	12	9	46	21
Inhibin beta A chain	INHBA_MOUSE	YES	5,00E-02	4,44	1,00E+00	NA	1,80E-02	NA	1,40E-01	NA	0	0	24	5
Triosephosphate isomerase	TPIS_MOUSE	NO	5,00E-02	0,72	6,00E-01	1,19	3,60E-02	0,59	8,70E-01	0,96	78	66	46	63
Acid sphingomyelinase-like phosphodiesterase 3a	ASM3A_MOUSE	YES	5,10E-02	1,33	5,60E-01	1,18	6,70E-03	2,46	5,90E-04	2,18	9	7	21	16
Monocyte differentiation antigen CD14	**CD14_MOUSE**	**YES**	**5,10E-02**	**1,16**	**4,40E-01**	**0,91**	**1,00E-06**	**3,86**	**4,20E-03**	**3,02**	**40**	**44**	**156**	**134**
Heat shock protein HSP 90-alpha	HS90A_MOUSE	NO	5,10E-02	0,56	9,90E-02	0,78	1,40E-01	0,60	3,60E-01	0,83	43	55	26	46

40S ribosomal protein SA	RSSA_MOUSE	YES	5,10E-02	0,46	8,90E-01	1,11	9,80E-02	0,40	9,40E-01	0,98	17	16	7	15
Transforming growth factor-beta-induced protein ig-h3	BGH3_MOUSE	YES	5,20E-02	0,48	3,70E-01	NA	3,80E-04	56,50	3,80E-03	NA	1	0	38	78
Legumain	LGMN_MOUSE	NO	5,30E-02	1,47	5,60E-01	1,00	7,10E-04	2,71	6,70E-02	1,85	31	31	85	58
Microtubule-associated protein RP/EB family member 1	MARE1_MOUSE	YES	5,30E-02	0,24	6,80E-01	1,57	4,40E-01	0,36	2,00E-01	2,43	4	2	1	6
Purine nucleoside phosphorylase	PNPH_MOUSE	NO	5,30E-02	0,75	5,00E-01	1,14	8,40E-03	1,05	9,10E-03	1,60	75	66	79	105
Proteasome subunit beta type-9	PSB9_MOUSE	NO	5,50E-02	0,20	4,80E-01	1,19	5,60E-03	0,11	1,20E-01	0,63	6	5	1	3
Cathepsin B	CATB_MOUSE	NO	5,60E-02	1,17	2,10E-01	1,13	3,60E-03	1,27	9,10E-02	1,22	450	399	570	486
S-formylglutathione hydrolase	ESTD_MOUSE	NO	5,70E-02	0,50	9,90E-01	1,06	3,40E-01	1,11	2,30E-02	2,32	19	18	21	41
Procollagen-lysine,2-oxoglutarate 5-dioxygenase 1	PLOD1_MOUSE	NO	5,70E-02	1,29	4,40E-01	0,89	3,20E-04	4,22	8,90E-03	2,90	32	36	135	104
Ubiquitin carboxyl-terminal hydrolase isozyme L1	UCHL1_MOUSE	NO	5,70E-02	0,36	9,80E-01	1,11	1,90E-01	0,38	6,50E-01	1,16	7	6	3	7
Properdin	PROP_MOUSE	YES	5,90E-02	2,20	3,50E-02	0,73	3,60E-02	0,63	5,30E-03	0,21	12	16	7	3
Tubulin alpha-1B chain	TBA1B_MOUSE	NO	5,90E-02	0,46	6,90E-02	1,31	1,60E-03	0,50	3,20E-01	1,41	21	16	11	23
Heat shock 70 kDa protein 1B	HS71B_MOUSE	NO	6,00E-02	0,57	2,90E-02	0,85	5,00E-03	0,40	6,60E-03	0,59	122	144	49	86
Ubiquitin	UBIQ_MOUSE	NO	6,00E-02	0,63	6,50E-02	0,60	5,80E-01	0,76	1,90E-01	0,72	22	37	17	27
60S ribosomal protein L22	RL22_MOUSE	NO	6,10E-02	0,15	1,00E+00	NA	3,70E-01	NA	2,30E-02	NA	0	0	1	7
T-complex protein 1 subunit gamma	TCPG_MOUSE	NO	6,10E-02	0,00	3,40E-01	1,38	1,40E-03	0,00	1,20E-01	0,46	17	12	0	6
Eukaryotic translation initiation factor 2 subunit 1	IF2A_MOUSE	NO	6,20E-02	0,20	1,00E+00	NA	3,70E-01	NA	1,00E-02	NA	0	0	1	3
N-acetylgalactosamine-6-sulfatase	GALNS_MOUSE	NO	6,30E-02	1,65	9,90E-01	1,09	2,90E-03	2,33	3,40E-01	1,55	4	4	9	6
Neurogenic locus notch homolog protein 2	NOTC2_MOUSE	YES	6,30E-02	2,38	6,80E-01	0,67	1,80E-02	4,75	7,30E-01	1,33	1	2	6	3
Proline synthetase co-transcribed bacterial homolog protein	PROSC_MOUSE	NO	6,30E-02	0,57	7,60E-01	1,10	4,90E-01	0,73	7,30E-02	1,40	7	7	5	9
L-amino-acid oxidase	OXLA_MOUSE	NO	6,40E-02	1,74	1,00E+00	NA	2,30E-03	NA	1,20E-02	NA	0	0	27	16
Sepiapterin reductase	SPRE_MOUSE	NO	6,40E-02	0,37	2,80E-01	1,26	8,10E-03	0,18	1,60E-02	0,61	13	10	2	6
Ubiquitin cross-reactive protein	UCRP_MOUSE	NO	6,60E-02	0,36	7,10E-01	0,82	1,10E-01	2,00	3,80E-02	4,55	3	4	6	17
F-actin-capping protein subunit alpha-2	CAZA2_MOUSE	NO	6,70E-02	0,69	5,10E-01	1,04	1,70E-01	0,58	4,90E-01	0,87	24	23	14	20
Dual specificity protein phosphatase 3	DUS3_MOUSE	NO	6,70E-02	1,26	5,30E-02	0,62	9,50E-01	0,83	6,10E-03	0,40	10	16	8	6
Extracellular matrix protein 1	ECM1_MOUSE	YES	6,70E-02	1,62	8,10E-01	1,10	7,10E-02	1,43	9,40E-01	0,97	26	23	37	23
Myosin light polypeptide 6	MYL6_MOUSE	NO	6,80E-02	0,67	7,00E-01	1,03	4,10E-04	0,44	1,70E-02	0,67	44	43	19	29
Ras-related protein Rab-14	RAB14_MOUSE	NO	6,80E-02	0,50	6,90E-01	0,94	8,30E-02	0,50	9,10E-01	0,94	11	11	5	11
4F2 cell-surface antigen heavy chain	4F2_MOUSE	YES	6,90E-02	1,63	3,80E-01	0,33	1,70E-04	13,00	1,50E-01	2,67	1	4	17	11
Laminin subunit gamma-1	LAMC1_MOUSE	YES	6,90E-02	2,71	1,00E+00	NA	9,80E-04	NA	2,30E-01	NA	0	0	13	5
Peptidyl-prolyl cis-trans isomerase B	PPIB_MOUSE	NO	6,90E-02	1,41	8,20E-01	1,00	6,10E-04	2,28	2,90E-01	1,61	12	12	27	19
Peroxiredoxin-2	PRDX2_MOUSE	NO	6,90E-02	0,64	4,00E-01	1,20	2,00E-03	0,35	1,30E-01	0,65	39	33	14	21
SAM domain and HD domain-containing protein 1	SAMH1_MOUSE	NO	6,90E-02	0,44	6,00E-01	0,85	1,20E-01	0,34	2,00E-01	0,65	35	41	12	27
Triggering receptor expressed on myeloid cells 2	TREM2_MOUSE	YES	7,00E-02	1,26	2,30E-01	1,22	1,50E-02	1,20	3,50E-01	1,16	20	16	24	19
Lysosomal alpha-glucosidase	LYAG_MOUSE	NO	7,10E-02	0,33	2,50E-01	NA	5,90E-01	0,45	4,00E-03	NA	4	0	2	5
Plasma glutamate carboxypeptidase	PGCP_MOUSE	YES	7,20E-02	1,69	6,10E-01	1,25	3,30E-01	1,10	6,60E-01	0,81	7	5	7	4
Bis(5'-nucleosyl)-tetraphosphatase [asymmetrical]	AP4A_MOUSE	NO	7,30E-02	1,55	1,90E-02	1,82	9,10E-01	0,85	9,00E-01	1,00	7	4	6	4
Tubulin alpha-1C chain	TBA1C_MOUSE	NO	7,30E-02	0,55	1,20E-01	1,14	1,10E-03	0,39	2,10E-01	0,81	181	159	71	129
Interferon-induced guanylate-binding protein 2	GBP2_MOUSE	YES	7,50E-02	0,54	9,40E-03	NA	2,80E-02	2,00	2,10E-03	NA	6	0	11	21
Sialoadhesin	SN_MOUSE	YES	7,50E-02	2,14	1,00E+00	NA	5,30E-04	NA	1,30E-01	NA	0	0	5	2
Dipeptidyl-peptidase 3	DPP3_MOUSE	NO	7,60E-02	1,38	3,70E-01	0,82	8,50E-02	1,19	3,00E-01	0,71	12	15	15	11
Endoplasmic reticulum aminopeptidase 1	ERAP1_MOUSE	YES	7,60E-02	3,40	1,40E-01	NA	7,60E-02	2,13	3,70E-01	NA	3	0	6	2
Transforming protein RhoA	RHOA_MOUSE	YES	7,60E-02	0,25	7,70E-01	1,15	1,30E-01	0,26	5,10E-01	1,21	13	11	3	13
Serine/threonine-protein phosphatase 2A 65 kDa regulatory subunit A alpha isoform	2AAA_MOUSE	NO	7,70E-02	0,00	6,80E-01	0,95	5,70E-03	0,00	1,40E-01	0,53	24	25	0	13
V-type proton ATPase subunit G 1	VATG1_MOUSE	YES	7,70E-02	0,26	7,60E-01	1,20	2,20E-01	0,25	3,00E-01	1,15	8	7	2	8
Annexin A5	ANXA5_MOUSE	NO	7,90E-02	1,64	1,20E-01	NA	1,10E-03	17,86	2,20E-02	NA	2	0	42	25
Ribonuclease 4	RNAS4_MOUSE	YES	8,00E-02	1,23	3,30E-01	0,81	6,60E-01	0,79	9,20E-02	0,53	16	20	13	10
Coronin-1C	COR1C_MOUSE	NO	8,30E-02	0,36	6,10E-02	0,64	1,70E-02	0,14	1,90E-03	0,25	22	34	3	8
Actin-related protein 2/3 complex subunit 1B	ARC1B_MOUSE	NO	8,60E-02	1,46	9,40E-01	1,02	1,00E-01	0,56	2,70E-02	0,39	21	20	12	8
ADP-ribosylation factor 1	ARF1_MOUSE	NO	8,70E-02	0,57	2,20E-01	1,42	9,50E-02	0,50	2,40E-01	1,25	11	8	6	10
Coatomer subunit epsilon	COPE_MOUSE	NO	8,70E-02	0,33	8,50E-01	1,00	3,10E-03	0,19	1,90E-01	0,58	9	9	2	5
Pleckstrin	PLEK_MOUSE	NO	8,90E-02	0,28	1,00E+00	NA	1,30E-01	NA	1,90E-02	NA	0	0	2	6
Adenine phosphoribosyltransferase	APT_MOUSE	NO	9,00E-02	0,22	8,60E-02	3,50	2,60E-01	0,36	4,40E-02	5,75	5	1	2	8
Sorting nexin-2	SNX2_MOUSE	NO	9,00E-02	0,18	7,70E-01	1,01	1,40E-03	0,15	5,90E-01	0,82	32	31	5	26
Cofilin-1	COF1_MOUSE	YES	9,10E-02	0,51	9,30E-01	1,06	8,90E-04	0,30	3,60E-02	0,61	94	89	28	54
Septin-2	SEPT2_MOUSE	YES	9,10E-02	0,38	1,70E-01	0,64	1,80E-01	0,38	1,60E-01	0,64	5	8	2	5
Talin-1	TLN1_MOUSE	YES	9,10E-02	0,52	3,50E-02	0,88	4,90E-05	0,38	5,70E-02	0,64	188	214	71	137
Apolipoprotein E	APOE_MOUSE	YES	9,30E-02	1,26	2,60E-03	1,77	5,70E-02	0,62	3,00E-01	0,87	154	87	96	76
EH domain-containing protein 4	EHD4_MOUSE	NO	9,30E-02	0,55	4,70E-01	1,58	9,00E-01	0,89	4,30E-02	2,58	6	4	6	10
Sorting nexin-5	SNX5_MOUSE	YES	9,30E-02	0,00	3,50E-01	0,93	1,30E-04	0,00	2,40E-02	0,34	21	22	0	8
Fatty acid-binding protein, epidermal	FABP5_MOUSE	NO	9,40E-02	0,73	2,00E-01	1,25	2,40E-02	0,50	1,30E-01	0,87	38	31	19	27
Platelet-activating factor acetylhydrolase	PAFA_MOUSE	YES	9,40E-02	0,39	1,00E+00	NA	2,70E-02	NA	1,20E-02	NA	0	0	4	11
Sulfhydryl oxidase 1	QSOX1_MOUSE	YES	9,40E-02	4,00	9,10E-01	1,17	8,60E-02	5,14	5,60E-01	1,50	2	2	12	3
Tubulin beta-5 chain	TBB5_MOUSE	NO	9,70E-02	0,59	1,80E-01	1,29	2,00E-02	0,47	8,10E-01	1,03	190	147	90	151
Interferon-induced protein with tetratricopeptide repeats 3	IFIT3_MOUSE	NO	9,90E-02	0,26	1,00E+00	NA	3,70E-01	NA	6,20E-03	NA	0	0	3	12
Proteasome subunit alpha type-2	PSA2_MOUSE	NO	9,90E-02	0,29	8,40E-01	1,12	7,90E-02	0,24	6,90E-01	0,92	10	9	2	8
Alpha-galactosidase A	AGAL_MOUSE	YES	1,00E-01	2,21	8,20E-01	1,12	2,40E-02	1,83	9,70E-01	0,92	10	9	18	8
Coatomer subunit gamma	COPG_MOUSE	NO	1,00E-01	0,12	8,70E-01	0,90	1,80E-02	0,04	2,90E-01	0,33	15	17	1	6
Dentin matrix protein 4	DMP4_MOUSE	YES	1,00E-01	1,35	7,90E-01	1,22	2,90E-04	13,55	1,10E-02	12,22	4	3	50	37
Vitamin K-dependent protein S	PROS_MOUSE	YES	1,00E-01	3,17	1,20E-01	0,00	3,20E-03	NA	9,70E-01	0,86	0	2	6	2
Annexin A3	ANXA3_MOUSE	NO	1,10E-01	2,09	3,70E-01	NA	2,70E-03	14,20	1,30E-01	NA	2	0	24	11
UPF0727 protein C6orf115 homolog	CF115_MOUSE	NO	1,10E-01	2,00	8,90E-03	0,68	4,00E-02	1,54	1,60E-01	0,53	4	6	7	3
D-dopachrome decarboxylase	DOPD_MOUSE	NO	1,10E-01	1,33	6,70E-01	1,18	6,30E-01	0,73	2,50E-02	0,64	11	9	8	6
Glutaredoxin-1	GLRX1_MOUSE	NO	1,10E-01	1,07	1,50E-01	0,80	2,50E-01	1,04	5,00E-02	0,77	9	12	10	9
Glutathione reductase, mitochondrial	GSHR_MOUSE	YES	1,10E-01	0,33	8,80E-01	0,95	3,10E-01	0,30	7,60E-01	0,86	7	7	2	6
Latexin	LXN_MOUSE	NO	1,10E-01	1,56	1,80E-01	2,00	4,80E-01	1,00	6,10E-01	1,29	5	2	5	3
Protein disulfide-isomerase	PDIA1_MOUSE	YES	1,10E-01	1,18	9,90E-01	1,05	2,90E-02	0,48	2,60E-03	0,43	46	44	22	19
Renin receptor	RENR_MOUSE	NO	1,10E-01	1,37	2,70E-01	1,53	1,20E-02	2,00	5,20E-02	2,24	9	6	17	13
60S acidic ribosomal protein P0	RLA0_MOUSE	NO	1,10E-01	0,41	3,30E-01	1,26	3,50E-03	0,18	7,10E-02	0,56	29	23	5	13
Vascular cell adhesion protein 1	VCAM1_MOUSE	NO	1,10E-01	1,21	1,00E+00	NA	5,70E-04	NA	4,90E-04	NA	0	0	8	6
Rho guanine nucleotide exchange factor 1	ARHG1_MOUSE	NO	1,20E-01	0,00	1,00E+00	NA	1,00E+00	NA	1,20E-01	NA	0	0	0	2
Chitinase-3-like protein 3	CH3L3_MOUSE	YES	1,20E-01	NA	1,00E+00	NA	1,20E-01	NA	1,00E+00	NA	0	0	1	0
UMP-CMP kinase 2, mitochondrial	CMPK2_MOUSE	NO	1,20E-01	0,60	4,50E-02	7,60	1,70E-02	3,26	1,80E-03	41,60	13	2	41	69
Complement C4-B	CO4B_MOUSE	YES	1,20E-01	NA	1,00E+00	NA	1,20E-01	NA	1,00E+00	NA	0	0	4	0
Cysteine and glycine-rich protein 1	CSRP1_MOUSE	NO	1,20E-01	0,00	1,90E-01	1,17	1,90E-05	0,00	1,20E-03	0,17	19	16	0	3
C-X-C motif chemokine 10	CXL10_MOUSE	YES	1,20E-01	1,33	1,00E+00	NA	2,40E-03	NA	6,20E-04	NA	0	0	8	6
Scavenger mRNA-decapping enzyme DcpS	DCPS_MOUSE	NO	1,20E-01	0,00	2,10E-01	0,78	3,00E-03	0,00	1,60E-01	0,50	5	6	0	3
Destrin	DEST_MOUSE	NO	1,20E-01	0,00	8,00E-01	0,78	3,70E-01	0,00	7,10E-01	1,33	2	3	0	4
Dynein light chain roadblock-type 1	DLRB1_MOUSE	NO	1,20E-01	0,00	7,50E-01	1,00	2,50E-07	0,00	1,90E-01	0,50	4	4	0	2
Eukaryotic translation initiation factor 3 subunit A	EIF3A_MOUSE	NO	1,20E-01	0,00	3,70E-01	0,00	1,00E+00	NA	7,20E-01	1,33	0	1	0	1
Coagulation factor V	FA5_MOUSE	YES	1,20E-01	NA	1,00E+00	NA	1,20E-01	NA	1,00E+00	NA	0	0	1	0
Fibroleukin	FGL2_MOUSE	YES	1,20E-01	NA	1,00E+00	NA	1,20E-01	NA	1,00E+00	NA	0	0	2	0
Heterogeneous nuclear ribonucleoprotein D0	HNRPD_MOUSE	NO	1,20E-01	0,00	5,70E-01	1,33	2,30E-02	0,00	3,00E-01	0,67	9	7	0	5
Heat shock protein HSP 90-beta	HS90B_MOUSE	NO	1,20E-01	0,71	2,40E-01	0,96	3,60E-02	0,68	4,90E-01	0,91	179	187	121	170
Huntingtin-interacting protein K	HYPK_MOUSE	NO	1,20E-01	0,00	7,80E-01	1,50	3,70E-01	0,00	2,90E-01	3,00	1	1	0	2
Alpha-L-iduronidase	IDUA_MOUSE	NO	1,20E-01	NA	3,70E-01	NA	2,20E-01	4,00	1,00E+00	NA	1	0	4	0
Eukaryotic translation initiation factor 5A-1	IF5A1_MOUSE	NO	1,20E-01	0,73	5,10E-01	0,89	4,60E-01	0,66	2,20E-02	0,81	22	24	14	20
Interleukin-1 alpha	IL1A_MOUSE	YES	1,20E-01	0,00	1,00E+00	NA	1,00E+00	NA	1,20E-01	NA	0	0	0	3
Interleukin-27 subunit alpha	IL27A_MOUSE	YES	1,20E-01	1,73	1,00E+00	NA	1,30E-02	NA	1,00E-03	NA	0	0	13	7
Myosin-9	MYH9_MOUSE	YES	1,20E-01	1,73	7,50E-03	0,50	6,40E-01	0,72	1,60E-04	0,21	26	52	19	11
Neutrophil cytosol factor 1	NCF1_MOUSE	NO	1,20E-01	0,00	1,00E+00	NA	1,00E+00	NA	1,20E-01	NA	0	0	0	2
Niban-like protein 1	NIBL1_MOUSE	NO	1,20E-01	0,00	3,70E-01	0,71	5,20E-02	0,00	4,30E-02	0,29	14	20	0	6
Obg-like ATPase 1	OLA1_MOUSE	NO	1,20E-01	0,00	4,30E-01	0,44	3,70E-01	0,00	8,70E-01	0,89	1	3	0	3
Group XV phospholipase A2	PAG15_MOUSE	YES	1,20E-01	NA	1,30E-01	2,23	2,90E-02	0,28	1,20E-01	0,00	10	4	3	0
Phosducin-like protein 3	PDCL3_MOUSE	NO	1,20E-01	0,00	1,00E+00	NA	1,00E+00	NA	1,20E-01	NA	0	0	0	1
Protein disulfide-isomerase A4	PDIA4_MOUSE	NO	1,20E-01	1,08	4,50E-01	0,56	1,40E-03	5,78	1,70E-02	3,00	3	5	17	16
Prefoldin subunit 2	PFD2_MOUSE	NO	1,20E-01	0,00	1,20E-01	0,64	2,40E-03	0,00	5,60E-02	0,32	5	7	0	2
Serine/threonine-protein phosphatase PP1-alpha catalytic subunit	PP1A_MOUSE	NO	1,20E-01	0,00	9,10E-01	1,14	1,40E-01	0,00	5,20E-01	1,71	3	2	0	4
Serine/threonine-protein phosphatase PP1-beta catalytic subunit	PP1B_MOUSE	NO	1,20E-01	0,00	3,70E-01	NA	3,70E-01	0,00	1,20E-01	NA	1	0	0	2
26S proteasome non-ATPase regulatory subunit 6	PSMD6_MOUSE	NO	1,20E-01	NA	9,80E-01	1,00	4,40E-01	2,00	3,70E-01	0,00	1	1	2	0
60S ribosomal protein L30	RL30_MOUSE	NO	1,20E-01	0,00	9,30E-01	1,33	3,70E-01	0,00	3,30E-01	3,33	1	1	0	3
60S ribosomal protein L9	RL9_MOUSE	NO	1,20E-01	0,00	1,00E+00	NA	1,00E+00	NA	1,20E-01	NA	0	0	0	2
60S acidic ribosomal protein P1	RLA1_MOUSE	NO	1,20E-01	0,00	7,10E-02	0,29	3,70E-01	0,00	1,40E-01	0,50	1	5	0	2
40S ribosomal protein S13	RS13_MOUSE	NO	1,20E-01	0,00	3,70E-01	NA	3,70E-01	0,00	1,20E-01	NA	1	0	0	2
40S ribosomal protein S20	RS20_MOUSE	NO	1,20E-01	0,00	3,70E-01	NA	3,70E-01	0,00	1,20E-01	NA	1	0	0	3
Small nuclear ribonucleoprotein E	RUXE_MOUSE	NO	1,20E-01	0,00	1,00E+00	NA	1,00E+00	NA	1,20E-01	NA	0	0	0	3

NAD-dependent deacetylase sirtuin-2	SIRT2_MOUSE	NO	1,20E-01	0,00	7,80E-01	1,43	1,70E-01	0,00	9,60E-01	1,00	3	2	0	2
Superoxide dismutase [Cu-Zn]	SODC_MOUSE	YES	1,20E-01	0,61	3,90E-01	0,84	8,90E-02	0,52	2,70E-01	0,72	16	19	8	14
Suppressor of G2 allele of SKP1 homolog	SUGT1_MOUSE	NO	1,20E-01	0,00	1,60E-01	2,80	2,80E-04	0,00	3,40E-01	2,80	5	2	0	5
Switch-associated protein 70	SWP70_MOUSE	YES	1,20E-01	0,00	1,20E-01	0,42	1,40E-01	0,00	1,70E-01	0,47	3	6	0	3
Thimet oligopeptidase	THOP1_MOUSE	NO	1,20E-01	0,00	1,00E+00	1,00	3,70E-01	0,00	4,70E-01	2,00	1	1	0	1
Ubiquitin carboxyl-terminal hydrolase 14	UBP14_MOUSE	YES	1,20E-01	0,00	8,70E-01	1,07	5,50E-05	0,00	2,40E-02	0,24	10	10	0	2
Ubiquitin carboxyl-terminal hydrolase 5	UBP5_MOUSE	NO	1,20E-01	0,00	3,50E-01	1,35	3,90E-03	0,00	1,00E-01	0,39	10	8	0	3
Tyrosine-protein kinase receptor UFO	UFO_MOUSE	NO	1,20E-01	NA	1,00E+00	NA	1,20E-01	NA	1,00E+00	NA	0	0	2	0
Antithrombin-III	ANT3_MOUSE	YES	1,30E-01	NA	3,70E-01	0,00	1,30E-01	NA	3,70E-01	0,00	0	1	4	0
Apolipoprotein A-I	APOA1_MOUSE	YES	1,30E-01	1,32	1,40E-01	0,36	1,80E-02	5,00	1,50E-01	1,36	2	5	8	6
Ester hydrolase C11orf54 homolog	CK054_MOUSE	NO	1,30E-01	0,00	9,10E-01	0,91	1,30E-01	0,00	4,70E-01	0,45	3	4	0	2
Cleavage and polyadenylation specificity factor subunit 5	CPSF5_MOUSE	NO	1,30E-01	0,00	8,30E-01	1,09	2,90E-03	0,00	1,70E-02	0,30	8	8	0	2
Granulocyte colony-stimulating factor	CSF3_MOUSE	YES	1,30E-01	1,73	1,00E+00	NA	1,00E-02	NA	8,90E-03	NA	0	0	19	11
Coagulation factor X	FA10_MOUSE	YES	1,30E-01	NA	1,00E+00	NA	1,30E-01	NA	1,00E+00	NA	0	0	2	0
Heat shock 70 kDa protein 13	HSP13_MOUSE	NO	1,30E-01	NA	1,00E+00	NA	1,30E-01	NA	1,00E+00	NA	0	0	4	0
Eukaryotic translation initiation factor 4E	IF4E_MOUSE	NO	1,30E-01	0,00	8,40E-01	0,83	1,30E-01	0,00	7,90E-01	1,17	2	2	0	2
Integrin alpha-4	ITA4_MOUSE	YES	1,30E-01	NA	1,00E+00	NA	1,30E-01	NA	1,00E+00	NA	0	0	2	0
Adenylate kinase 2, mitochondrial	KAD2_MOUSE	NO	1,30E-01	0,64	5,80E-01	1,19	1,90E-01	0,58	5,70E-01	1,08	14	12	8	13
Voltage-gated potassium channel subunit beta-2	KCAB2_MOUSE	NO	1,30E-01	0,00	3,70E-01	0,00	1,00E+00	NA	3,80E-01	2,50	0	1	0	2
Lysosomal alpha-mannosidase	MA2B1_MOUSE	NO	1,30E-01	1,10	8,20E-03	1,42	9,70E-01	0,83	3,00E-01	1,08	79	55	66	60
Protein MEMO1	MEMO1_MOUSE	NO	1,30E-01	0,00	1,00E+00	NA	1,00E+00	NA	1,30E-01	NA	0	0	0	2
Myoferlin	MYOF_MOUSE	YES	1,30E-01	0,00	9,80E-01	1,00	3,70E-01	0,00	5,80E-01	1,67	1	1	0	2
Adaptin ear-binding coat-associated protein 2	NECP2_MOUSE	YES	1,30E-01	0,00	6,10E-02	0,71	3,10E-04	0,00	3,90E-01	0,64	3	5	0	3
Sialidase-1	NEUR1_MOUSE	YES	1,30E-01	NA	1,00E+00	NA	1,30E-01	NA	1,00E+00	NA	0	0	2	0
Proteasome subunit beta type-5	PSB5_MOUSE	NO	1,30E-01	NA	7,30E-01	0,75	2,40E-01	4,00	1,20E-01	0,00	1	1	4	0
Ras-related protein Rab-5C	RAB5C_MOUSE	YES	1,30E-01	0,62	8,10E-01	1,20	2,40E-01	1,28	7,00E-02	2,47	6	5	8	12
Rho-related GTP-binding protein RhoG	RHOG_MOUSE	YES	1,30E-01	0,00	1,00E+00	NA	1,00E+00	NA	1,30E-01	NA	0	0	0	3
40S ribosomal protein S14	RS14_MOUSE	NO	1,30E-01	0,00	1,00E+00	NA	1,00E+00	NA	1,30E-01	NA	0	0	0	2
40S ribosomal protein S3a	RS3A_MOUSE	NO	1,30E-01	0,00	1,00E+00	NA	1,00E+00	NA	1,30E-01	NA	0	0	0	3
Splicing factor, proline- and glutamine-rich	SFPQ_MOUSE	NO	1,30E-01	0,00	1,80E-01	1,38	2,20E-04	0,00	8,80E-02	0,38	10	7	0	3
Transforming growth factor beta-1	TGFB1_MOUSE	YES	1,30E-01	3,00	3,70E-01	NA	1,60E-02	7,50	3,70E-01	NA	1	0	5	2
Tropomodulin-3	TMOD3_MOUSE	NO	1,30E-01	0,00	2,20E-01	1,60	4,60E-03	0,00	7,10E-01	1,30	5	3	0	4
Fermitin family homolog 3	URP2_MOUSE	YES	1,30E-01	0,47	7,20E-01	1,10	2,30E-02	0,43	9,40E-01	1,01	32	29	14	29
Xaa-Pro aminopeptidase 1	XPP1_MOUSE	NO	1,30E-01	0,00	8,20E-01	0,83	1,20E-01	0,00	6,70E-01	0,67	3	4	0	3
Aminopeptidase N	AMPN_MOUSE	NO	1,40E-01	1,50	1,80E-01	2,10	8,30E-01	0,79	7,60E-01	1,10	14	7	11	7
Acidic leucine-rich nuclear phosphoprotein 32 family member B	AN32B_MOUSE	NO	1,40E-01	0,67	9,50E-01	1,04	4,20E-02	1,52	6,90E-03	2,35	9	9	14	20
Flavin reductase	BLVRB_MOUSE	NO	1,40E-01	0,65	9,90E-01	1,08	3,50E-01	0,65	7,10E-01	1,08	19	18	12	19
Carbonic anhydrase 2	CAH2_MOUSE	NO	1,40E-01	2,18	1,60E-02	5,50	7,00E-02	3,36	2,50E-02	8,50	4	1	12	6
Coiled-coil domain-containing protein 22	CCD22_MOUSE	NO	1,40E-01	0,00	1,00E+00	NA	1,00E+00	NA	1,40E-01	NA	0	0	0	2
Collagen alpha-1(XVIII) chain	COIA1_MOUSE	YES	1,40E-01	NA	1,00E+00	NA	1,40E-01	NA	1,00E+00	NA	0	0	2	0
N-acetyllactosaminide alpha-1,3-galactosyltransferase	GGTA1_MOUSE	NO	1,40E-01	NA	1,00E+00	NA	1,40E-01	NA	1,00E+00	NA	0	0	4	0

Heat shock cognate 71 kDa protein	HSP7C_MOUSE	YES	1,40E-01	0,76	4,40E-01	1,02	6,10E-02	0,66	3,60E-02	0,88	253	249	167	219
Multiple inositol polyphosphate phosphatase 1	MINP1_MOUSE	YES	1,40E-01	NA	1,00E+00	NA	1,40E-01	NA	1,00E+00	NA	0	0	4	0
Tubulin-specific chaperone A	TBCA_MOUSE	NO	1,40E-01	0,00	8,80E-01	1,00	1,20E-01	0,00	8,30E-01	0,83	2	2	0	2
Three prime repair exonuclease 1	TREX1_MOUSE	NO	1,40E-01	0,00	1,00E+00	NA	1,00E+00	NA	1,40E-01	NA	0	0	0	5
Beta-2-microglobulin	B2MG_MOUSE	YES	1,50E-01	1,39	5,50E-01	1,44	2,30E-01	1,24	5,90E-01	1,27	30	21	37	26
Complement component C1q receptor	C1QR1_MOUSE	YES	1,50E-01	NA	6,60E-01	1,67	6,70E-01	1,20	3,70E-01	0,00	2	1	2	0
Adenylyl cyclase-associated protein 1	CAP1_MOUSE	YES	1,50E-01	0,48	7,00E-01	1,00	3,40E-03	0,28	6,20E-02	0,59	73	72	20	43
C-C motif chemokine 9	CCL9_MOUSE	YES	1,50E-01	1,43	6,70E-03	NA	2,60E-02	2,14	1,10E-02	NA	5	0	10	7
Cystatin-C	CYTC_MOUSE	YES	1,50E-01	1,12	8,60E-01	1,11	5,50E-01	0,92	6,80E-01	0,91	106	96	98	87
Stress-70 protein, mitochondrial	GRP75_MOUSE	NO	1,50E-01	0,00	9,70E-01	1,00	1,80E-01	0,00	4,60E-01	0,62	4	4	0	3
Interleukin-1 receptor antagonist protein	IL1RA_MOUSE	YES	1,50E-01	1,18	3,90E-01	0,86	2,30E-05	21,75	3,80E-03	15,86	4	5	87	74
Macrophage mannose receptor 1	MRC1_MOUSE	NO	1,50E-01	1,32	4,60E-02	1,31	1,40E-01	1,13	4,30E-01	1,13	94	71	106	80
Neuropeptide Y	NPY_MOUSE	YES	1,50E-01	0,56	1,00E+00	NA	3,30E-04	NA	9,30E-03	NA	0	0	3	6
Programmed cell death protein 5	PDCD5_MOUSE	NO	1,50E-01	0,00	2,80E-01	0,54	1,20E-01	0,00	2,40E-01	0,46	2	4	0	2
Phospholipase D4	PLD4_MOUSE	NO	1,50E-01	1,90	1,10E-02	2,23	3,60E-02	0,39	2,70E-03	0,45	16	7	6	3
Peptidyl-prolyl cis-trans isomerase C	PPIC_MOUSE	NO	1,50E-01	0,33	1,00E+00	NA	3,70E-01	NA	3,80E-06	NA	0	0	1	3
Proteasome subunit beta type-10	PSB10_MOUSE	NO	1,50E-01	0,47	4,10E-01	1,60	1,40E-01	0,44	4,10E-01	1,50	5	3	2	5
Serum amyloid A-3 protein	SAA3_MOUSE	YES	1,50E-01	1,17	1,00E+00	NA	1,30E-03	NA	2,60E-06	NA	0	0	40	34
Asparaginyl-tRNA synthetase, cytoplasmic	SYNC_MOUSE	NO	1,50E-01	0,00	6,10E-01	1,42	7,30E-02	0,00	4,70E-01	0,50	6	4	0	2
T-complex protein 1 subunit theta	TCPQ_MOUSE	NO	1,50E-01	0,00	8,60E-01	0,97	1,50E-03	0,00	1,10E-01	0,35	19	20	0	7
Ubiquitin-conjugating enzyme E2 variant 1	UB2V1_MOUSE	NO	1,50E-01	0,64	4,50E-01	0,79	7,60E-01	0,93	8,50E-01	1,16	5	6	5	7
Alcohol dehydrogenase class-3	ADHX_MOUSE	NO	1,60E-01	0,48	3,30E-01	1,58	5,70E-01	0,63	7,50E-02	2,08	6	4	4	8
Fructose-bisphosphate aldolase A	ALDOA_MOUSE	NO	1,60E-01	0,77	9,20E-01	1,04	2,70E-01	0,72	9,20E-01	0,98	195	186	141	182
Actin-related protein 2/3 complex subunit 5-like protein	ARP5L_MOUSE	NO	1,60E-01	0,33	3,30E-01	2,14	4,10E-02	0,20	7,20E-01	1,29	5	2	1	3
45 kDa calcium-binding protein	CAB45_MOUSE	NO	1,60E-01	2,70	3,70E-01	0,00	3,30E-02	NA	4,20E-01	2,50	0	1	9	3
Cullin-associated NEDD8-dissociated protein 1	CAND1_MOUSE	NO	1,60E-01	0,29	8,80E-02	1,46	4,50E-04	0,08	5,80E-02	0,42	33	22	3	9
Early endosome antigen 1	EEA1_MOUSE	YES	1,60E-01	0,19	8,70E-02	0,75	9,00E-03	0,10	2,60E-02	0,40	20	27	2	11
Protein FAM3A	FAM3A_MOUSE	YES	1,60E-01	NA	1,00E+00	NA	1,60E-01	NA	1,00E+00	NA	0	0	2	0
Rho GDP-dissociation inhibitor 1	GDIR1_MOUSE	YES	1,60E-01	0,80	5,60E-01	0,98	8,30E-02	0,68	2,20E-01	0,82	71	72	48	60
Hemoglobin subunit beta-1	HBB1_MOUSE	NO	1,60E-01	1,40	2,90E-01	1,30	5,30E-01	0,99	6,60E-01	0,92	89	68	88	63
Interferon-activable protein 205-B	IFI5B_MOUSE	NO	1,60E-01	0,00	8,60E-01	1,12	1,00E-02	0,00	7,50E-01	0,76	6	6	0	4
Importin-5	IPO5_MOUSE	NO	1,60E-01	0,42	4,40E-01	1,23	4,00E-03	0,13	3,10E-02	0,39	25	20	3	8
Bifunctional purine biosynthesis protein PURH	PUR9_MOUSE	NO	1,60E-01	0,00	4,30E-01	1,37	1,50E-02	0,00	8,20E-01	0,85	12	9	0	8
Stabilin-1	STAB1_MOUSE	YES	1,60E-01	1,08	1,20E-01	0,73	1,00E-02	1,56	6,30E-01	1,05	94	129	147	136
Aldose reductase-related protein 2	ALD2_MOUSE	NO	1,70E-01	0,68	6,30E-01	0,63	1,20E-01	2,60	8,10E-02	2,38	2	3	4	6
Aldose reductase	ALDR_MOUSE	NO	1,70E-01	0,61	8,20E-01	0,93	9,50E-01	0,81	2,40E-01	1,24	9	10	7	12
Complement C3	CO3_MOUSE	YES	1,70E-01	1,12	5,40E-01	1,21	6,30E-07	10,52	2,40E-03	11,41	65	54	684	612
Histone H2A type 1-F	H2A1F_MOUSE	NO	1,70E-01	0,46	8,10E-01	1,00	8,50E-02	0,34	3,50E-01	0,75	11	11	4	8
High mobility group protein B2	HMGB2_MOUSE	NO	1,70E-01	0,43	1,20E-01	0,00	1,50E-01	NA	5,10E-01	1,40	0	3	2	5
Hexokinase-3	HXK3_MOUSE	NO	1,70E-01	0,66	5,70E-01	1,16	5,90E-03	0,44	3,70E-01	0,77	49	43	22	33
Ras GTPase-activating-like protein IQGAP1	IQGA1_MOUSE	YES	1,70E-01	0,51	9,40E-02	1,14	3,50E-05	0,23	2,20E-02	0,51	151	133	35	68
Polyadenylate-binding protein 1	PABP1_MOUSE	NO	1,70E-01	0,67	7,10E-01	0,94	4,70E-01	0,68	9,10E-01	0,96	17	18	11	17
Plectin-1	PLEC1_MOUSE	NO	1,70E-01	0,54	1,30E-01	0,74	4,70E-04	0,13	4,90E-03	0,19	131	177	18	33
Phospholipid transfer protein	PLTP_MOUSE	YES	1,70E-01	1,12	9,90E-01	1,05	7,30E-01	0,80	7,80E-02	0,75	74	71	60	53
Glycogen phosphorylase, liver form	PYGL_MOUSE	NO	1,70E-01	0,00	8,10E-01	1,00	1,70E-03	0,00	3,90E-03	0,17	14	14	0	2
Ganglioside GM2 activator	SAP3_MOUSE	NO	1,70E-01	1,38	8,90E-02	0,62	7,60E-02	1,57	2,30E-01	0,71	7	11	11	8
Bifunctional aminoacyl-tRNA synthetase	SYEP_MOUSE	NO	1,70E-01	0,00	6,20E-01	0,57	3,70E-01	0,00	6,50E-01	1,43	1	2	0	3
Metalloproteinase inhibitor 1	TIMP1_MOUSE	YES	1,70E-01	0,00	1,00E+00	NA	1,00E+00	NA	1,70E-01	NA	0	0	0	2
14-3-3 protein zeta/delta	1433Z_MOUSE	NO	1,80E-01	0,68	6,60E-01	1,03	1,40E-01	0,57	3,60E-01	0,86	49	47	28	41
Cytoplasmic dynein 1 heavy chain 1	DYHC1_MOUSE	NO	1,80E-01	0,73	9,00E-01	0,95	6,60E-01	0,66	7,80E-01	0,86	37	39	25	34
Inter-alpha-trypsin inhibitor heavy chain H2	ITIH2_MOUSE	YES	1,80E-01	1,03	1,10E-01	1,15	3,60E-03	1,19	2,30E-02	1,33	26	22	31	30
6-phosphofructokinase, liver type	K6PL_MOUSE	NO	1,80E-01	0,00	1,00E+00	NA	1,00E+00	NA	1,80E-01	NA	0	0	0	4
Platelet factor 4	PLF4_MOUSE	YES	1,80E-01	1,29	4,30E-01	0,44	2,10E-02	4,43	4,40E-01	1,50	2	5	10	8
Sorting nexin-3	SNX3_MOUSE	NO	1,80E-01	0,39	2,60E-01	2,22	1,80E-01	0,35	2,60E-01	2,00	7	3	2	6
Twinfilin-1	TWF1_MOUSE	NO	1,80E-01	1,45	6,80E-02	0,79	2,40E-01	0,62	8,70E-04	0,33	9	11	5	4
Synaptobrevin homolog YKT6	YKT6_MOUSE	YES	1,80E-01	1,80	6,50E-01	1,16	1,10E-02	0,31	3,80E-02	0,20	10	8	3	2
BRO1 domain-containing protein BROX	BROX_MOUSE	NO	1,90E-01	6,50	2,10E-01	0,63	3,50E-01	0,50	1,10E-02	0,05	9	14	4	1
Complement factor B	CFAB_MOUSE	YES	1,90E-01	1,12	3,70E-01	NA	9,00E-05	178,00	1,30E-03	NA	1	0	237	212
UPF0556 protein C19orf10 homolog	CS010_MOUSE	YES	1,90E-01	0,76	5,70E-01	1,21	3,10E-01	0,76	4,00E-01	1,21	6	5	4	6
Eukaryotic translation initiation factor 3 subunit L	EIF3L_MOUSE	NO	1,90E-01	0,00	1,00E+00	NA	1,00E+00	NA	1,90E-01	NA	0	0	0	3
Furin	FURIN_MOUSE	YES	1,90E-01	1,75	1,00E+00	NA	4,90E-05	NA	1,40E-01	NA	0	0	5	3
Hematopoietic lineage cell-specific protein	HCLS1_MOUSE	NO	1,90E-01	0,63	4,40E-01	0,84	9,00E-01	0,87	5,10E-01	1,16	10	12	9	14
Lysosome-associated membrane glycoprotein 2	LAMP2_MOUSE	YES	1,90E-01	1,12	9,30E-01	1,05	4,00E-03	0,55	2,80E-02	0,52	28	27	16	14
Platelet-activating factor acetylhydrolase IB subunit alpha	LIS1_MOUSE	NO	1,90E-01	0,31	1,40E-01	0,00	3,70E-01	NA	2,00E-01	2,00	0	3	2	5
Leucine zipper transcription factor-like protein 1	LZTL1_MOUSE	NO	1,90E-01	0,42	1,00E+00	NA	1,40E-01	NA	1,00E-02	NA	0	0	2	4
60S acidic ribosomal protein P2	RLA2_MOUSE	NO	1,90E-01	0,58	3,40E-01	0,85	1,10E-01	0,47	1,10E-01	0,68	15	18	7	12
Transcobalamin-2	TCO2_MOUSE	YES	1,90E-01	1,26	9,00E-01	1,09	3,70E-04	3,92	3,20E-02	3,39	8	8	33	26
Tumor necrosis factor receptor superfamily member 1B	TNR1B_MOUSE	NO	1,90E-01	1,76	1,20E-01	NA	3,40E-03	5,42	1,20E-01	NA	4	0	22	12
Vinculin	VINC_MOUSE	YES	1,90E-01	0,00	5,50E-01	0,86	3,20E-03	0,00	3,40E-02	0,20	10	12	0	2
Acyloxyacyl hydrolase	AOAH_MOUSE	YES	2,00E-01	1,06	3,70E-01	3,00	1,20E-03	5,83	5,60E-04	16,50	4	1	23	22
Peptidyl-prolyl cis-trans isomerase FKBP1A	FKB1A_MOUSE	NO	2,00E-01	1,92	2,50E-01	1,83	6,10E-01	0,70	5,10E-01	0,67	11	6	8	4
Osteoclast-stimulating factor 1	OSTF1_MOUSE	NO	2,00E-01	0,64	2,10E-02	0,73	1,00E-01	0,56	2,10E-02	0,64	20	28	11	18
Phosphatidylethanolamine-binding protein 1	PEBP1_MOUSE	NO	2,00E-01	0,77	3,40E-01	1,34	1,50E-01	0,62	6,10E-01	1,07	18	14	11	15
Sulfated glycoprotein 1	SAP_MOUSE	YES	2,00E-01	1,05	2,60E-01	1,15	2,10E-02	1,11	7,80E-02	1,22	208	180	230	219
Thioredoxin domain-containing protein 5	TXND5_MOUSE	NO	2,00E-01	5,50	1,30E-01	0,00	1,20E-01	NA	3,30E-01	0,29	0	2	4	1
Glucose-6-phosphate 1-dehydrogenase X	G6PD1_MOUSE	NO	2,10E-01	0,00	1,30E-01	1,39	2,00E-04	0,00	4,90E-02	0,30	34	25	0	7
Galectin-9	LEG9_MOUSE	YES	2,10E-01	6,00	1,00E+00	NA	1,30E-01	NA	3,70E-01	NA	0	0	6	1
Nucleolin	NUCL_MOUSE	NO	2,10E-01	0,71	1,30E-01	NA	2,10E-03	7,40	7,80E-04	NA	2	0	12	17
von Willebrand factor A domain-containing protein 5A	VMA5A_MOUSE	NO	2,10E-01	0,64	9,00E-01	1,07	8,40E-03	0,28	4,50E-03	0,47	68	64	19	30
Aspartate aminotransferase, mitochondrial	AATM_MOUSE	YES	2,20E-01	1,48	8,30E-01	1,08	8,30E-01	0,79	4,90E-03	0,58	13	12	10	7
Elongation factor 1-delta	EF1D_MOUSE	NO	2,20E-01	0,54	3,10E-01	1,18	5,40E-03	0,32	1,90E-01	0,70	16	13	5	9
Ferritin heavy chain	FRIH_MOUSE	NO	2,20E-01	0,65	4,10E-01	0,82	9,80E-01	0,84	8,60E-01	1,05	10	13	9	13
Nitric oxide synthase, inducible	NOS2_MOUSE	NO	2,20E-01	0,00	1,00E+00	NA	1,00E+00	NA	2,20E-01	NA	0	0	0	8
Out at first protein homolog	OAF_MOUSE	NO	2,20E-01	2,67	1,00E+00	NA	2,70E-02	NA	3,70E-01	NA	0	0	5	2
Poly(rC)-binding protein 1	PCBP1_MOUSE	NO	2,20E-01	0,72	8,20E-01	1,11	3,70E-01	0,69	5,60E-01	1,06	17	16	12	17
Proteasome subunit alpha type-5	PSA5_MOUSE	NO	2,20E-01	0,76	3,60E-01	0,93	1,80E-02	1,26	2,30E-02	1,54	14	15	18	24
UDP-GlcNAc:betaGal beta-1,3-N-acetylglucosaminyltransferase 2	B3GN2_MOUSE	NO	2,30E-01	1,42	1,00E+00	NA	3,40E-03	NA	2,70E-02	NA	0	0	9	6
Brain acid soluble protein 1	BASP1_MOUSE	YES	2,30E-01	0,00	2,20E-01	0,79	1,30E-06	0,00	7,10E-03	0,10	24	31	0	3
C-C motif chemokine 12	CCL12_MOUSE	YES	2,30E-01	1,35	1,00E+00	NA	4,90E-03	NA	1,10E-02	NA	0	0	8	6
Kinesin-1 heavy chain	KINH_MOUSE	NO	2,30E-01	0,00	4,30E-01	2,50	1,80E-01	0,00	4,80E-01	2,50	3	1	0	3
Syntenin-1	SDCB1_MOUSE	YES	2,30E-01	1,82	2,20E-01	0,60	2,90E-02	3,33	8,20E-01	1,10	2	3	7	4
Beta-galactosidase	BGAL_MOUSE	NO	2,40E-01	1,63	4,50E-01	1,60	7,30E-01	0,97	9,40E-01	0,95	11	7	10	6
Cathepsin Z	CATZ_MOUSE	NO	2,40E-01	1,14	1,40E-01	1,38	1,10E-03	3,83	6,10E-03	4,62	34	25	130	114
Clathrin heavy chain 1	CLH_MOUSE	YES	2,40E-01	0,61	8,60E-01	1,08	5,10E-02	0,41	3,20E-01	0,74	123	114	51	84
Glutathione S-transferase P 1	GSTP1_MOUSE	NO	2,40E-01	1,30	6,30E-01	1,29	3,40E-02	1,44	4,40E-01	1,43	3	2	4	3
Hemoglobin subunit alpha	HBA_MOUSE	NO	2,40E-01	1,44	7,70E-01	1,14	4,90E-01	1,05	4,70E-01	0,83	78	68	82	57
Ribosyldihydronicotinamide dehydrogenase [quinone]	NQO2_MOUSE	NO	2,40E-01	2,80	3,80E-01	0,67	4,40E-01	1,40	1,80E-01	0,33	3	5	5	2
Proteasome activator complex subunit 1	PSME1_MOUSE	NO	2,40E-01	0,67	5,90E-01	1,09	3,60E-03	0,36	7,50E-03	0,59	30	27	11	16
Serine-threonine kinase receptor-associated protein	STRAP_MOUSE	NO	2,40E-01	0,18	3,70E-01	0,00	3,70E-01	NA	2,20E-01	5,50	0	1	1	4
Cytoplasmic FMR1-interacting protein 1	CYFP1_MOUSE	YES	2,50E-01	0,22	7,10E-01	0,81	2,10E-01	0,08	8,70E-02	0,28	9	11	1	3
Serpin B6	SPB6_MOUSE	NO	2,50E-01	1,06	6,40E-01	1,13	6,30E-02	0,58	2,80E-02	0,61	51	45	29	28
V-type proton ATPase subunit E 1	VATE1_MOUSE	YES	2,50E-01	0,41	7,60E-02	0,30	2,20E-01	4,00	1,00E-01	2,90	1	3	4	10
Apolipoprotein A-I-binding protein	AIBP_MOUSE	YES	2,60E-01	0,64	5,50E-01	1,14	1,30E-02	0,44	3,90E-01	0,78	14	12	6	9
Calmodulin	CALM_MOUSE	NO	2,60E-01	0,80	5,60E-01	1,00	1,20E-02	0,56	7,40E-03	0,70	26	26	15	18
Soluble calcium-activated nucleotidase 1	CANT1_MOUSE	NO	2,60E-01	NA	1,00E+00	NA	2,60E-01	NA	1,00E+00	NA	0	0	4	0
F-actin-capping protein subunit beta	CAPZB_MOUSE	NO	2,60E-01	0,68	8,70E-01	1,07	9,50E-01	0,85	2,10E-01	1,34	31	29	26	39
DnaJ homolog subfamily B member 11	DJB11_MOUSE	NO	2,60E-01	NA	1,00E+00	NA	2,60E-01	NA	1,00E+00	NA	0	0	4	0
Myosin regulatory light chain 12B	ML12B_MOUSE	NO	2,60E-01	1,69	9,60E-01	1,06	1,30E-01	1,22	7,20E-01	0,76	6	6	7	4
Prostaglandin reductase 1	PTGR1_MOUSE	NO	2,60E-01	1,25	6,40E-01	0,93	7,80E-01	0,77	5,80E-02	0,57	9	9	7	5
[Protein ADP-ribosylarginine] hydrolase	ADPRH_MOUSE	NO	2,70E-01	4,50	1,00E+00	NA	1,60E-01	NA	3,70E-01	NA	0	0	3	1
Beta-glucuronidase	BGLR_MOUSE	NO	2,70E-01	0,84	5,80E-01	1,13	8,80E-01	0,86	8,20E-02	1,15	76	68	65	78
Growth/differentiation factor 15	GDF15_MOUSE	YES	2,70E-01	4,00	1,00E+00	NA	1,50E-01	NA	3,70E-01	NA	0	0	3	1
Eukaryotic initiation factor 4A-I	IF4A1_MOUSE	NO	2,70E-01	0,56	9,40E-01	1,06	4,20E-01	0,65	4,60E-01	1,24	22	21	14	26
S-methyl-5'-thioadenosine phosphorylase	MTAP_MOUSE	NO	2,70E-01	0,68	6,50E-01	0,71	6,40E-02	1,30	5,10E-01	1,36	3	5	4	6
Alpha-2-macroglobulin	A2M_MOUSE	YES	2,80E-01	3,00	1,00E+00	NA	1,20E-01	NA	3,70E-01	NA	0	0	3	1
Calcium-binding protein 39	CAB39_MOUSE	NO	2,80E-01	1,20	1,50E-01	1,69	2,00E-01	0,67	9,80E-01	0,94	9	5	6	5

Protein canopy homolog 2	CNPY2_MOUSE	NO	2,80E-01	1,56	9,10E-01	1,06	9,30E-01	0,82	2,10E-01	0,56	6	5	5	3
Cystatin-F	CYTF_MOUSE	YES	2,80E-01	1,22	1,00E+00	NA	5,00E-03	NA	3,20E-03	NA	0	0	7	6
H-2 class I histocompatibility antigen, Q8 alpha chain	HA18_MOUSE	YES	2,80E-01	2,67	1,00E+00	NA	1,20E-01	NA	3,70E-01	NA	0	0	11	4
Integral membrane protein 2B	ITM2B_MOUSE	YES	2,80E-01	1,53	3,70E-01	NA	6,60E-02	5,75	9,90E-03	NA	1	0	8	5
Signal transducer and activator of transcription 1	STAT1_MOUSE	NO	2,80E-01	0,50	1,20E-01	3,17	1,60E-01	1,42	6,10E-02	9,00	6	2	9	18
Stress-induced-phosphoprotein 1	STIP1_MOUSE	NO	2,80E-01	0,48	8,60E-01	0,97	1,20E-02	0,43	8,00E-01	0,87	12	13	5	11
Biliverdin reductase A	BIEA_MOUSE	NO	2,90E-01	1,08	6,40E-01	1,27	5,90E-01	0,97	6,50E-01	1,13	22	17	21	20
Coronin-1A	COR1A_MOUSE	YES	2,90E-01	0,26	5,00E-01	0,96	9,30E-03	0,14	1,90E-01	0,53	26	27	4	14
Protein CREG1	CREG1_MOUSE	YES	2,90E-01	0,64	9,00E-01	1,05	7,90E-02	1,09	1,90E-01	1,77	8	7	8	13
Elongation factor 1-gamma	EF1G_MOUSE	NO	2,90E-01	0,49	4,40E-01	0,95	1,00E-03	0,14	3,50E-03	0,27	43	45	6	12
Glutathione S-transferase Mu 1	GSTM1_MOUSE	NO	2,90E-01	1,03	3,50E-01	0,89	4,30E-01	0,97	2,20E-01	0,83	21	23	20	19
Lamin-A/C	LMNA_MOUSE	NO	2,90E-01	0,66	1,50E-01	0,88	4,00E-04	0,13	4,60E-04	0,17	70	79	9	14
Nascent polypeptide-associated complex subunit alpha, muscle-specific form	NACAM_MOUSE	NO	2,90E-01	0,84	5,90E-01	1,11	5,30E-03	1,39	3,90E-04	1,82	10	9	14	17
Phosphoglucomutase-1	PGM1_MOUSE	NO	2,90E-01	1,42	5,00E-01	0,91	7,20E-01	0,95	1,30E-01	0,60	13	14	12	9
Proteasome subunit beta type-4	PSB4_MOUSE	NO	2,90E-01	0,65	7,50E-01	0,92	1,60E-01	0,48	3,70E-01	0,68	8	8	4	6
Tubulin-folding cofactor B	TBCB_MOUSE	NO	2,90E-01	0,27	3,70E-01	0,00	3,70E-01	NA	2,60E-01	3,75	0	1	1	5
Disintegrin and metalloproteinase domain-containing protein 8	ADAM8_MOUSE	YES	3,00E-01	1,56	6,40E-01	0,67	1,50E-01	2,33	9,90E-01	1,00	2	3	5	3
60 kDa heat shock protein, mitochondrial	CH60_MOUSE	YES	3,00E-01	1,30	4,30E-01	0,64	3,00E-01	1,44	5,10E-01	0,71	3	5	4	3
Hypoxia up-regulated protein 1	HYOU1_MOUSE	NO	3,00E-01	1,26	2,70E-01	1,67	9,30E-02	1,60	1,00E-01	2,11	5	3	8	6
3,2-trans-enoyl-CoA isomerase, mitochondrial	D3D2_MOUSE	NO	3,10E-01	3,00	5,80E-01	0,60	5,90E-01	1,50	3,00E-01	0,30	2	3	3	1
Oligoribonuclease, mitochondrial	ORN_MOUSE	NO	3,10E-01	3,00	8,80E-01	1,25	7,60E-01	1,20	7,10E-01	0,50	2	1	2	1
Profilin-1	PROF1_MOUSE	YES	3,10E-01	0,81	7,70E-02	1,27	4,90E-03	0,56	4,20E-01	0,88	138	109	78	96
Proteasome subunit beta type-2	PSB2_MOUSE	NO	3,10E-01	1,15	5,80E-01	1,22	3,10E-01	0,59	1,20E-02	0,63	13	11	8	7
Poly(rC)-binding protein 2	PCBP2_MOUSE	NO	3,20E-01	0,72	6,10E-01	0,83	8,20E-01	0,95	3,60E-01	1,09	6	8	6	8
Reticulon-4	RTN4_MOUSE	NO	3,20E-01	1,21	9,60E-01	1,05	5,60E-01	1,00	5,80E-01	0,86	8	7	8	6
Cathepsin L1	CATL1_MOUSE	NO	3,30E-01	1,07	7,80E-01	1,01	7,70E-05	2,81	1,50E-02	2,65	78	78	220	206
Complement factor H	CFAH_MOUSE	YES	3,30E-01	0,71	8,40E-02	0,64	5,80E-01	0,69	5,50E-02	0,63	12	19	8	12
Cytokine receptor-like factor 2	CRLF2_MOUSE	YES	3,30E-01	4,50	1,00E+00	NA	2,20E-01	NA	3,70E-01	NA	0	0	3	1
C-X-C motif chemokine 2	CXCL2_MOUSE	YES	3,30E-01	1,73	1,00E+00	NA	7,50E-02	NA	1,00E-02	NA	0	0	9	5
Dystroglycan	DAG1_MOUSE	YES	3,30E-01	1,13	6,20E-01	0,73	1,10E-02	3,18	2,00E-01	2,07	4	5	12	10
Eukaryotic translation initiation factor 6	IF6_MOUSE	NO	3,30E-01	1,44	3,80E-01	1,17	6,10E-02	0,62	1,60E-01	0,50	7	6	4	3
Epididymis-specific alpha-mannosidase	MA2B2_MOUSE	YES	3,30E-01	1,53	7,30E-03	1,76	8,40E-01	0,87	9,10E-01	1,00	10	6	9	6
Proteasome subunit beta type-3	PSB3_MOUSE	NO	3,30E-01	0,81	1,20E-01	0,85	1,30E-01	0,66	1,10E-02	0,69	18	21	12	14
Disintegrin and metalloproteinase domain-containing protein 15	ADA15_MOUSE	YES	3,40E-01	1,14	3,60E-01	3,00	5,70E-03	4,17	1,10E-02	11,00	2	1	8	7
Acidic leucine-rich nuclear phosphoprotein 32 family member E	AN32E_MOUSE	NO	3,40E-01	0,46	1,00E+00	NA	3,60E-02	NA	7,10E-02	NA	0	0	4	8
Mesencephalic astrocyte-derived neurotrophic factor	MANF_MOUSE	YES	3,40E-01	2,67	2,80E-02	0,37	9,60E-01	0,80	3,50E-03	0,11	3	9	3	1
Macrophage migration inhibitory factor	MIF_MOUSE	YES	3,40E-01	0,65	5,10E-01	1,60	1,00E-01	0,33	7,40E-01	0,80	13	8	4	7
Eukaryotic translation initiation factor 3 subunit K	EIF3K_MOUSE	NO	3,50E-01	0,33	6,50E-01	0,75	6,20E-01	0,50	8,50E-01	1,13	2	3	1	3
Hippocalcin-like protein 1	HPCL1_MOUSE	NO	3,50E-01	2,50	1,20E-02	1,50	5,10E-01	0,63	1,60E-01	0,38	8	5	5	2
Malate dehydrogenase, cytoplasmic	MDHC_MOUSE	NO	3,50E-01	0,74	1,10E-01	1,29	2,80E-03	0,44	2,90E-01	0,77	43	33	19	25
Staphylococcal nuclease domain-containing protein 1	SND1_MOUSE	NO	3,50E-01	0,32	8,80E-01	0,91	4,40E-02	0,11	2,40E-01	0,33	18	19	2	6

Alpha-2-macroglobulin-P	A2MP_MOUSE	YES	3,60E-01	0,68	9,00E-01	1,11	1,20E-01	1,90	6,20E-02	3,11	3	3	6	9
FK506-binding protein 2	FKBP2_MOUSE	NO	3,60E-01	1,10	9,30E-01	1,00	4,70E-01	0,65	1,90E-01	0,59	6	6	4	3
Growth-regulated alpha protein	GROA_MOUSE	YES	3,60E-01	0,69	1,00E+00	NA	6,40E-04	NA	8,80E-03	NA	0	0	4	5
Plastin-2	PLSL_MOUSE	YES	3,60E-01	0,86	6,60E-01	1,07	8,40E-03	0,67	1,10E-02	0,83	395	370	266	309
Ribonuclease inhibitor	RINI_MOUSE	NO	3,60E-01	0,73	1,00E+00	1,04	1,30E-02	0,48	1,40E-01	0,68	69	67	33	45
Aldehyde dehydrogenase family 16 member A1	A16A1_MOUSE	NO	3,70E-01	NA	5,00E-01	2,20	3,50E-01	0,27	3,70E-01	0,00	4	2	1	0
Apolipoprotein B-100 receptor	AB48R_MOUSE	NO	3,70E-01	0,00	7,00E-01	1,23	4,30E-02	0,00	8,00E-02	0,23	11	9	0	2
Acylphosphatase-1	ACYP1_MOUSE	NO	3,70E-01	0,00	4,50E-01	1,00	2,50E-07	0,00	3,80E-02	0,25	4	4	0	1
Fructose-bisphosphate aldolase C	ALDOC_MOUSE	NO	3,70E-01	NA	9,50E-01	1,00	9,20E-01	1,00	3,70E-01	0,00	1	1	1	0
DNA-(apurinic or apyrimidinic site) lyase	APEX1_MOUSE	NO	3,70E-01	0,00	1,00E+00	NA	1,00E+00	NA	3,70E-01	NA	0	0	0	1
Argininosuccinate synthase	ASSY_MOUSE	NO	3,70E-01	0,00	1,00E+00	NA	1,00E+00	NA	3,70E-01	NA	0	0	0	1
Copper transport protein ATOX1	ATOX1_MOUSE	NO	3,70E-01	0,00	1,00E+00	NA	1,00E+00	NA	3,70E-01	NA	0	0	0	2
Beta-1,4 N-acetylgalactosaminyltransferase 1	B4GN1_MOUSE	NO	3,70E-01	NA	1,00E+00	NA	3,70E-01	NA	1,00E+00	NA	0	0	2	0
Beta-1,4-galactosyltransferase 1	B4GT1_MOUSE	YES	3,70E-01	NA	3,70E-01	NA	7,70E-01	1,00	1,00E+00	NA	1	0	1	0
Barrier-to-autointegration factor	BAF_MOUSE	NO	3,70E-01	0,00	1,20E-01	0,00	1,00E+00	NA	3,70E-01	0,33	0	2	0	1
Biotinidase	BTD_MOUSE	YES	3,70E-01	NA	1,00E+00	NA	3,70E-01	NA	1,00E+00	NA	0	0	1	0
Complement component 1 Q subcomponent-binding protein, mitochondrial	C1QBP_MOUSE	NO	3,70E-01	NA	1,00E+00	NA	3,70E-01	NA	1,00E+00	NA	0	0	1	0
UPF0587 protein C1orf123 homolog	CA123_MOUSE	NO	3,70E-01	0,00	6,80E-01	0,85	1,50E-01	0,00	1,10E-01	0,31	4	4	0	1
Calnexin	CALX_MOUSE	NO	3,70E-01	NA	1,00E+00	NA	3,70E-01	NA	1,00E+00	NA	0	0	1	0
Caspase-1	CASP1_MOUSE	YES	3,70E-01	0,00	1,00E+00	NA	1,00E+00	NA	3,70E-01	NA	0	0	0	1
CD180 antigen	CD180_MOUSE	YES	3,70E-01	0,00	8,50E-01	1,17	1,20E-01	0,00	3,80E-01	0,33	2	2	0	1
Cell division control protein 42 homolog	CDC42_MOUSE	YES	3,70E-01	0,00	3,70E-01	NA	3,70E-01	0,00	3,70E-01	NA	2	0	0	1
Carbohydrate sulfotransferase 14	CHSTE_MOUSE	NO	3,70E-01	NA	1,00E+00	NA	3,70E-01	NA	1,00E+00	NA	0	0	1	0
Citrate synthase, mitochondrial	CISY_MOUSE	NO	3,70E-01	0,00	9,90E-01	1,08	1,30E-01	0,00	5,70E-02	0,25	4	4	0	1
CMRF35-like molecule 3	CLM3_MOUSE	YES	3,70E-01	NA	1,00E+00	NA	3,70E-01	NA	1,00E+00	NA	0	0	2	0
Coatomer subunit beta	COPB_MOUSE	NO	3,70E-01	0,00	8,20E-01	0,88	1,20E-01	0,00	9,40E-02	0,13	7	8	0	1
Calcineurin-like phosphoesterase domain-containing protein 1	CPPED_MOUSE	NO	3,70E-01	0,00	1,00E+00	NA	1,00E+00	NA	3,70E-01	NA	0	0	0	1
Cysteine-rich with EGF-like domain protein 2	CREL2_MOUSE	YES	3,70E-01	NA	1,00E+00	NA	3,70E-01	NA	1,00E+00	NA	0	0	2	0
Versican core protein	CSPG2_MOUSE	YES	3,70E-01	0,00	1,00E+00	NA	1,00E+00	NA	3,70E-01	NA	0	0	0	1
UPF0368 protein Cxorf26 homolog	CX026_MOUSE	NO	3,70E-01	NA	5,80E-03	6,67	3,30E-02	0,20	3,70E-01	0,00	7	1	1	0
C-X-C motif chemokine 3	CXCL3_MOUSE	YES	3,70E-01	0,00	1,00E+00	NA	1,00E+00	NA	3,70E-01	NA	0	0	0	1
Cytochrome b5	CYB5_MOUSE	NO	3,70E-01	NA	3,10E-01	1,86	4,00E-02	0,15	1,20E-01	0,00	4	2	1	0
Drebrin-like protein	DBNL_MOUSE	NO	3,70E-01	0,00	1,00E+00	NA	1,00E+00	NA	3,70E-01	NA	0	0	0	2
Cytoplasmic dynein 1 light intermediate chain 1	DC1L1_MOUSE	NO	3,70E-01	0,00	5,80E-02	4,00	1,60E-03	0,00	8,00E-01	0,67	4	1	0	1
Trans-1,2-dihydrobenzene-1,2-diol dehydrogenase	DHDH_MOUSE	NO	3,70E-01	0,00	2,30E-01	0,22	3,70E-01	0,00	2,40E-01	0,22	1	3	0	1
Sorbitol dehydrogenase	DHSO_MOUSE	NO	3,70E-01	NA	1,00E+00	NA	3,70E-01	NA	1,00E+00	NA	0	0	1	0
Protein diaphanous homolog 1	DIAP1_MOUSE	YES	3,70E-01	NA	1,50E-01	0,54	1,70E-01	0,09	1,00E-04	0,00	7	14	1	0
Deoxyribonuclease-2-alpha	DNS2A_MOUSE	NO	3,70E-01	0,00	1,00E+00	NA	1,00E+00	NA	3,70E-01	NA	0	0	0	1
Probable D-tyrosyl-tRNA(Tyr) deacylase 2	DTD2_MOUSE	NO	3,70E-01	0,00	3,80E-01	0,38	3,70E-01	0,00	4,10E-01	0,38	1	3	0	1
Dynein light chain Tctex-type 1	DYLT1_MOUSE	NO	3,70E-01	0,00	1,00E+00	NA	1,00E+00	NA	3,70E-01	NA	0	0	0	1
Eukaryotic translation initiation factor 2A	EIF2A_MOUSE	NO	3,70E-01	0,00	7,10E-01	1,33	1,20E-01	0,00	3,70E-01	0,33	3	2	0	1
Eukaryotic translation initiation factor 3 subunit B	EIF3B_MOUSE	NO	3,70E-01	0,00	1,80E-01	0,00	1,00E+00	NA	5,10E-01	0,50	0	4	0	2
Eukaryotic translation initiation factor 3 subunit C	EIF3C_MOUSE	NO	3,70E-01	0,00	1,00E+00	NA	1,00E+00	NA	3,70E-01	NA	0	0	0	1
Eukaryotic translation initiation factor 3 subunit E	EIF3E_MOUSE	NO	3,70E-01	0,00	1,00E+00	NA	1,00E+00	NA	3,70E-01	NA	0	0	0	1
Eukaryotic translation initiation factor 3 subunit M	EIF3M_MOUSE	NO	3,70E-01	0,00	1,00E+00	NA	1,00E+00	NA	3,70E-01	NA	0	0	0	1
Endothelial protein C receptor	EPCR_MOUSE	NO	3,70E-01	NA	1,00E+00	NA	3,70E-01	NA	1,00E+00	NA	0	0	1	0
Eukaryotic peptide chain release factor subunit 1	ERF1_MOUSE	NO	3,70E-01	0,00	4,20E-01	1,23	1,00E-03	0,00	1,10E-01	0,31	5	4	0	1
BRISC complex subunit Abro1	F175B_MOUSE	NO	3,70E-01	0,00	1,00E+00	NA	1,00E+00	NA	3,70E-01	NA	0	0	0	1
Ferric-chelate reductase 1	FRRS1_MOUSE	NO	3,70E-01	NA	1,00E+00	NA	3,70E-01	NA	1,00E+00	NA	0	0	1	0
Tissue alpha-L-fucosidase	FUCO_MOUSE	NO	3,70E-01	NA	1,00E+00	NA	3,70E-01	NA	1,00E+00	NA	0	0	1	0
RNA-binding protein FUS	FUS_MOUSE	NO	3,70E-01	0,00	3,90E-01	1,82	5,90E-02	0,00	3,70E-01	0,36	7	4	0	1
Ras GTPase-activating protein-binding protein 1	G3BP1_MOUSE	YES	3,70E-01	0,00	9,70E-01	1,13	1,90E-02	0,00	2,50E-01	0,27	6	5	0	1
Galactocerebrosidase	GALC_MOUSE	NO	3,70E-01	NA	1,00E+00	NA	3,70E-01	NA	1,00E+00	NA	0	0	1	0
Galactokinase	GALK1_MOUSE	NO	3,70E-01	0,00	1,00E+00	NA	1,00E+00	NA	3,70E-01	NA	0	0	0	1
Polypeptide N-acetylgalactosaminyltransferase 1	GALT1_MOUSE	YES	3,70E-01	NA	1,00E+00	NA	3,70E-01	NA	1,00E+00	NA	0	0	1	0
Guanylate-binding protein 4	GBP4_MOUSE	NO	3,70E-01	0,00	1,00E+00	NA	1,00E+00	NA	3,70E-01	NA	0	0	0	2
Glycolipid transfer protein	GLTP_MOUSE	NO	3,70E-01	NA	9,50E-01	1,00	4,70E-01	0,38	1,30E-01	0,00	3	3	1	0
Glyoxylate reductase/hydroxypyruvate reductase	GRHPR_MOUSE	NO	3,70E-01	0,00	1,00E+00	NA	1,00E+00	NA	3,70E-01	NA	0	0	0	1
H-2 class I histocompatibility antigen, K-D alpha chain	HA1D_MOUSE	YES	3,70E-01	NA	1,00E+00	NA	3,70E-01	NA	1,00E+00	NA	0	0	3	0
Hepatoma-derived growth factor	HDGF_MOUSE	YES	3,70E-01	0,00	7,40E-01	1,22	1,10E-02	0,00	3,40E-02	0,09	9	8	0	1
Haloacid dehalogenase-like hydrolase domain-containing protein 2	HDHD2_MOUSE	NO	3,70E-01	NA	3,70E-01	0,00	3,70E-01	NA	3,70E-01	0,00	0	1	1	0
Histidine triad nucleotide-binding protein 1	HINT1_MOUSE	NO	3,70E-01	0,33	7,00E-02	1,42	2,50E-03	0,09	4,40E-02	0,38	11	8	1	3
Heme oxygenase 2	HMOX2_MOUSE	NO	3,70E-01	0,00	4,30E-01	0,60	1,60E-01	0,00	5,30E-02	0,12	5	8	0	1
Heterogeneous nuclear ribonucleoprotein H	HNRH1_MOUSE	NO	3,70E-01	0,00	3,70E-01	NA	3,70E-01	0,00	3,70E-01	NA	1	0	0	2
Heterogeneous nuclear ribonucleoproteins C1/C2	HNRPC_MOUSE	NO	3,70E-01	0,00	5,00E-01	0,50	3,70E-01	0,00	3,60E-01	0,38	3	5	0	2
Heterogeneous nuclear ribonucleoprotein Q	HNRPQ_MOUSE	NO	3,70E-01	0,00	3,10E-01	0,60	1,60E-01	0,00	4,10E-01	0,53	3	5	0	3
Heat shock protein 105 kDa	HS105_MOUSE	NO	3,70E-01	0,00	3,70E-01	NA	3,70E-01	0,00	3,70E-01	NA	1	0	0	1
Heat shock protein beta-1	HSPB1_MOUSE	YES	3,70E-01	0,00	3,70E-01	NA	3,70E-01	0,00	3,70E-01	NA	1	0	0	1
Interleukin-18-binding protein	I18BP_MOUSE	YES	3,70E-01	NA	1,00E+00	NA	3,70E-01	NA	1,00E+00	NA	0	0	1	0
Isoamyl acetate-hydrolyzing esterase 1 homolog	IAH1_MOUSE	NO	3,70E-01	0,00	1,00E+00	NA	1,00E+00	NA	3,70E-01	NA	0	0	0	1
ICOS ligand	ICOSL_MOUSE	YES	3,70E-01	1,50	1,00E+00	NA	8,90E-07	NA	1,80E-01	NA	0	0	5	3
Eukaryotic translation initiation factor 4B	IF4B_MOUSE	NO	3,70E-01	0,00	3,70E-01	0,00	1,00E+00	NA	9,30E-01	1,00	0	1	0	1
Interferon-induced protein with tetratricopeptide repeats 1	IFIT1_MOUSE	NO	3,70E-01	0,00	1,00E+00	NA	1,00E+00	NA	3,70E-01	NA	0	0	0	1
Interferon-inducible GTPase 1	IIGP1_MOUSE	YES	3,70E-01	0,00	1,00E+00	NA	1,00E+00	NA	3,70E-01	NA	0	0	0	1
Cytokine receptor common gamma chain	IL2RG_MOUSE	YES	3,70E-01	0,00	1,00E+00	NA	1,00E+00	NA	3,70E-01	NA	0	0	0	1
Integrin beta-5	ITB5_MOUSE	YES	3,70E-01	NA	1,00E+00	NA	3,70E-01	NA	1,00E+00	NA	0	0	1	0
Keratin, type II cytoskeletal 1	K2C1_MOUSE	YES	3,70E-01	NA	1,00E+00	NA	3,70E-01	NA	1,00E+00	NA	0	0	1	0
Keratin, type II cytoskeletal 6A	K2C6A_MOUSE	NO	3,70E-01	0,00	1,00E+00	NA	1,00E+00	NA	3,70E-01	NA	0	0	0	1
6-phosphofructokinase type C	K6PP_MOUSE	NO	3,70E-01	0,00	1,00E+00	NA	1,00E+00	NA	3,70E-01	NA	0	0	0	1
Protein kinase C delta type	KPCD_MOUSE	YES	3,70E-01	0,00	1,00E+00	NA	1,00E+00	NA	3,70E-01	NA	0	0	0	1
Keratin, type I cuticular Ha4	KRT34_MOUSE	NO	3,70E-01	0,00	3,70E-01	NA	3,70E-01	0,00	3,70E-01	NA	2	0	0	1
Tyrosine-protein kinase SYK	KSYK_MOUSE	YES	3,70E-01	0,00	1,00E+00	NA	1,00E+00	NA	3,70E-01	NA	0	0	0	1
Galectin-8	LEG8_MOUSE	NO	3,70E-01	NA	1,00E+00	NA	3,70E-01	NA	1,00E+00	NA	0	0	1	0
LIM and senescent cell antigen-like-containing domain protein 1	LIMS1_MOUSE	YES	3,70E-01	0,00	1,00E+00	NA	1,00E+00	NA	3,70E-01	NA	0	0	0	1
Vesicular integral-membrane protein VIP36	LMAN2_MOUSE	NO	3,70E-01	2,50	1,00E+00	NA	1,20E-01	NA	3,70E-01	NA	0	0	3	1
Leucine-rich repeat-containing protein 25	LRC25_MOUSE	NO	3,70E-01	0,00	3,70E-01	0,00	1,00E+00	NA	8,70E-01	1,50	0	1	0	1
Leucine-rich repeat-containing protein 47	LRC47_MOUSE	NO	3,70E-01	0,00	1,00E+00	NA	1,00E+00	NA	3,70E-01	NA	0	0	0	1
Leucine-rich repeat-containing protein 59	LRC59_MOUSE	NO	3,70E-01	0,00	1,00E+00	NA	1,00E+00	NA	3,70E-01	NA	0	0	0	2
Lumican	LUM_MOUSE	NO	3,70E-01	0,00	1,00E+00	NA	1,00E+00	NA	3,70E-01	NA	0	0	0	2
Microtubule-associated protein 4	MAP4_MOUSE	NO	3,70E-01	0,00	3,30E-01	3,00	1,30E-01	0,00	9,80E-01	1,00	4	1	0	1
S-adenosylmethionine synthetase isoform type-2	METK2_MOUSE	NO	3,70E-01	0,00	1,00E+00	NA	1,00E+00	NA	3,70E-01	NA	0	0	0	1
Alpha-1,6-mannosyl-glycoprotein 2-beta-N-acetylglucosaminyltransferase	MGAT2_MOUSE	NO	3,70E-01	NA	1,00E+00	NA	3,70E-01	NA	1,00E+00	NA	0	0	1	0
Magnesium-dependent phosphatase 1	MGDP1_MOUSE	NO	3,70E-01	0,00	3,70E-01	2,67	1,20E-01	0,00	9,90E-01	1,00	3	1	0	1
Protein mago nashi homolog 1-related	MGNR_MOUSE	NO	3,70E-01	0,00	3,10E-01	3,33	1,30E-01	0,00	5,70E-01	2,67	3	1	0	3
Mitogen-activated protein kinase scaffold protein 1	MPKS1_MOUSE	NO	3,70E-01	0,00	3,70E-01	NA	3,70E-01	0,00	3,70E-01	NA	1	0	0	1
MARCKS-related protein	MRP_MOUSE	NO	3,70E-01	0,00	1,00E+00	NA	1,00E+00	NA	3,70E-01	NA	0	0	0	1
Nicotinamide phosphoribosyltransferase	NAMPT_MOUSE	NO	3,70E-01	NA	7,20E-01	1,18	4,90E-02	0,12	3,00E-03	0,00	11	9	1	0
Neural cell adhesion molecule 1	NCAM1_MOUSE	YES	3,70E-01	NA	1,00E+00	NA	3,70E-01	NA	1,00E+00	NA	0	0	1	0
Neutrophil cytosol factor 2	NCF2_MOUSE	NO	3,70E-01	0,00	1,00E+00	NA	1,00E+00	NA	3,70E-01	NA	0	0	0	2
Neutrophil cytosol factor 4	NCF4_MOUSE	NO	3,70E-01	0,00	1,00E+00	NA	1,00E+00	NA	3,70E-01	NA	0	0	0	2
NEDD8	NEDD8_MOUSE	NO	3,70E-01	0,00	9,50E-05	0,00	1,00E+00	NA	5,20E-02	0,25	0	4	0	1
Nuclear factor NF-kappa-B p100 subunit	NFKB2_MOUSE	NO	3,70E-01	0,00	1,00E+00	NA	1,00E+00	NA	3,70E-01	NA	0	0	0	1
NHL repeat-containing protein 3	NHLC3_MOUSE	NO	3,70E-01	NA	3,70E-01	NA	7,40E-01	0,50	1,00E+00	NA	1	0	1	0
Glycylpeptide N-tetradecanoyltransferase 1	NMT1_MOUSE	NO	3,70E-01	NA	6,60E-01	1,43	2,40E-01	0,20	1,30E-01	0,00	3	2	1	0
Nucleosome assembly protein 1-like 1	NP1L1_MOUSE	NO	3,70E-01	0,00	1,00E+00	NA	1,00E+00	NA	3,70E-01	NA	0	0	0	2
Nucleosome assembly protein 1-like 4	NP1L4_MOUSE	NO	3,70E-01	0,00	1,30E-01	0,00	1,00E+00	NA	4,30E-01	0,40	0	2	0	1
Nuclear transport factor 2	NTF2_MOUSE	NO	3,70E-01	0,00	3,70E-01	NA	3,70E-01	0,00	3,70E-01	NA	2	0	0	1
Platelet-activating factor acetylhydrolase IB subunit beta	PA1B2_MOUSE	NO	3,70E-01	0,00	5,90E-01	1,80	1,60E-01	0,00	9,00E-01	0,80	3	2	0	1
Retinal rod rhodopsin-sensitive cGMP 3',5'-cyclic phosphodiesterase subunit delta	PDE6D_MOUSE	NO	3,70E-01	0,00	5,40E-01	0,57	3,70E-01	0,00	4,60E-01	0,43	1	2	0	1
Astrocytic phosphoprotein PEA-15	PEA15_MOUSE	NO	3,70E-01	0,00	3,60E-01	0,40	3,70E-01	0,00	2,70E-01	0,27	2	5	0	1
Prefoldin subunit 6	PFD6_MOUSE	NO	3,70E-01	0,00	5,90E-01	1,67	1,30E-01	0,00	3,10E-01	0,33	3	2	0	1
Putative phospholipase B-like 2	PLBL2_MOUSE	NO	3,70E-01	0,00	3,60E-01	3,00	1,60E-01	0,00	7,40E-01	1,50	2	1	0	1
Phosphatidylcholine transfer protein	PPCT_MOUSE	NO	3,70E-01	NA	3,70E-01	NA	7,30E-01	1,50	1,00E+00	NA	1	0	1	0
Serine/threonine-protein phosphatase 6 catalytic subunit	PPP6_MOUSE	NO	3,70E-01	0,00	3,70E-01	NA	3,70E-01	0,00	3,70E-01	NA	1	0	0	1
Thioredoxin-dependent peroxide reductase, mitochondrial	PRDX3_MOUSE	NO	3,70E-01	NA	7,40E-01	0,86	4,10E-01	0,33	9,40E-03	0,00	6	7	2	0
26S protease regulatory subunit S10B	PRS10_MOUSE	NO	3,70E-01	0,00	8,50E-02	2,17	9,10E-05	0,00	9,80E-01	1,00	4	2	0	2

Proteasome subunit alpha type-4	PSA4_MOUSE	NO	3,70E-01	0,81	3,10E-02	1,67	3,40E-02	0,56	2,80E-01	1,15	15	9	8	10
Proteasome subunit beta type-7	PSB7_MOUSE	NO	3,70E-01	0,00	7,40E-01	2,00	3,70E-01	0,00	7,00E-01	2,00	1	1	0	1
26S proteasome non-ATPase regulatory subunit 11	PSD11_MOUSE	NO	3,70E-01	0,00	3,80E-01	1,55	2,10E-02	0,00	1,10E-01	0,20	10	7	0	1
26S proteasome non-ATPase regulatory subunit 1	PSMD1_MOUSE	NO	3,70E-01	0,00	5,70E-01	1,32	2,80E-02	0,00	9,80E-02	0,27	10	7	0	2
26S proteasome non-ATPase regulatory subunit 2	PSMD2_MOUSE	NO	3,70E-01	0,00	7,90E-01	0,90	1,40E-01	0,00	1,50E-01	0,33	6	7	0	2
26S proteasome non-ATPase regulatory subunit 4	PSMD4_MOUSE	NO	3,70E-01	0,00	5,50E-01	0,86	6,90E-03	0,00	4,30E-02	0,18	6	7	0	1
Polypyrimidine tract-binding protein 1	PTBP1_MOUSE	NO	3,70E-01	0,00	2,30E-01	2,09	5,60E-03	0,00	2,70E-01	0,27	8	4	0	1
6-pyruvoyl tetrahydrobiopterin synthase	PTPS_MOUSE	NO	3,70E-01	0,00	4,40E-01	2,33	1,20E-01	0,00	9,90E-01	1,00	2	1	0	1
Ras-related protein Rab-21	RAB21_MOUSE	NO	3,70E-01	0,00	1,00E+00	NA	1,00E+00	NA	3,70E-01	NA	0	0	0	1
Ras-related protein Rab-31	RAB31_MOUSE	YES	3,70E-01	0,00	1,30E-01	0,00	1,00E+00	NA	6,60E-01	0,60	0	2	0	1
Radixin	RADI_MOUSE	YES	3,70E-01	0,00	3,60E-01	0,31	3,70E-01	0,00	3,10E-01	0,31	2	5	0	2
Putative RNA-binding protein 3	RBM3_MOUSE	NO	3,70E-01	0,00	2,10E-01	0,69	8,10E-04	0,00	3,30E-02	0,15	6	9	0	1
UV excision repair protein RAD23 homolog B	RD23B_MOUSE	NO	3,70E-01	NA	9,80E-01	1,00	9,20E-01	1,00	3,70E-01	0,00	1	1	1	0
60S ribosomal protein L38	RL38_MOUSE	NO	3,70E-01	0,00	1,00E+00	NA	1,00E+00	NA	3,70E-01	NA	0	0	0	1
Ribosome-binding protein 1	RRBP1_MOUSE	NO	3,70E-01	0,00	5,90E-01	2,50	3,70E-01	0,00	4,10E-01	12,00	2	1	0	8
40S ribosomal protein S16	RS16_MOUSE	NO	3,70E-01	NA	8,30E-01	1,00	1,50E-01	0,29	1,40E-03	0,00	5	5	1	0
40S ribosomal protein S17	RS17_MOUSE	NO	3,70E-01	0,00	1,00E+00	NA	1,00E+00	NA	3,70E-01	NA	0	0	0	1
40S ribosomal protein S2	RS2_MOUSE	NO	3,70E-01	0,00	1,00E+00	NA	1,00E+00	NA	3,70E-01	NA	0	0	0	1
U2 small nuclear ribonucleoprotein A'	RU2A_MOUSE	NO	3,70E-01	0,00	9,80E-01	1,08	2,80E-03	0,00	6,80E-01	0,67	4	4	0	3
Protein S100-A4	S10A4_MOUSE	NO	3,70E-01	0,00	6,20E-01	1,50	1,20E-01	0,00	3,80E-01	0,33	3	2	0	1
Adenosylhomocysteinase	SAHH_MOUSE	NO	3,70E-01	0,00	4,50E-01	2,25	1,20E-01	0,00	9,90E-01	1,00	3	1	0	1
Semaphorin-4C	SEM4C_MOUSE	YES	3,70E-01	NA	1,00E+00	NA	3,70E-01	NA	1,00E+00	NA	0	0	1	0
Splicing factor, arginine/serine-rich 3	SFRS3_MOUSE	NO	3,70E-01	0,00	1,00E+00	NA	1,00E+00	NA	3,70E-01	NA	0	0	0	1
Endophilin-A2	SH3G1_MOUSE	NO	3,70E-01	0,00	1,00E+00	NA	1,00E+00	NA	3,70E-01	NA	0	0	0	1
Sialate O-acetylesterase	SIAE_MOUSE	NO	3,70E-01	NA	1,00E+00	NA	3,70E-01	NA	1,00E+00	NA	0	0	1	0
Nucleotide exchange factor SIL1	SIL1_MOUSE	NO	3,70E-01	NA	1,00E+00	NA	3,70E-01	NA	1,00E+00	NA	0	0	1	0
Sorting nexin-12	SNX12_MOUSE	NO	3,70E-01	0,00	6,10E-01	0,82	3,70E-01	0,00	5,40E-02	0,27	3	4	0	1
Sorting nexin-6	SNX6_MOUSE	NO	3,70E-01	0,00	8,40E-01	1,00	5,70E-03	0,00	9,20E-03	0,16	6	6	0	1
StAR-related lipid transfer protein 5	STAR5_MOUSE	NO	3,70E-01	NA	3,70E-01	0,00	3,70E-01	NA	3,70E-01	0,00	0	1	1	0
Signal transducer and activator of transcription 3	STAT3_MOUSE	YES	3,70E-01	0,00	1,00E+00	NA	1,00E+00	NA	3,70E-01	NA	0	0	0	1
Syntaxin-7	STX7_MOUSE	NO	3,70E-01	0,00	1,40E-01	NA	1,40E-01	0,00	3,70E-01	NA	3	0	0	1
Aspartyl-tRNA synthetase, cytoplasmic	SYDC_MOUSE	NO	3,70E-01	0,00	1,00E+00	NA	1,00E+00	NA	3,70E-01	NA	0	0	0	1
Histidyl-tRNA synthetase, cytoplasmic	SYHC_MOUSE	NO	3,70E-01	NA	6,50E-01	1,24	3,90E-02	0,12	2,10E-02	0,00	9	7	1	0
Threonyl-tRNA synthetase, cytoplasmic	SYTC_MOUSE	NO	3,70E-01	0,00	2,50E-01	0,60	1,50E-01	0,00	5,00E-03	0,13	3	5	0	1
Valyl-tRNA synthetase	SYVC_MOUSE	NO	3,70E-01	0,00	3,60E-01	1,55	5,50E-05	0,00	1,70E-01	0,10	10	7	0	1
Transaldolase	TALDO_MOUSE	NO	3,70E-01	0,72	7,40E-01	1,15	3,90E-02	0,57	7,80E-01	0,91	25	22	14	20
T-complex protein 1 subunit beta	TCPB_MOUSE	NO	3,70E-01	0,00	9,70E-01	1,03	2,70E-02	0,00	1,60E-01	0,10	13	13	0	1
T-complex protein 1 subunit delta	TCPD_MOUSE	NO	3,70E-01	NA	8,70E-01	1,05	6,90E-02	0,07	1,20E-01	0,00	15	14	1	0
T-complex protein 1 subunit epsilon	TCPE_MOUSE	NO	3,70E-01	0,00	3,30E-01	1,46	1,40E-02	0,00	1,60E-02	0,16	18	12	0	2
T-complex protein 1 subunit zeta	TCPZ_MOUSE	NO	3,70E-01	0,00	8,40E-01	1,12	1,80E-02	0,00	7,30E-02	0,23	10	9	0	2
Toll-interacting protein	TOLIP_MOUSE	NO	3,70E-01	0,00	1,00E+00	NA	1,00E+00	NA	3,70E-01	NA	0	0	0	1
Trafficking protein particle complex subunit 3	TPPC3_MOUSE	NO	3,70E-01	0,00	1,00E+00	NA	1,00E+00	NA	3,70E-01	NA	0	0	0	2
UPF0566 protein	U566_MOUSE	NO	3,70E-01	0,00	9,20E-01	1,00	3,70E-01	0,00	9,60E-01	1,00	1	1	0	1
NEDD8-conjugating enzyme Ubc12	UBC12_MOUSE	NO	3,70E-01	0,00	9,80E-01	1,00	3,70E-01	0,00	9,50E-01	1,00	1	1	0	1
Ubiquitin-like protein 4A	UBL4A_MOUSE	NO	3,70E-01	0,00	6,10E-01	0,67	1,20E-01	0,00	2,40E-01	0,22	2	3	0	1
E3 ubiquitin-protein ligase UBR4	UBR4_MOUSE	NO	3,70E-01	0,00	1,00E+00	NA	1,00E+00	NA	3,70E-01	NA	0	0	0	1
Ribonuclease UK114	UK114_MOUSE	NO	3,70E-01	NA	1,00E+00	NA	3,70E-01	NA	1,00E+00	NA	0	0	1	0
Exportin-1	XPO1_MOUSE	NO	3,70E-01	0,00	1,30E-01	3,13	3,50E-02	0,00	4,10E-01	0,38	8	3	0	1
Exportin-2	XPO2_MOUSE	NO	3,70E-01	0,00	1,80E-02	2,22	4,50E-04	0,00	3,80E-02	0,17	13	6	0	1
Nuclease-sensitive element-binding protein 1	YBOX1_MOUSE	YES	3,70E-01	0,00	2,50E-01	1,33	2,30E-03	0,00	6,30E-02	0,27	15	11	0	3
Activator of 90 kDa heat shock protein ATPase homolog 1	AHSA1_MOUSE	NO	3,80E-01	0,45	3,00E-01	0,84	5,90E-02	0,24	4,00E-02	0,44	7	8	2	4
Apoptosis regulator BAX	BAX_MOUSE	NO	3,80E-01	0,72	2,10E-01	1,38	7,60E-01	0,92	5,40E-02	1,77	12	9	11	15
Proteasome subunit beta type-8	PSB8_MOUSE	NO	3,80E-01	1,08	2,00E-01	1,40	1,90E-01	1,14	5,90E-02	1,48	12	8	13	12
Ras-related protein Rab-1A	RAB1A_MOUSE	NO	3,80E-01	0,57	9,40E-01	1,06	9,80E-01	0,68	2,30E-01	1,28	6	6	4	8
Ras-related protein Rab-11B	RB11B_MOUSE	YES	3,80E-01	2,00	7,80E-01	1,11	2,50E-01	0,53	1,00E-01	0,30	10	9	5	3
Thioredoxin domain-containing protein 17	TXD17_MOUSE	NO	3,80E-01	0,27	5,80E-01	1,60	2,30E-01	0,19	8,50E-01	1,10	5	3	1	4
Galectin-3-binding protein	LG3BP_MOUSE	YES	3,90E-01	0,96	2,40E-01	1,17	7,10E-05	1,87	8,50E-04	2,28	66	57	124	129
Ras-related protein Rab-32	RAB32_MOUSE	NO	3,90E-01	2,40	3,70E-01	NA	4,30E-01	2,00	3,70E-01	NA	2	0	4	2
14-3-3 protein beta/alpha	1433B_MOUSE	NO	4,00E-01	0,46	6,50E-01	0,84	7,10E-01	0,62	2,30E-01	1,14	12	15	8	17
Filamin-B	FLNB_MOUSE	YES	4,00E-01	0,41	5,20E-01	1,25	2,70E-02	0,36	9,60E-01	1,10	8	7	3	7
Nidogen-2	NID2_MOUSE	YES	4,00E-01	2,33	1,00E+00	NA	1,20E-01	NA	3,70E-01	NA	0	0	2	1
6-phosphogluconolactonase	6PGL_MOUSE	NO	4,10E-01	0,78	4,40E-01	0,90	3,70E-01	1,02	3,20E-01	1,18	15	16	15	19
Glucosidase 2 subunit beta	GLU2B_MOUSE	NO	4,10E-01	1,23	1,20E-01	NA	4,90E-02	4,00	2,30E-03	NA	1	0	5	4
UMP-CMP kinase	KCY_MOUSE	NO	4,10E-01	1,00	5,20E-01	1,26	2,00E-01	0,53	4,60E-02	0,67	28	22	15	15
V-type proton ATPase subunit S1	VAS1_MOUSE	YES	4,10E-01	1,04	4,20E-01	0,89	1,20E-02	2,37	4,40E-03	2,04	17	19	40	39
Elongation factor 1-beta	EF1B_MOUSE	NO	4,20E-01	0,71	7,60E-01	1,13	1,30E-01	0,50	5,40E-01	0,80	11	10	6	8
Hydroxyacyl-coenzyme A dehydrogenase, mitochondrial	HCDH_MOUSE	NO	4,20E-01	2,25	5,10E-01	2,00	7,00E-01	1,13	9,30E-01	1,00	3	1	3	1
Transitional endoplasmic reticulum ATPase	TERA_MOUSE	NO	4,20E-01	0,78	1,00E-01	0,93	2,40E-03	0,49	1,10E-02	0,59	94	101	46	59
Actin-related protein 2/3 complex subunit 2	ARPC2_MOUSE	YES	4,30E-01	0,78	2,50E-01	1,70	2,10E-01	1,11	2,90E-02	2,39	19	11	21	26
Dihydropteridine reductase	DHPR_MOUSE	NO	4,30E-01	1,14	1,40E-01	2,43	1,60E-01	1,41	4,50E-02	3,00	6	2	8	7
BTB/POZ domain-containing protein KCTD12	KCD12_MOUSE	YES	4,30E-01	0,81	5,80E-01	1,21	4,40E-01	0,71	6,50E-01	1,06	25	21	18	22
Low molecular weight phosphotyrosine protein phosphatase	PPAC_MOUSE	NO	4,30E-01	0,80	3,80E-01	1,25	5,10E-02	0,48	1,90E-01	0,75	8	7	4	5
Cysteinyl-tRNA synthetase, cytoplasmic	SYCC_MOUSE	NO	4,30E-01	0,57	5,90E-01	0,93	2,70E-02	0,29	5,10E-02	0,47	9	10	3	5
Complement C1r-A subcomponent	C1RA_MOUSE	NO	4,40E-01	1,45	1,00E+00	NA	9,40E-03	NA	1,40E-01	NA	0	0	5	4
Proteasome subunit alpha type-7	PSA7_MOUSE	NO	4,40E-01	0,96	8,30E-01	1,02	8,30E-01	0,82	3,90E-01	0,87	18	18	15	16
40S ribosomal protein S12	RS12_MOUSE	NO	4,40E-01	0,62	4,20E-01	1,25	5,80E-02	0,32	8,10E-02	0,65	8	7	3	4
Tumor necrosis factor ligand superfamily member 9	TNFL9_MOUSE	YES	4,40E-01	0,63	1,00E+00	NA	1,20E-01	NA	3,60E-05	NA	0	0	5	8
Vacuolar protein sorting-associated protein 26A	VP26A_MOUSE	NO	4,40E-01	1,37	6,00E-01	0,83	3,40E-01	1,37	7,80E-01	0,83	6	8	9	6
Leukocyte immunoglobulin-like receptor subfamily B member 4	LIRB4_MOUSE	YES	4,50E-01	2,25	1,00E+00	NA	1,60E-01	NA	3,70E-01	NA	0	0	3	1
N-acetyltransferase NAT13	NAT13_MOUSE	NO	4,50E-01	2,25	1,00E+00	NA	1,50E-01	NA	3,70E-01	NA	0	0	3	1
Ras-related C3 botulinum toxin substrate 1	RAC1_MOUSE	YES	4,50E-01	0,67	4,00E-01	0,87	6,50E-01	0,73	8,60E-01	0,95	11	13	8	12
Retinoid-inducible serine carboxypeptidase	RISC_MOUSE	YES	4,50E-01	1,63	1,30E-01	2,44	5,60E-01	1,18	5,80E-01	1,78	7	3	9	5
Ubiquitin-conjugating enzyme E2 variant 2	UB2V2_MOUSE	NO	4,50E-01	0,62	9,50E-01	1,06	2,10E-01	0,42	1,90E-01	0,72	6	6	3	4
Peptidyl-prolyl cis-trans isomerase A	PPIA_MOUSE	NO	4,60E-01	0,86	6,50E-01	1,02	1,10E-02	0,68	9,10E-02	0,80	227	224	154	180
Puromycin-sensitive aminopeptidase	PSA_MOUSE	NO	4,60E-01	0,38	3,20E-01	1,36	1,20E-02	0,07	8,90E-03	0,24	15	11	1	3
tRNA methyltransferase 112 homolog	TR112_MOUSE	NO	4,60E-01	0,43	7,40E-01	1,67	8,10E-01	0,60	4,00E-01	2,33	2	1	1	2
V-type proton ATPase subunit B, brain isoform	VATB2_MOUSE	YES	4,60E-01	0,31	2,50E-01	1,33	2,70E-03	0,09	1,60E-01	0,40	18	13	2	5
WD repeat-containing protein 1	WDR1_MOUSE	NO	4,60E-01	0,77	7,80E-01	1,02	1,90E-03	0,29	1,20E-03	0,38	83	81	24	31
AP-1 complex subunit beta-1	AP1B1_MOUSE	NO	4,70E-01	0,40	6,00E-01	1,29	3,70E-02	0,04	1,80E-02	0,14	15	12	1	2
Bleomycin hydrolase	BLMH_MOUSE	NO	4,70E-01	1,25	7,90E-01	0,98	2,40E-01	0,61	8,40E-02	0,48	14	14	8	7
Protein disulfide-isomerase A6	PDIA6_MOUSE	YES	4,70E-01	1,09	1,00E+00	1,06	7,90E-02	0,55	1,80E-02	0,53	29	28	16	15
26S proteasome non-ATPase regulatory subunit 9	PSMD9_MOUSE	NO	4,70E-01	1,42	1,70E-01	2,75	2,10E-01	1,55	3,30E-01	3,00	4	1	6	4
Tumor protein D52	TPD52_MOUSE	NO	4,70E-01	1,08	3,30E-01	0,86	8,40E-02	0,50	1,00E-02	0,40	19	22	9	9
14-3-3 protein theta	1433T_MOUSE	NO	4,80E-01	0,93	9,80E-02	1,23	6,20E-01	0,86	2,70E-01	1,14	14	12	12	13
Ferritin light chain 1	FRIL1_MOUSE	NO	4,80E-01	0,86	9,70E-01	1,05	3,30E-01	0,92	3,60E-01	1,13	34	32	31	36
Insulin-like growth factor-binding protein 4	IBP4_MOUSE	YES	4,80E-01	1,21	1,70E-01	0,67	9,50E-01	0,85	8,40E-02	0,47	7	10	6	5
Dihydrofolate reductase	DYR_MOUSE	NO	4,90E-01	0,43	1,60E-01	0,56	3,90E-01	0,33	7,00E-02	0,44	3	5	1	2
Glutathione S-transferase omega-1	GSTO1_MOUSE	NO	4,90E-01	1,06	5,80E-01	1,17	7,30E-01	0,90	8,10E-01	1,00	7	6	6	6
Malate dehydrogenase, mitochondrial	MDHM_MOUSE	NO	4,90E-01	1,00	9,80E-01	1,05	2,50E-01	1,08	4,10E-01	1,13	37	35	40	40
Thioredoxin domain-containing protein 12	TXD12_MOUSE	NO	4,90E-01	0,43	8,60E-01	0,92	3,80E-01	0,25	2,40E-01	0,54	4	4	1	2
Proto-oncogene tyrosine-protein kinase MER	MERTK_MOUSE	NO	5,00E-01	1,67	7,40E-01	2,00	5,30E-01	1,67	6,10E-01	2,00	2	1	3	2
Alpha-soluble NSF attachment protein	SNAA_MOUSE	NO	5,00E-01	1,23	6,70E-01	1,27	7,60E-01	0,96	9,60E-01	1,00	9	7	9	7
Superoxide dismutase [Mn], mitochondrial	SODM_MOUSE	NO	5,00E-01	0,43	4,80E-01	1,40	5,50E-02	0,21	7,60E-01	0,70	5	3	1	2
Di-N-acetylchitobiase	DIAC_MOUSE	NO	5,10E-01	0,44	1,00E+00	NA	3,70E-01	NA	1,60E-01	NA	0	0	1	3
Guanine nucleotide-binding protein subunit beta-2-like 1	GBLP_MOUSE	YES	5,10E-01	0,78	6,60E-01	1,14	2,30E-01	0,60	2,90E-01	0,87	32	28	19	25
Protein jagged-1	JAG1_MOUSE	YES	5,10E-01	1,31	1,00E+00	NA	5,80E-04	NA	1,40E-01	NA	0	0	13	10
Lysozyme C-2	LYZ2_MOUSE	YES	5,10E-01	0,82	5,20E-01	1,26	7,70E-01	0,88	2,00E-01	1,36	105	83	92	113
Isocitrate dehydrogenase [NADP] cytoplasmic	IDHC_MOUSE	NO	5,20E-01	1,30	6,80E-01	0,99	2,20E-01	0,52	2,80E-02	0,40	27	28	14	11
Proliferating cell nuclear antigen	PCNA_MOUSE	NO	5,20E-01	1,19	6,50E-01	1,22	6,90E-01	0,72	3,80E-01	0,74	24	19	17	14
Proteasome subunit beta type-6	PSB6_MOUSE	NO	5,20E-01	1,31	9,30E-02	0,60	4,70E-01	1,13	2,00E-01	0,52	5	8	6	4
Leukotriene A-4 hydrolase	LKHA4_MOUSE	NO	5,30E-01	1,67	9,20E-01	1,00	3,20E-01	0,31	1,60E-02	0,19	11	11	3	2
Mannosyl-oligosaccharide 1,2-alpha-mannosidase IA	MA1A1_MOUSE	NO	5,30E-01	1,11	1,30E-02	0,59	7,20E-03	3,59	1,30E-01	1,89	9	15	32	29
Nucleoside diphosphate kinase A	NDKA_MOUSE	NO	5,30E-01	0,99	1,80E-01	1,24	4,50E-01	0,94	1,50E-01	1,17	31	25	29	29
Programmed cell death 6-interacting protein	PDC6I_MOUSE	NO	5,30E-01	0,83	9,20E-01	1,02	7,70E-04	0,27	1,40E-02	0,33	43	42	12	14
14-3-3 protein eta	1433F_MOUSE	NO	5,40E-01	0,67	1,80E-01	1,07	2,70E-01	0,68	2,90E-01	1,09	21	19	14	21
Macrophage colony-stimulating factor 1	CSF1_MOUSE	YES	5,40E-01	1,38	1,00E+00	NA	1,20E-01	NA	2,50E-03	NA	0	0	4	3

Serine/threonine-protein phosphatase 2A regulatory subunit B'	PTPA_MOUSE	NO	5,40E-01	0,61	8,60E-01	1,08	2,40E-01	0,41	1,60E-01	0,72	9	8	4	6
Ribonuclease T2	RNT2_MOUSE	YES	5,40E-01	1,16	3,70E-01	NA	3,90E-02	16,67	2,40E-03	NA	1	0	17	14
SH3 domain-binding glutamic acid-rich-like protein 3	SH3L3_MOUSE	NO	5,40E-01	1,03	8,10E-02	0,78	6,90E-01	0,79	2,20E-02	0,60	16	20	12	12
Actin-related protein 2/3 complex subunit 4	ARPC4_MOUSE	NO	5,50E-01	0,83	6,80E-01	0,97	1,90E-02	0,54	8,00E-02	0,63	30	31	16	20
ELAV-like protein 1	ELAV1_MOUSE	NO	5,50E-01	0,53	6,90E-01	0,50	3,30E-01	4,00	2,30E-01	3,75	1	1	3	5
Exostosin-like 2	EXTL2_MOUSE	NO	5,50E-01	1,75	1,00E+00	NA	1,30E-01	NA	3,70E-01	NA	0	0	2	1
V-type proton ATPase subunit D	VATD_MOUSE	NO	5,50E-01	0,75	8,70E-01	1,09	3,60E-01	1,25	1,70E-01	1,82	4	4	5	7
Carbonic anhydrase 1	CAH1_MOUSE	NO	5,60E-01	1,33	1,00E+00	NA	1,30E-01	NA	2,70E-03	NA	0	0	5	4
Ezrin	EZRI_MOUSE	YES	5,60E-01	1,00	1,10E-01	0,96	1,20E-01	0,86	1,80E-02	0,83	7	8	6	6
Glycogen phosphorylase, brain form	PYGB_MOUSE	NO	5,60E-01	0,50	6,70E-01	1,17	4,20E-04	0,05	1,60E-02	0,11	14	12	1	1
Ras suppressor protein 1	RSU1_MOUSE	NO	5,60E-01	0,55	9,50E-05	0,00	1,20E-01	NA	7,40E-01	1,22	0	3	2	4
Gelsolin	GELS_MOUSE	YES	5,70E-01	0,96	7,20E-01	1,01	7,90E-02	0,64	6,80E-03	0,67	86	85	55	57
cAMP-dependent protein kinase catalytic subunit alpha	KAPCA_MOUSE	YES	5,70E-01	0,50	1,30E-01	NA	4,80E-01	0,40	1,20E-01	NA	2	0	1	1
Protein transport protein Sec23B	SC23B_MOUSE	NO	5,70E-01	0,54	4,50E-01	0,56	9,40E-01	0,78	5,70E-01	0,81	3	5	2	4
Lactoylglutathione lyase	LGUL_MOUSE	NO	5,80E-01	0,83	7,20E-01	1,44	5,70E-01	1,15	3,00E-01	2,00	4	3	5	6
Peptidyl-prolyl cis-trans isomerase NIMA-interacting 1	PIN1_MOUSE	NO	5,80E-01	0,85	1,10E-01	0,50	5,80E-01	1,10	4,00E-02	0,65	3	7	4	4
Proteasome activator complex subunit 2	PSME2_MOUSE	NO	5,80E-01	0,61	5,10E-01	1,61	2,80E-01	0,46	8,40E-01	1,22	12	8	6	9
Rab GDP dissociation inhibitor beta	GDIB_MOUSE	NO	5,90E-01	0,94	3,60E-01	0,96	8,60E-06	0,35	1,30E-03	0,36	117	121	41	44
Thymosin beta-4	TYB4_MOUSE	NO	5,90E-01	0,71	3,10E-01	0,76	1,80E-01	0,38	1,70E-02	0,41	9	11	3	5
Ubiquitin-conjugating enzyme E2 N	UBE2N_MOUSE	NO	5,90E-01	1,08	1,60E-01	1,50	5,70E-02	0,39	8,00E-03	0,54	12	8	5	4
Urokinase-type plasminogen activator	UROK_MOUSE	YES	5,90E-01	1,75	9,30E-02	0,37	1,40E-01	0,18	2,30E-02	0,04	13	34	2	1
Apoptosis-associated speck-like protein containing a CARD	ASC_MOUSE	YES	6,00E-01	0,78	1,00E-01	1,32	2,70E-03	0,44	2,70E-01	0,74	22	17	10	12
C-C motif chemokine 5	CCL5_MOUSE	YES	6,00E-01	1,33	1,00E+00	NA	1,20E-01	NA	1,20E-01	NA	0	0	3	2
Dipeptidyl-peptidase 2	DPP2_MOUSE	YES	6,00E-01	1,32	4,80E-02	3,00	8,90E-01	0,93	9,20E-02	2,11	9	3	8	6
EMILIN-2	EMIL2_MOUSE	YES	6,00E-01	1,01	9,30E-01	1,14	4,10E-04	18,00	6,80E-03	20,29	3	2	48	47
Haptoglobin	HPT_MOUSE	YES	6,00E-01	0,79	1,00E+00	NA	2,90E-03	NA	3,40E-03	NA	0	0	11	14
Pyridoxal kinase	PDXK_MOUSE	NO	6,00E-01	1,02	9,20E-01	1,04	3,30E-01	0,98	8,40E-01	1,00	19	18	19	18
Actin-related protein 2	ARP2_MOUSE	NO	6,10E-01	1,09	2,60E-01	1,48	4,00E-01	0,61	3,40E-01	0,83	47	32	29	26
Cathepsin S	CATS_MOUSE	NO	6,10E-01	0,97	5,80E-01	1,12	1,80E-03	1,63	1,30E-02	1,87	162	145	264	272
Glyoxalase domain-containing protein 4	GLOD4_MOUSE	NO	6,10E-01	1,00	5,60E-01	0,88	1,60E-02	2,14	4,40E-02	1,88	5	5	10	10
Epididymal secretory protein E1	NPC2_MOUSE	YES	6,10E-01	0,94	9,20E-01	1,03	3,60E-01	1,03	4,30E-01	1,13	21	20	21	23
Spliceosome RNA helicase Bat1	UAP56_MOUSE	NO	6,10E-01	1,57	1,60E-02	1,81	8,60E-03	0,19	1,10E-02	0,22	19	11	4	2
Wiskott-Aldrich syndrome protein family member 2	WASF2_MOUSE	NO	6,10E-01	1,67	3,70E-01	0,00	1,30E-01	NA	7,50E-01	1,50	0	1	2	1
Mitogen-activated protein kinase 1	MK01_MOUSE	NO	6,30E-01	1,60	7,90E-01	1,25	9,20E-01	0,80	7,50E-01	0,63	3	3	3	2
Proteasome subunit beta type-1	PSB1_MOUSE	NO	6,30E-01	0,80	7,70E-01	1,00	3,50E-02	0,52	2,10E-01	0,65	21	21	11	13
Spermidine synthase	SPEE_MOUSE	NO	6,30E-01	1,25	3,30E-01	3,00	2,80E-01	2,50	2,00E-02	6,00	2	1	5	4
Alpha-actinin-4	ACTN4_MOUSE	NO	6,40E-01	0,93	1,30E-01	1,18	1,70E-04	0,38	1,10E-03	0,48	172	146	66	70
Ceruloplasmin	CERU_MOUSE	YES	6,40E-01	1,01	1,00E+00	NA	1,30E-06	NA	7,70E-03	NA	0	0	94	94
Coatomer subunit alpha	COPA_MOUSE	YES	6,40E-01	1,40	4,90E-01	0,68	1,10E-01	0,21	7,90E-02	0,10	11	17	2	2
Glucose-6-phosphate isomerase	G6PI_MOUSE	YES	6,40E-01	0,81	3,70E-01	0,90	1,20E-02	0,38	1,40E-02	0,43	94	105	36	45
Glucosamine-6-phosphate isomerase 1	GNPI1_MOUSE	NO	6,40E-01	1,03	3,10E-01	0,88	9,30E-01	0,86	1,70E-01	0,73	12	14	10	10
Proteasome subunit alpha type-1	PSA1_MOUSE	NO	6,40E-01	1,04	3,80E-01	0,84	5,10E-01	1,04	5,10E-01	0,84	16	19	16	16
Ras-related protein Rab-7a	RAB7A_MOUSE	NO	6,40E-01	0,83	6,50E-01	1,17	3,70E-02	0,48	2,40E-01	0,67	14	12	7	8
Actin-related protein 2/3 complex subunit 3	ARPC3_MOUSE	NO	6,50E-01	0,83	5,10E-01	0,89	1,20E-01	0,44	1,20E-02	0,47	18	21	8	10
Dynactin subunit 3	DCTN3_MOUSE	NO	6,50E-01	0,40	1,00E+00	NA	3,70E-01	NA	3,70E-01	NA	0	0	1	2
Arginyl-tRNA synthetase, cytoplasmic	SYRC_MOUSE	NO	6,50E-01	0,67	8,20E-01	1,13	3,50E-01	0,47	6,40E-01	0,80	6	5	3	4
Vesicle-associated membrane protein-associated protein A	VAPA_MOUSE	YES	6,50E-01	1,08	1,60E-01	0,45	6,80E-01	1,08	1,10E-01	0,45	4	10	5	4
Cystatin-B	CYTB_MOUSE	NO	6,60E-01	0,82	2,00E-01	0,90	1,30E-03	0,33	3,30E-03	0,36	47	52	16	19
Dynein light chain 2, cytoplasmic	DYL2_MOUSE	NO	6,60E-01	2,00	6,30E-02	0,27	6,30E-01	2,00	8,50E-02	0,27	1	4	2	1
Procollagen-lysine,2-oxoglutarate 5-dioxygenase 3	PLOD3_MOUSE	NO	6,60E-01	2,00	1,00E+00	NA	3,70E-01	NA	3,70E-01	NA	0	0	3	1
Peroxiredoxin-5, mitochondrial	PRDX5_MOUSE	NO	6,60E-01	0,86	9,40E-02	1,28	7,90E-01	0,81	6,70E-02	1,21	34	27	28	32
SLAM family member 7	SLAF7_MOUSE	YES	6,60E-01	0,79	1,00E+00	NA	1,80E-02	NA	9,10E-03	NA	0	0	13	16
Moesin	MOES_MOUSE	YES	6,70E-01	0,86	8,70E-01	1,07	5,90E-02	0,61	7,90E-02	0,75	128	119	77	90
Myotrophin	MTPN_MOUSE	NO	6,70E-01	0,80	1,40E-01	0,78	4,50E-01	0,69	1,30E-01	0,68	10	12	7	8
Septin-7	SEPT7_MOUSE	NO	6,70E-01	0,40	4,50E-01	0,89	3,40E-02	0,13	5,30E-02	0,28	11	12	1	3
Acid ceramidase	ASAH1_MOUSE	NO	6,80E-01	1,75	4,70E-01	1,21	6,20E-02	0,21	3,90E-04	0,14	11	9	2	1
Calcyclin-binding protein	CYBP_MOUSE	NO	6,80E-01	0,60	1,00E+00	NA	3,70E-01	NA	1,30E-01	NA	0	0	1	2
Protein DJ-1	PARK7_MOUSE	NO	6,80E-01	0,84	2,20E-02	1,73	1,00E-01	0,60	1,60E-01	1,23	15	9	9	11
Ubiquitin-conjugating enzyme E2 L3	UB2L3_MOUSE	NO	6,80E-01	0,73	2,20E-01	1,38	1,80E-02	0,22	2,60E-02	0,42	12	9	3	4
EGF-like module-containing mucin-like hormone receptor-like 1	EMR1_MOUSE	YES	6,90E-01	0,86	9,00E-01	1,25	8,10E-03	6,00	1,80E-03	8,75	2	1	10	12
NSFL1 cofactor p47	NSF1C_MOUSE	NO	6,90E-01	0,77	2,40E-01	1,44	5,30E-01	0,64	3,60E-01	1,20	12	8	8	10
Xaa-Pro dipeptidase	PEPD_MOUSE	NO	6,90E-01	1,28	4,50E-01	1,43	2,10E-01	0,46	5,10E-01	0,51	17	12	8	6
N-acetylglucosamine-6-sulfatase	GNS_MOUSE	NO	7,00E-01	0,97	1,80E-02	1,68	3,40E-01	0,95	9,90E-02	1,64	12	7	12	12
Napsin-A	NAPSA_MOUSE	YES	7,00E-01	1,40	7,60E-01	0,75	3,50E-01	2,33	9,20E-01	1,25	1	1	2	2
5'(3')-deoxyribonucleotidase, cytosolic type	NT5C_MOUSE	NO	7,00E-01	0,86	2,40E-01	1,44	3,70E-02	0,46	2,80E-01	0,78	9	6	4	5
Ubiquitin-conjugating enzyme E2 K	UBE2K_MOUSE	NO	7,00E-01	1,08	7,90E-01	1,13	1,00E-01	0,52	2,10E-01	0,54	9	8	5	4
Cathepsin H	CATH_MOUSE	NO	7,10E-01	0,76	1,00E+00	NA	6,00E-03	NA	4,10E-02	NA	0	0	4	6
Inositol monophosphatase	IMPA1_MOUSE	NO	7,10E-01	1,43	8,10E-01	0,85	9,10E-01	0,91	6,50E-01	0,54	4	4	3	2
Peroxiredoxin-6	PRDX6_MOUSE	NO	7,10E-01	0,82	9,80E-01	1,05	2,30E-01	0,63	2,00E-01	0,81	39	37	24	30
Thioredoxin	THIO_MOUSE	YES	7,20E-01	0,84	3,80E-01	0,78	9,80E-01	0,84	3,20E-01	0,78	8	11	7	8
Growth factor receptor-bound protein 2	GRB2_MOUSE	NO	7,30E-01	0,84	9,30E-01	1,07	1,50E-02	0,36	1,80E-02	0,45	15	14	5	6
Heterogeneous nuclear ribonucleoproteins A2/B1	ROA2_MOUSE	NO	7,30E-01	0,85	2,00E-01	0,89	9,20E-01	0,82	3,00E-01	0,87	47	53	39	46
Serotransferrin	TRFE_MOUSE	YES	7,30E-01	0,93	5,30E-02	1,52	5,90E-01	0,78	1,20E-02	1,27	111	73	86	93
COP9 signalosome complex subunit 7a	CSN7A_MOUSE	NO	7,40E-01	0,67	9,80E-01	1,00	7,40E-01	1,50	3,20E-01	2,25	1	1	2	3
Carboxypeptidase D	CBPD_MOUSE	NO	7,50E-01	1,50	1,00E+00	NA	3,70E-01	NA	3,70E-01	NA	0	0	1	1
C-C motif chemokine 8	CCL8_MOUSE	YES	7,50E-01	1,17	1,00E+00	NA	5,20E-02	NA	1,30E-01	NA	0	0	5	4
C-type lectin domain family 6 member A	CLC6A_MOUSE	NO	7,50E-01	0,64	1,00E+00	NA	1,90E-01	NA	2,50E-01	NA	0	0	2	4
Interleukin-6	IL6_MOUSE	YES	7,50E-01	0,86	1,00E+00	NA	1,50E-03	NA	4,20E-04	NA	0	0	50	58
Isochorismatase domain-containing protein 1	ISOC1_MOUSE	NO	7,50E-01	0,63	8,70E-01	0,75	6,90E-01	1,67	4,90E-01	2,00	1	1	2	3
Beta-mannosidase	MANBA_MOUSE	NO	7,50E-01	1,50	3,80E-01	2,67	9,10E-01	0,75	7,20E-01	1,33	3	1	2	1
14-3-3 protein epsilon	1433E_MOUSE	NO	7,60E-01	0,96	2,90E-01	1,21	6,80E-01	0,92	2,50E-01	1,15	47	39	43	45
Cytosolic 5'-nucleotidase 3	5NT3_MOUSE	NO	7,60E-01	0,83	1,00E+00	NA	2,00E-02	NA	2,10E-03	NA	0	0	7	8
Nucleoside diphosphate kinase B	NDKB_MOUSE	YES	7,60E-01	1,00	4,20E-01	1,00	5,20E-01	0,30	3,50E-01	0,30	8	8	2	2
Stathmin	STMN1_MOUSE	NO	7,60E-01	0,70	4,40E-01	1,20	9,20E-03	0,17	1,50E-02	0,29	14	12	2	3
Enhancer of rudimentary homolog	ERH_MOUSE	NO	7,70E-01	1,50	2,20E-01	2,80	1,10E-01	0,21	6,40E-01	0,40	5	2	1	1
Galectin-1	LEG1_MOUSE	YES	7,70E-01	0,87	4,20E-01	0,96	2,10E-01	0,67	7,90E-02	0,74	29	30	19	22
Dual specificity mitogen-activated protein kinase kinase 1	MP2K1_MOUSE	NO	7,70E-01	1,50	7,90E-01	0,67	7,30E-01	1,50	8,40E-01	0,67	1	1	1	1
Phosphoserine aminotransferase	SERC_MOUSE	NO	7,70E-01	1,33	9,20E-01	1,05	1,10E-01	0,38	1,30E-01	0,30	7	7	3	2
Actin-related protein 3	ARP3_MOUSE	NO	7,80E-01	0,95	4,10E-02	0,85	3,30E-02	0,54	9,80E-04	0,48	100	118	54	57
Macrophage-capping protein	CAPG_MOUSE	YES	7,80E-01	0,87	5,60E-01	0,96	1,90E-01	0,67	1,10E-01	0,74	62	65	42	48
60S ribosomal protein L10a	RL10A_MOUSE	NO	7,80E-01	1,00	1,00E-01	0,60	9,30E-02	2,56	8,10E-02	1,53	3	5	8	8
Translationally-controlled tumor protein	TCTP_MOUSE	NO	7,80E-01	0,98	8,80E-01	1,14	6,40E-01	0,73	6,80E-01	0,86	19	16	14	14
Thioredoxin reductase 1, cytoplasmic	TRXR1_MOUSE	NO	7,80E-01	0,67	1,60E-01	1,65	6,40E-03	0,07	4,40E-02	0,18	19	11	1	2
Thioredoxin-like protein 1	TXNL1_MOUSE	NO	7,80E-01	0,96	5,20E-01	0,88	1,20E-01	1,38	2,20E-01	1,26	12	14	17	18
Insulin-like growth factor I	IGF1_MOUSE	YES	7,90E-01	0,95	6,00E-01	0,98	7,90E-03	0,43	1,30E-02	0,44	16	17	7	7
Meteorin-like protein	METRL_MOUSE	YES	7,90E-01	0,83	7,10E-01	1,50	5,00E-02	7,33	2,20E-04	13,25	2	1	15	18
Lysosomal Pro-X carboxypeptidase	PCP_MOUSE	NO	7,90E-01	1,00	8,00E-01	1,33	2,60E-01	1,67	1,80E-01	2,22	4	3	7	7
60S ribosomal protein L12	RL12_MOUSE	NO	7,90E-01	0,86	7,20E-01	1,13	6,70E-03	0,38	3,20E-02	0,51	26	23	10	12
Translin	TSN_MOUSE	NO	8,00E-01	0,75	7,70E-01	0,97	2,00E-02	0,21	2,40E-02	0,28	9	10	2	3
Calreticulin	CALR_MOUSE	YES	8,10E-01	0,98	5,90E-01	1,18	4,50E-02	0,52	1,80E-01	0,63	33	28	17	17
FK506-binding protein 3	FKBP3_MOUSE	NO	8,10E-01	1,20	2,30E-02	0,21	5,60E-01	1,50	7,20E-02	0,26	1	6	2	2
Inter-alpha-trypsin inhibitor heavy chain H3	ITIH3_MOUSE	YES	8,10E-01	1,20	1,00E+00	NA	3,70E-01	NA	3,70E-01	NA	0	0	2	2
Phosphoglycerate kinase 1	PGK1_MOUSE	NO	8,10E-01	0,94	7,80E-01	1,08	9,40E-02	0,62	1,20E-02	0,71	210	195	131	139
Aspartate aminotransferase, cytoplasmic	AATC_MOUSE	NO	8,20E-01	0,80	2,10E-01	0,86	2,50E-01	0,48	5,20E-03	0,52	8	10	4	5
Disintegrin and metalloproteinase domain-containing protein 17	ADA17_MOUSE	YES	8,20E-01	0,87	1,00E+00	NA	3,40E-03	NA	9,90E-06	NA	0	0	9	10
UPF0160 protein MYG1, mitochondrial	MYG1_MOUSE	NO	8,20E-01	0,67	4,60E-01	1,22	3,90E-03	0,07	1,00E-02	0,13	9	8	1	1
Heat shock 70 kDa protein 4	HSP74_MOUSE	NO	8,30E-01	0,86	4,30E-01	1,27	4,70E-02	0,46	3,00E-01	0,68	78	61	36	42
Beta-1,3-N-acetylglucosaminyltransferase lunatic fringe	LFNG_MOUSE	NO	8,30E-01	1,00	1,20E-01	0,27	1,60E-02	6,00	3,80E-01	1,60	1	5	8	8
26S proteasome non-ATPase regulatory subunit 7	PSD7_MOUSE	NO	8,30E-01	0,85	9,80E-01	1,17	1,70E-01	1,57	3,10E-01	2,17	2	2	4	4
Protein FAM49B	FA49B_MOUSE	NO	8,40E-01	0,88	5,20E-01	1,17	9,50E-02	1,06	1,20E-01	1,41	23	20	24	28
Sorcin	SORCN_MOUSE	YES	8,40E-01	0,60	3,00E-01	0,75	1,60E-01	0,25	1,10E-01	0,31	4	5	1	2
Prostaglandin E synthase 3	TEBP_MOUSE	NO	8,40E-01	0,75	5,00E-01	1,50	3,20E-01	0,50	9,70E-01	1,00	6	4	3	4
C-C motif chemokine 2	CCL2_MOUSE	YES	8,50E-01	0,94	1,00E+00	NA	6,30E-04	NA	4,40E-03	NA	0	0	22	24
CD5 antigen-like	CD5L_MOUSE	YES	8,50E-01	1,22	2,80E-01	0,86	1,80E-02	0,18	6,10E-03	0,13	21	24	4	3
Beta-hexosaminidase subunit alpha	HEXA_MOUSE	NO	8,50E-01	0,92	6,40E-03	1,42	3,40E-01	0,89	2,20E-02	1,38	44	31	39	43
High mobility group protein B1	HMGB1_MOUSE	YES	8,50E-01	0,92	1,00E+00	NA	2,70E-03	NA	6,70E-03	NA	0	0	7	8

Programmed cell death protein 6	PDCD6_MOUSE	NO	8,50E-01	0,67	3,70E-01	3,00	4,60E-01	0,33	7,40E-01	1,50	2	1	1	1
Proteasome subunit alpha type-3	PSA3_MOUSE	NO	8,50E-01	0,87	7,60E-01	1,00	2,20E-01	1,18	1,20E-01	1,35	11	11	13	15
Chromobox protein homolog 3	CBX3_MOUSE	NO	8,60E-01	0,95	3,10E-01	1,13	3,00E-02	0,48	3,60E-03	0,56	15	13	7	7
Coatomer subunit delta	COPD_MOUSE	NO	8,60E-01	0,81	9,50E-01	1,03	3,10E-01	0,42	2,70E-02	0,53	10	10	4	5
Ubiquitin thioesterase OTUB1	OTUB1_MOUSE	NO	8,60E-01	0,94	2,90E-01	1,16	4,30E-01	1,00	6,60E-02	1,24	10	8	10	10
40S ribosomal protein S18	RS18_MOUSE	NO	8,60E-01	0,87	6,90E-01	0,95	4,50E-01	0,72	4,10E-01	0,79	6	6	4	5
Alcohol dehydrogenase [NADP+]	AK1A1_MOUSE	YES	8,70E-01	0,92	2,70E-01	0,90	9,40E-02	0,70	5,80E-02	0,68	47	52	33	36
Integrin beta-1	ITB1_MOUSE	YES	8,70E-01	0,88	3,20E-01	0,33	3,10E-02	7,00	4,40E-02	2,67	1	2	5	5
Disintegrin and metalloproteinase domain-containing protein 10	ADA10_MOUSE	YES	8,80E-01	1,20	1,00E+00	NA	3,70E-01	NA	3,70E-01	NA	0	0	2	2
Eukaryotic translation initiation factor 4H	IF4H_MOUSE	NO	8,80E-01	0,75	3,30E-01	3,00	3,90E-01	0,33	8,00E-01	1,33	3	1	1	1
Synaptic vesicle membrane protein VAT-1 homolog	VAT1_MOUSE	NO	8,80E-01	0,84	9,40E-01	1,04	3,40E-02	0,20	1,50E-02	0,25	52	50	10	12
Aminopeptidase B	AMPB_MOUSE	YES	8,90E-01	0,87	1,80E-01	1,36	2,70E-04	0,28	6,00E-02	0,44	49	36	14	16
Actin-related protein 2/3 complex subunit 5	ARPC5_MOUSE	NO	8,90E-01	0,86	4,40E-01	1,17	1,80E-01	0,65	6,20E-01	0,88	16	14	11	12
Charged multivesicular body protein 4b	CHM4B_MOUSE	NO	8,90E-01	0,94	1,00E+00	NA	2,10E-02	NA	1,90E-03	NA	0	0	5	6
Fatty acid synthase	FAS_MOUSE	NO	8,90E-01	0,95	8,70E-01	0,98	1,40E-01	0,37	1,40E-02	0,38	18	18	7	7
Proto-oncogene C-crk	CRK_MOUSE	YES	9,00E-01	0,82	8,50E-01	1,20	5,20E-01	1,50	4,50E-01	2,20	2	2	3	4
Protein tyrosine kinase 2 beta	FAK2_MOUSE	YES	9,00E-01	1,00	1,00E+00	NA	3,70E-01	NA	3,70E-01	NA	0	0	1	1
Eukaryotic translation initiation factor 1A	IF1A_MOUSE	NO	9,00E-01	1,00	4,60E-01	0,44	5,90E-01	1,50	7,00E-01	0,67	1	3	2	2
Proliferation-associated protein 2G4	PA2G4_MOUSE	NO	9,00E-01	0,82	7,90E-01	1,13	1,70E-01	0,43	3,00E-01	0,60	18	16	8	9
Polypeptide N-acetylgalactosaminyltransferase 6	GALT6_MOUSE	NO	9,10E-01	0,95	1,00E+00	1,00	2,10E-02	5,00	7,70E-02	5,25	1	1	7	7
Glutamate--cysteine ligase regulatory subunit	GSH0_MOUSE	NO	9,10E-01	0,89	2,10E-01	0,43	1,10E-01	2,67	6,10E-02	1,29	2	5	5	6
L-lactate dehydrogenase A chain	LDHA_MOUSE	NO	9,10E-01	0,91	9,30E-01	1,05	8,80E-01	0,85	9,70E-01	0,98	136	129	116	127
Glutaminyl-peptide cyclotransferase	QPCT_MOUSE	YES	9,10E-01	0,75	1,00E+00	NA	3,70E-01	NA	3,70E-01	NA	0	0	1	1
Heterogeneous nuclear ribonucleoprotein F	HNRPF_MOUSE	NO	9,20E-01	0,95	8,30E-01	0,94	6,00E-01	0,56	4,30E-01	0,56	11	11	6	6
Isopentenyl-diphosphate Delta-isomerase 1	IDI1_MOUSE	NO	9,20E-01	1,00	3,70E-01	0,00	1,30E-01	NA	4,00E-01	2,33	0	1	2	2
Interleukin-27 subunit beta	IL27B_MOUSE	YES	9,20E-01	0,82	1,00E+00	NA	3,70E-01	NA	3,70E-01	NA	0	0	3	4
Galectin-3	LEG3_MOUSE	YES	9,20E-01	0,89	8,00E-01	1,06	8,00E-02	1,09	2,40E-02	1,30	93	88	102	114
Lipoprotein lipase	LIPL_MOUSE	YES	9,20E-01	0,90	2,80E-03	0,71	8,80E-01	0,83	5,70E-02	0,66	89	125	74	83
Ras-related protein Rab-2A	RAB2A_MOUSE	NO	9,20E-01	0,88	2,30E-01	1,64	8,50E-01	0,78	1,80E-01	1,45	6	4	5	5
14-3-3 protein gamma	1433G_MOUSE	NO	9,30E-01	1,00	1,60E-01	1,54	7,70E-01	0,83	3,00E-01	1,27	13	9	11	11
Histone H4	H4_MOUSE	NO	9,30E-01	0,94	5,30E-01	1,24	9,00E-01	0,81	7,00E-01	1,06	7	6	6	6
Protein S100-A13	S10AD_MOUSE	YES	9,30E-01	1,00	3,70E-01	0,00	3,70E-01	NA	8,10E-01	0,67	0	1	1	1
UDP-N-acetylhexosamine pyrophosphorylase-like protein 1	UAP1L_MOUSE	NO	9,30E-01	0,94	3,20E-01	0,92	5,60E-03	0,29	5,50E-03	0,28	35	38	10	11
SH3 domain-binding glutamic acid-rich-like protein	SH3L1_MOUSE	NO	9,40E-01	0,89	4,00E-01	1,35	5,90E-01	0,74	5,70E-01	1,12	15	11	11	13
Beta-1,4-galactosyltransferase 5	B4GT5_MOUSE	NO	9,50E-01	0,90	1,00E+00	NA	1,50E-03	NA	6,80E-03	NA	0	0	15	17
Transcription elongation factor B polypeptide 2	ELOB_MOUSE	NO	9,50E-01	0,80	3,70E-01	0,00	3,70E-01	NA	7,60E-01	0,71	0	2	1	2
Prothrombin	THRB_MOUSE	NO	9,50E-01	0,85	1,00E+00	NA	2,00E-01	NA	9,70E-03	NA	0	0	4	4
Transmembrane glycoprotein NMB	GPNMB_MOUSE	YES	9,60E-01	0,91	7,40E-02	1,39	2,10E-01	0,74	2,20E-01	1,13	31	22	23	25
Thrombospondin-1	TSP1_MOUSE	NO	9,60E-01	0,90	3,30E-01	0,50	5,00E-04	40,83	1,40E-02	22,58	2	4	82	90
Ankyrin repeat and FYVE domain-containing protein 1	ANFY1_MOUSE	NO	9,70E-01	1,00	4,30E-01	1,43	4,80E-02	0,13	7,20E-02	0,19	10	7	1	1
3'(2'),5'-bisphosphate nucleotidase 1	BPNT1_MOUSE	NO	9,70E-01	1,00	1,00E+00	NA	3,70E-01	NA	3,70E-01	NA	0	0	1	1
Coactosin-like protein	COTL1_MOUSE	NO	9,70E-01	0,91	1,10E-01	1,35	1,70E-02	0,46	7,90E-02	0,68	36	26	16	18
Guanine nucleotide-binding protein G(i), alpha-2 subunit	GNAI2_MOUSE	NO	9,70E-01	1,00	1,00E+00	NA	3,70E-01	NA	3,70E-01	NA	0	0	1	1
Macrophage metalloelastase	MMP12_MOUSE	YES	9,70E-01	0,91	1,60E-02	0,48	3,00E-02	1,69	7,90E-01	0,89	17	36	29	32
Protein-L-isoaspartate(D-aspartate) O-methyltransferase	PIMT_MOUSE	NO	9,70E-01	0,91	3,00E-01	2,33	8,00E-01	0,71	3,70E-01	1,83	5	2	3	4
TIP41-like protein	TIPRL_MOUSE	NO	9,70E-01	1,00	1,00E+00	NA	3,70E-01	NA	3,70E-01	NA	0	0	1	1
Protein tyrosine phosphatase type IVA 2	TP4A2_MOUSE	YES	9,70E-01	1,00	6,40E-04	NA	4,10E-02	0,20	3,70E-01	NA	3	0	1	1
Alpha-actinin-1	ACTN1_MOUSE	YES	9,80E-01	0,50	3,10E-01	0,92	7,10E-03	0,05	9,60E-03	0,10	31	34	2	3
C-type lectin domain family 4 member E	CLC4E_MOUSE	NO	9,80E-01	0,92	1,00E+00	NA	5,40E-04	NA	1,60E-01	NA	0	0	4	4
Hsc70-interacting protein	F10A1_MOUSE	NO	9,80E-01	0,88	1,60E-02	0,70	5,80E-02	0,48	1,70E-01	0,39	10	15	5	6
26S proteasome non-ATPase regulatory subunit 8	PSMD8_MOUSE	NO	9,80E-01	0,88	3,70E-01	0,00	1,80E-01	NA	4,70E-01	2,00	0	1	2	3
Glycyl-tRNA synthetase	SYG_MOUSE	NO	9,80E-01	0,92	3,70E-01	0,00	1,20E-02	NA	3,70E-01	3,00	0	1	4	4
L-xylulose reductase	DCXR_MOUSE	YES	9,90E-01	0,88	9,00E-01	1,00	6,60E-01	0,58	3,90E-01	0,67	4	4	2	3
Prefoldin subunit 5	PFD5_MOUSE	NO	9,90E-01	0,90	5,10E-01	0,88	6,30E-01	0,64	3,20E-01	0,63	5	5	3	3
Heterogeneous nuclear ribonucleoprotein A1	ROA1_MOUSE	NO	9,90E-01	0,97	9,70E-02	0,79	7,40E-01	1,19	3,30E-02	0,97	9	11	10	11
Amyloid beta A4 protein	A4_MOUSE	NO	1,00E+00	NA	6,10E-01	0,73	1,40E-01	0,00	1,30E-01	0,00	3	4	0	0
Amyloid beta A4 precursor protein-binding family B member 1-interacting protein	AB1IP_MOUSE	YES	1,00E+00	NA	3,70E-01	NA	3,70E-01	0,00	1,00E+00	NA	2	0	0	0
Acyl-CoA-binding protein	ACBP_MOUSE	NO	1,00E+00	NA	9,50E-01	1,03	2,00E-02	0,00	7,30E-04	0,00	11	10	0	0
Cytoplasmic aconitate hydratase	ACOC_MOUSE	NO	1,00E+00	NA	6,20E-01	0,78	5,70E-03	0,00	7,00E-02	0,00	5	6	0	0
Aconitate hydratase, mitochondrial	ACON_MOUSE	NO	1,00E+00	NA	9,00E-01	1,07	1,70E-02	0,00	1,20E-01	0,00	5	5	0	0
Acyl-coenzyme A thioesterase 2, mitochondrial	ACOT2_MOUSE	NO	1,00E+00	NA	7,20E-01	0,67	3,70E-01	0,00	1,20E-01	0,00	1	2	0	0
Beta-actin-like protein 2	ACTBL_MOUSE	NO	1,00E+00	NA	6,40E-01	2,17	1,20E-01	0,00	3,70E-01	0,00	9	4	0	0
Alpha-centractin	ACTZ_MOUSE	NO	1,00E+00	NA	8,10E-01	1,09	2,20E-03	0,00	6,80E-03	0,00	4	4	0	0
Arf-GAP domain and FG repeats-containing protein 1	AGFG1_MOUSE	NO	1,00E+00	NA	3,70E-01	NA	3,70E-01	0,00	1,00E+00	NA	1	0	0	0
Allograft inflammatory factor 1	AIF1_MOUSE	YES	1,00E+00	NA	3,70E-01	0,00	1,00E+00	NA	3,70E-01	0,00	0	2	0	0
Apoptosis-inducing factor 1, mitochondrial	AIFM1_MOUSE	NO	1,00E+00	NA	9,90E-01	1,00	3,70E-01	0,00	1,20E-01	0,00	1	1	0	0
Aminoacyl tRNA synthetase complex-interacting multifunctional protein 1	AIMP1_MOUSE	YES	1,00E+00	NA	3,70E-01	0,00	1,00E+00	NA	3,70E-01	0,00	0	1	0	0
4-trimethylaminobutyraldehyde dehydrogenase	AL9A1_MOUSE	NO	1,00E+00	NA	7,70E-02	4,67	1,90E-02	0,00	3,70E-01	0,00	5	1	0	0
AMP deaminase 3	AMPD3_MOUSE	NO	1,00E+00	NA	3,70E-01	0,00	1,00E+00	NA	3,70E-01	0,00	0	1	0	0
Cytosol aminopeptidase	AMPL_MOUSE	NO	1,00E+00	NA	7,80E-01	0,67	3,70E-01	0,00	3,70E-01	0,00	1	1	0	0
Ankyrin repeat domain-containing protein 13A	AN13A_MOUSE	NO	1,00E+00	NA	3,70E-01	NA	3,70E-01	0,00	1,00E+00	NA	1	0	0	0
AP-1 complex subunit gamma-1	AP1G1_MOUSE	NO	1,00E+00	NA	3,70E-01	NA	3,70E-01	0,00	1,00E+00	NA	1	0	0	0
AP-1 complex subunit mu-1	AP1M1_MOUSE	NO	1,00E+00	NA	3,50E-01	0,82	6,20E-04	0,00	5,40E-03	0,00	8	9	0	0
AP-2 complex subunit alpha-1	AP2A1_MOUSE	YES	1,00E+00	NA	3,70E-01	NA	3,70E-01	0,00	1,00E+00	NA	1	0	0	0
AP-2 complex subunit alpha-2	AP2A2_MOUSE	YES	1,00E+00	NA	3,70E-01	0,00	1,00E+00	NA	3,70E-01	0,00	0	1	0	0
AP-2 complex subunit sigma	AP2S1_MOUSE	YES	1,00E+00	NA	3,70E-01	NA	3,70E-01	0,00	1,00E+00	NA	1	0	0	0
Apoptosis inhibitor 5	API5_MOUSE	NO	1,00E+00	NA	9,20E-01	0,92	1,30E-01	0,00	1,40E-01	0,00	4	4	0	0
Protein archease	ARCH_MOUSE	NO	1,00E+00	NA	3,70E-01	0,00	1,00E+00	NA	3,70E-01	0,00	0	1	0	0
Argininosuccinate lyase	ARLY_MOUSE	NO	1,00E+00	NA	7,20E-01	0,84	1,80E-02	0,00	7,10E-02	0,00	5	6	0	0
Armadillo repeat-containing protein 10	ARM10_MOUSE	NO	1,00E+00	NA	8,60E-01	1,20	1,60E-01	0,00	3,70E-01	0,00	2	2	0	0
Tether containing UBX domain for GLUT4	ASPC1_MOUSE	YES	1,00E+00	NA	3,70E-01	0,00	1,00E+00	NA	3,70E-01	0,00	0	1	0	0
Autophagy-related protein 7	ATG7_MOUSE	NO	1,00E+00	NA	3,70E-01	0,00	1,00E+00	NA	3,70E-01	0,00	0	1	0	0
ATP synthase subunit beta, mitochondrial	ATPB_MOUSE	NO	1,00E+00	NA	3,70E-01	0,00	1,00E+00	NA	3,70E-01	0,00	0	2	0	0
Large proline-rich protein BAT3	BAT3_MOUSE	NO	1,00E+00	NA	1,30E-01	NA	1,30E-01	0,00	1,00E+00	NA	2	0	0	0
Myc box-dependent-interacting protein 1	BIN1_MOUSE	NO	1,00E+00	NA	7,90E-01	0,91	1,20E-01	0,00	2,60E-03	0,00	7	7	0	0
Valacyclovir hydrolase	BPHL_MOUSE	NO	1,00E+00	NA	3,70E-01	0,00	1,00E+00	NA	3,70E-01	0,00	0	1	0	0
Calpain-1 catalytic subunit	CAN1_MOUSE	YES	1,00E+00	NA	4,10E-01	0,40	3,70E-01	0,00	1,30E-01	0,00	1	2	0	0
Calpain-2 catalytic subunit	CAN2_MOUSE	YES	1,00E+00	NA	8,00E-01	1,50	3,70E-01	0,00	3,70E-01	0,00	1	1	0	0
Caspase-6	CASP6_MOUSE	NO	1,00E+00	NA	8,90E-01	1,00	3,70E-01	0,00	3,70E-01	0,00	1	1	0	0
Caspase-8	CASP8_MOUSE	NO	1,00E+00	NA	3,70E-01	0,00	1,00E+00	NA	3,70E-01	0,00	0	1	0	0
Catalase	CATA_MOUSE	NO	1,00E+00	NA	9,00E-01	1,00	1,30E-02	0,00	4,00E-03	0,00	16	16	0	0
Chromobox protein homolog 1	CBX1_MOUSE	NO	1,00E+00	NA	3,70E-01	0,00	1,00E+00	NA	3,70E-01	0,00	0	1	0	0
Coiled-coil domain-containing protein 115	CC115_MOUSE	NO	1,00E+00	NA	3,70E-01	NA	3,70E-01	0,00	1,00E+00	NA	1	0	0	0
Platelet glycoprotein 4	CD36_MOUSE	YES	1,00E+00	NA	8,30E-03	0,15	3,70E-01	0,00	5,90E-04	0,00	1	7	0	0
Macrosialin	CD68_MOUSE	YES	1,00E+00	NA	6,20E-01	0,40	3,70E-01	0,00	3,70E-01	0,00	1	2	0	0
Cell division control protein 2 homolog	CDC2_MOUSE	NO	1,00E+00	NA	3,70E-01	NA	3,70E-01	0,00	1,00E+00	NA	1	0	0	0
Hsp90 co-chaperone Cdc37	CDC37_MOUSE	NO	1,00E+00	NA	5,70E-01	1,27	7,60E-03	0,00	2,90E-02	0,00	5	4	0	0
Protein CDV3	CDV3_MOUSE	NO	1,00E+00	NA	9,30E-01	1,08	6,10E-03	0,00	9,50E-05	0,00	4	4	0	0
Craniofacial development protein 1	CFDP1_MOUSE	YES	1,00E+00	NA	3,70E-01	NA	3,70E-01	0,00	1,00E+00	NA	1	0	0	0
10 kDa heat shock protein, mitochondrial	CH10_MOUSE	NO	1,00E+00	NA	2,10E-01	5,00	1,20E-01	0,00	3,70E-01	0,00	3	1	0	0
Charged multivesicular body protein 5	CHMP5_MOUSE	NO	1,00E+00	NA	3,70E-01	NA	3,70E-01	0,00	1,00E+00	NA	1	0	0	0
Uncharacterized protein C11orf73 homolog	CK073_MOUSE	NO	1,00E+00	NA	9,20E-01	1,00	3,70E-01	0,00	3,70E-01	0,00	1	1	0	0
CAP-Gly domain-containing linker protein 1	CLIP1_MOUSE	NO	1,00E+00	NA	5,50E-01	1,75	1,80E-01	0,00	1,20E-01	0,00	2	1	0	0
UPF0317 protein C14orf159 homolog, mitochondrial	CN159_MOUSE	NO	1,00E+00	NA	3,70E-01	0,00	1,00E+00	NA	3,70E-01	0,00	0	1	0	0
UPF0568 protein C14orf166 homolog	CN166_MOUSE	NO	1,00E+00	NA	3,50E-01	3,50	1,30E-01	0,00	3,70E-01	0,00	2	1	0	0
Cellular nucleic acid-binding protein	CNBP_MOUSE	NO	1,00E+00	NA	1,80E-01	0,00	1,00E+00	NA	1,80E-01	0,00	0	2	0	0
Cofilin-2	COF2_MOUSE	NO	1,00E+00	NA	3,70E-01	NA	3,70E-01	0,00	1,00E+00	NA	1	0	0	0
COMM domain-containing protein 3	COMD3_MOUSE	NO	1,00E+00	NA	3,30E-01	3,00	1,20E-01	0,00	3,70E-01	0,00	3	1	0	0
COMM domain-containing protein 4	COMD4_MOUSE	NO	1,00E+00	NA	3,70E-01	NA	3,70E-01	0,00	1,00E+00	NA	1	0	0	0
COMM domain-containing protein 7	COMD7_MOUSE	NO	1,00E+00	NA	3,70E-01	1,71	2,50E-07	0,00	1,40E-01	0,00	4	2	0	0
COMM domain-containing protein 8	COMD8_MOUSE	NO	1,00E+00	NA	3,70E-01	NA	3,70E-01	0,00	1,00E+00	NA	1	0	0	0
COMM domain-containing protein 9	COMD9_MOUSE	NO	1,00E+00	NA	3,70E-01	0,00	1,00E+00	NA	3,70E-01	0,00	0	1	0	0
Coatomer subunit beta'	COPB2_MOUSE	NO	1,00E+00	NA	7,90E-01	0,67	3,70E-01	0,00	3,70E-01	0,00	1	1	0	0
Coronin-1B	COR1B_MOUSE	NO	1,00E+00	NA	2,40E-02	0,18	3,70E-01	0,00	3,80E-03	0,00	1	6	0	0
Coronin-7	CORO7_MOUSE	NO	1,00E+00	NA	6,10E-01	1,36	6,90E-03	0,00	1,80E-01	0,00	6	5	0	0
Lambda-crystallin homolog	CRYL1_MOUSE	NO	1,00E+00	NA	3,70E-01	NA	3,70E-01	0,00	1,00E+00	NA	1	0	0	0

Uncharacterized protein C19orf43 homolog	CS043_MOUSE	NO	1,00E+00	NA	8,50E-01	1,33	3,70E-01	0,00	3,70E-01	0,00	1	1	0	0
COP9 signalosome complex subunit 6	CSN6_MOUSE	NO	1,00E+00	NA	9,50E-01	1,33	3,70E-01	0,00	3,70E-01	0,00	1	1	0	0
COP9 signalosome complex subunit 8	CSN8_MOUSE	NO	1,00E+00	NA	3,70E-01	NA	3,70E-01	0,00	1,00E+00	NA	1	0	0	0
UPF0687 protein C20orf27 homolog	CT027_MOUSE	NO	1,00E+00	NA	1,20E-01	0,00	1,00E+00	NA	1,20E-01	0,00	0	2	0	0
Cullin-3	CUL3_MOUSE	NO	1,00E+00	NA	9,80E-01	1,00	3,70E-01	0,00	3,70E-01	0,00	1	1	0	0
Cytochrome c oxidase subunit 6B1	CX6B1_MOUSE	NO	1,00E+00	NA	2,70E-01	1,75	6,70E-03	0,00	1,20E-01	0,00	5	3	0	0
Cytochrome c, somatic	CYC_MOUSE	NO	1,00E+00	NA	3,50E-01	1,71	1,90E-02	0,00	1,30E-01	0,00	4	2	0	0
Cytoplasmic dynein 1 intermediate chain 2	DC1I2_MOUSE	NO	1,00E+00	NA	3,70E-01	NA	3,70E-01	0,00	1,00E+00	NA	1	0	0	0
Deoxycytidine kinase	DCK_MOUSE	NO	1,00E+00	NA	4,30E-01	0,43	3,70E-01	0,00	1,30E-01	0,00	1	2	0	0
DCN1-like protein 1	DCNL1_MOUSE	NO	1,00E+00	NA	3,70E-01	0,00	1,00E+00	NA	3,70E-01	0,00	0	1	0	0
Dynactin subunit 1	DCTN1_MOUSE	NO	1,00E+00	NA	6,40E-01	1,67	1,30E-01	0,00	3,70E-01	0,00	2	1	0	0
Dynactin subunit 2	DCTN2_MOUSE	NO	1,00E+00	NA	3,50E-01	0,96	1,40E-04	0,00	6,80E-05	0,00	8	8	0	0
DNA damage-binding protein 1	DDB1_MOUSE	NO	1,00E+00	NA	6,00E-01	2,50	3,70E-01	0,00	3,70E-01	0,00	2	1	0	0
Protein DDI1 homolog 2	DDI2_MOUSE	NO	1,00E+00	NA	4,80E-01	2,67	1,40E-01	0,00	3,70E-01	0,00	3	1	0	0
Probable ATP-dependent RNA helicase DDX58	DDX58_MOUSE	NO	1,00E+00	NA	3,70E-01	NA	3,70E-01	0,00	1,00E+00	NA	1	0	0	0
Putative deoxyribose-phosphate aldolase	DEOC_MOUSE	NO	1,00E+00	NA	3,70E-01	NA	3,70E-01	0,00	1,00E+00	NA	1	0	0	0
Peroxisomal multifunctional enzyme type 2	DHB4_MOUSE	NO	1,00E+00	NA	1,30E-01	NA	1,30E-01	0,00	1,00E+00	NA	2	0	0	0
DnaJ homolog subfamily A member 1	DNJA1_MOUSE	NO	1,00E+00	NA	3,70E-01	0,00	1,00E+00	NA	3,70E-01	0,00	0	1	0	0
DnaJ homolog subfamily C member 8	DNJC8_MOUSE	NO	1,00E+00	NA	6,50E-01	1,80	5,00E-03	0,00	3,70E-01	0,00	3	2	0	0
DnaJ homolog subfamily C member 9	DNJC9_MOUSE	NO	1,00E+00	NA	3,70E-01	0,00	1,00E+00	NA	3,70E-01	0,00	0	1	0	0
DNA (cytosine-5)-methyltransferase 1	DNMT1_MOUSE	NO	1,00E+00	NA	5,30E-03	0,00	1,00E+00	NA	5,30E-03	0,00	0	4	0	0
Aspartyl aminopeptidase	DNPEP_MOUSE	NO	1,00E+00	NA	9,70E-01	1,06	1,20E-02	0,00	1,60E-03	0,00	6	6	0	0
Dynamin-2	DYN2_MOUSE	YES	1,00E+00	NA	3,70E-01	NA	3,70E-01	0,00	1,00E+00	NA	1	0	0	0
Band 4.1-like protein 2	E41L2_MOUSE	NO	1,00E+00	NA	7,50E-01	0,60	3,70E-01	0,00	3,70E-01	0,00	1	2	0	0
Endothelial differentiation-related factor 1	EDF1_MOUSE	NO	1,00E+00	NA	3,70E-01	NA	3,70E-01	0,00	1,00E+00	NA	1	0	0	0
Eukaryotic translation initiation factor 1b	EIF1B_MOUSE	NO	1,00E+00	NA	1,20E-01	NA	1,20E-01	0,00	1,00E+00	NA	3	0	0	0
Eukaryotic translation initiation factor 3 subunit G	EIF3G_MOUSE	NO	1,00E+00	NA	3,70E-01	NA	3,70E-01	0,00	1,00E+00	NA	1	0	0	0
Transcription elongation factor B polypeptide 1	ELOC_MOUSE	NO	1,00E+00	NA	1,20E-01	NA	1,20E-01	0,00	1,00E+00	NA	2	0	0	0
Epidermal growth factor receptor substrate 15-like 1	EP15R_MOUSE	YES	1,00E+00	NA	1,00E+00	1,00	3,70E-01	0,00	3,70E-01	0,00	1	1	0	0
Extended synaptotagmin-1	ESYT1_MOUSE	NO	1,00E+00	NA	7,10E-02	0,29	3,70E-01	0,00	8,60E-04	0,00	2	6	0	0
RNA-binding protein EWS	EWS_MOUSE	YES	1,00E+00	NA	3,70E-01	NA	3,70E-01	0,00	1,00E+00	NA	1	0	0	0
Protein FAM107B	F107B_MOUSE	NO	1,00E+00	NA	7,80E-01	0,75	3,70E-01	0,00	1,20E-01	0,00	1	1	0	0
Protein FAM136A	F136A_MOUSE	NO	1,00E+00	NA	1,00E+00	1,00	1,30E-01	0,00	1,20E-01	0,00	2	2	0	0
GDP-L-fucose synthetase	FCL_MOUSE	NO	1,00E+00	NA	3,70E-01	0,00	1,00E+00	NA	3,70E-01	0,00	0	1	0	0
FK506-binding protein 15	FKB15_MOUSE	NO	1,00E+00	NA	2,20E-01	1,43	5,70E-03	0,00	3,70E-07	0,00	7	5	0	0
Protein flightless-1 homolog	FLII_MOUSE	NO	1,00E+00	NA	8,50E-01	1,33	3,70E-01	0,00	3,70E-01	0,00	1	1	0	0
Frataxin, mitochondrial	FRDA_MOUSE	NO	1,00E+00	NA	3,70E-01	0,00	1,00E+00	NA	3,70E-01	0,00	0	1	0	0
Far upstream element-binding protein 1	FUBP1_MOUSE	NO	1,00E+00	NA	3,70E-01	NA	3,70E-01	0,00	1,00E+00	NA	1	0	0	0
Fumarate hydratase, mitochondrial	FUMH_MOUSE	NO	1,00E+00	NA	6,00E-01	1,57	1,20E-01	0,00	1,80E-01	0,00	4	2	0	0
FYN-binding protein	FYB_MOUSE	NO	1,00E+00	NA	5,70E-01	0,67	1,20E-01	0,00	1,20E-01	0,00	2	3	0	0
GTPase-activating protein and VPS9 domain-containing protein 1	GAPD1_MOUSE	NO	1,00E+00	NA	9,80E-01	1,00	3,70E-01	0,00	3,70E-01	0,00	1	1	0	0
Gamma-aminobutyric acid receptor-associated protein-like 1	GBRL1_MOUSE	NO	1,00E+00	NA	5,90E-01	2,00	2,10E-01	0,00	3,70E-01	0,00	3	1	0	0
Hydroxyacylglutathione hydrolase, mitochondrial	GLO2_MOUSE	NO	1,00E+00	NA	3,70E-01	NA	3,70E-01	0,00	1,00E+00	NA	1	0	0	0
Glia maturation factor beta	GMFB_MOUSE	NO	1,00E+00	NA	3,70E-01	NA	3,70E-01	0,00	1,00E+00	NA	1	0	0	0
Glia maturation factor gamma	GMFG_MOUSE	NO	1,00E+00	NA	3,70E-01	NA	3,70E-01	0,00	1,00E+00	NA	1	0	0	0
G-protein-signaling modulator 3	GPSM3_MOUSE	NO	1,00E+00	NA	3,70E-01	0,00	1,00E+00	NA	3,70E-01	0,00	0	1	0	0
Glutathione peroxidase 1	GPX1_MOUSE	NO	1,00E+00	NA	7,30E-01	0,71	3,70E-01	0,00	1,60E-01	0,00	2	2	0	0
GrpE protein homolog 1, mitochondrial	GRPE1_MOUSE	NO	1,00E+00	NA	3,70E-01	NA	3,70E-01	0,00	1,00E+00	NA	1	0	0	0
Guanine deaminase	GUAD_MOUSE	NO	1,00E+00	NA	2,90E-03	0,00	1,00E+00	NA	2,90E-03	0,00	0	5	0	0
HCLS1-binding protein 3	H1BP3_MOUSE	NO	1,00E+00	NA	1,30E-01	NA	1,30E-01	0,00	1,00E+00	NA	2	0	0	0
Histone H2B type 1-M	H2B1M_MOUSE	NO	1,00E+00	NA	3,70E-01	NA	3,70E-01	0,00	1,00E+00	NA	1	0	0	0
Delta-aminolevulinic acid dehydratase	HEM2_MOUSE	NO	1,00E+00	NA	5,90E-01	2,00	2,10E-01	0,00	3,70E-01	0,00	3	1	0	0
Histidine triad nucleotide-binding protein 2, mitochondrial	HINT2_MOUSE	NO	1,00E+00	NA	9,30E-01	1,00	1,20E-01	0,00	1,40E-01	0,00	2	2	0	0
Huntingtin-interacting protein 1	HIP1_MOUSE	NO	1,00E+00	NA	3,70E-01	NA	3,70E-01	0,00	1,00E+00	NA	1	0	0	0
High mobility group protein HMG-I/HMG-Y	HMGA1_MOUSE	NO	1,00E+00	NA	7,80E-01	1,36	1,20E-03	0,00	2,10E-01	0,00	5	4	0	0
Non-histone chromosomal protein HMG-14	HMGN1_MOUSE	NO	1,00E+00	NA	3,70E-01	0,00	1,00E+00	NA	3,70E-01	0,00	0	1	0	0
Minor histocompatibility protein HA-1	HMHA1_MOUSE	NO	1,00E+00	NA	3,70E-01	0,00	1,00E+00	NA	3,70E-01	0,00	0	3	0	0
Hyaluronan mediated motility receptor	HMMR_MOUSE	NO	1,00E+00	NA	3,70E-01	0,00	1,00E+00	NA	3,70E-01	0,00	0	1	0	0
Hematological and neurological expressed 1 protein	HN1_MOUSE	NO	1,00E+00	NA	3,70E-01	NA	3,70E-01	0,00	1,00E+00	NA	1	0	0	0
Hematological and neurological expressed 1-like protein	HN1L_MOUSE	NO	1,00E+00	NA	2,60E-01	1,35	3,60E-03	0,00	7,20E-05	0,00	10	8	0	0
Heterogeneous nuclear ribonucleoprotein G	HNRPG_MOUSE	NO	1,00E+00	NA	1,20E-01	NA	1,20E-01	0,00	1,00E+00	NA	4	0	0	0
Heterogeneous nuclear ribonucleoprotein U	HNRPU_MOUSE	NO	1,00E+00	NA	1,00E+00	1,14	1,20E-01	0,00	2,10E-01	0,00	3	2	0	0
Heat shock 70 kDa protein 1L	HS71L_MOUSE	NO	1,00E+00	NA	3,70E-01	0,00	1,00E+00	NA	3,70E-01	0,00	0	1	0	0
Hexokinase-1	HXK1_MOUSE	NO	1,00E+00	NA	3,70E-01	0,00	1,00E+00	NA	3,70E-01	0,00	0	1	0	0
Insulin-degrading enzyme	IDE_MOUSE	NO	1,00E+00	NA	8,10E-01	0,67	3,70E-01	0,00	3,70E-01	0,00	1	1	0	0
Eukaryotic translation initiation factor 2 subunit 2	IF2B_MOUSE	NO	1,00E+00	NA	8,90E-01	0,86	3,70E-01	0,00	1,80E-01	0,00	2	2	0	0
Eukaryotic translation initiation factor 2 subunit 3, X-linked	IF2G_MOUSE	NO	1,00E+00	NA	1,00E+00	1,00	2,80E-02	0,00	1,20E-01	0,00	6	6	0	0
Eukaryotic translation initiation factor 4 gamma 1	IF4G1_MOUSE	NO	1,00E+00	NA	6,20E-01	0,82	1,50E-01	0,00	1,80E-03	0,00	3	4	0	0
Interferon-activable protein 204	IFI4_MOUSE	NO	1,00E+00	NA	3,70E-01	0,00	1,00E+00	NA	3,70E-01	0,00	0	1	0	0
Importin subunit alpha-4	IMA4_MOUSE	NO	1,00E+00	NA	8,40E-01	0,75	3,70E-01	0,00	3,70E-01	0,00	1	1	0	0
Inositol-3-phosphate synthase 1	INO1_MOUSE	NO	1,00E+00	NA	7,70E-01	0,82	2,30E-02	0,00	1,20E-01	0,00	5	6	0	0
Inosine triphosphate pyrophosphatase	ITPA_MOUSE	NO	1,00E+00	NA	5,70E-01	0,57	3,70E-01	0,00	1,20E-01	0,00	1	2	0	0
GTP:AMP phosphotransferase mitochondrial	KAD3_MOUSE	NO	1,00E+00	NA	8,60E-01	1,17	1,30E-01	0,00	1,60E-01	0,00	2	2	0	0
Lupus La protein homolog	LA_MOUSE	NO	1,00E+00	NA	1,60E-01	NA	1,60E-01	0,00	1,00E+00	NA	2	0	0	0
Lamina-associated polypeptide 2, isoforms alpha/zeta	LAP2A_MOUSE	NO	1,00E+00	NA	9,70E-01	1,03	9,80E-05	0,00	1,80E-03	0,00	10	10	0	0
Lysosomal acid lipase/cholesteryl ester hydrolase	LICH_MOUSE	NO	1,00E+00	NA	3,70E-01	NA	3,70E-01	0,00	1,00E+00	NA	1	0	0	0
Lamin-B1	LMNB1_MOUSE	NO	1,00E+00	NA	2,80E-01	0,77	2,70E-02	0,00	7,00E-05	0,00	7	9	0	0
Lamin-B2	LMNB2_MOUSE	NO	1,00E+00	NA	3,70E-01	0,00	1,00E+00	NA	3,70E-01	0,00	0	1	0	0
Leupaxin	LPXN_MOUSE	NO	1,00E+00	NA	1,30E-01	0,00	1,00E+00	NA	1,30E-01	0,00	0	2	0	0
Leucine-rich repeat-containing protein 20	LRC20_MOUSE	NO	1,00E+00	NA	3,70E-01	NA	3,70E-01	0,00	1,00E+00	NA	1	0	0	0
Low-density lipoprotein receptor-related protein 4	LRP4_MOUSE	YES	1,00E+00	NA	3,70E-01	0,00	1,00E+00	NA	3,70E-01	0,00	0	1	0	0
Leucine-rich repeat flightless-interacting protein 1	LRRF1_MOUSE	NO	1,00E+00	NA	1,30E-01	NA	1,30E-01	0,00	1,00E+00	NA	3	0	0	0
U6 snRNA-associated Sm-like protein LSm2	LSM2_MOUSE	NO	1,00E+00	NA	3,70E-01	0,00	1,00E+00	NA	3,70E-01	0,00	0	1	0	0
Lymphocyte-specific protein 1	LSP1_MOUSE	YES	1,00E+00	NA	8,80E-01	1,00	1,70E-02	0,00	2,60E-03	0,00	26	26	0	0
Myristoylated alanine-rich C-kinase substrate	MARCS_MOUSE	NO	1,00E+00	NA	1,50E-01	NA	1,50E-01	0,00	1,00E+00	NA	2	0	0	0
Matrin-3	MATR3_MOUSE	NO	1,00E+00	NA	3,70E-01	0,00	1,00E+00	NA	3,70E-01	0,00	0	1	0	0
DNA replication licensing factor MCM6	MCM6_MOUSE	NO	1,00E+00	NA	4,50E-01	0,43	3,70E-01	0,00	1,30E-01	0,00	1	2	0	0
Malignant T cell amplified sequence 1	MCTS1_MOUSE	NO	1,00E+00	NA	1,00E-01	4,00	1,70E-02	0,00	3,70E-01	0,00	3	1	0	0
Mitotic spindle assembly checkpoint protein MAD2A	MD2L1_MOUSE	NO	1,00E+00	NA	2,50E-01	4,00	1,20E-01	0,00	3,70E-01	0,00	3	1	0	0
N-terminal acetyltransferase B complex subunit MDM20	MDM20_MOUSE	NO	1,00E+00	NA	3,70E-01	NA	3,70E-01	0,00	1,00E+00	NA	1	0	0	0
Mitogen-activated protein kinase 3	MK03_MOUSE	NO	1,00E+00	NA	5,40E-01	0,60	3,70E-01	0,00	1,40E-01	0,00	1	2	0	0
Mitogen-activated protein kinase 14	MK14_MOUSE	NO	1,00E+00	NA	1,20E-01	NA	1,20E-01	0,00	1,00E+00	NA	3	0	0	0
Mps one binder kinase activator-like 3	MOBL3_MOUSE	NO	1,00E+00	NA	3,70E-01	NA	3,70E-01	0,00	1,00E+00	NA	1	0	0	0
Peptide methionine sulfoxide reductase	MSRA_MOUSE	NO	1,00E+00	NA	8,10E-01	1,22	1,50E-01	0,00	2,20E-03	0,00	4	3	0	0
1,2-dihydroxy-3-keto-5-methylthiopentene dioxygenase	MTND_MOUSE	YES	1,00E+00	NA	3,70E-01	NA	3,70E-01	0,00	1,00E+00	NA	1	0	0	0
Putative N-acetylglucosamine-6-phosphate deacetylase	NAGA_MOUSE	NO	1,00E+00	NA	4,10E-01	2,67	1,40E-01	0,00	3,70E-01	0,00	3	1	0	0
Nuclear autoantigenic sperm protein	NASP_MOUSE	NO	1,00E+00	NA	3,70E-01	NA	3,70E-01	0,00	1,00E+00	NA	1	0	0	0
N-acylneuraminate cytidylyltransferase	NEUA_MOUSE	NO	1,00E+00	NA	1,20E-01	0,00	1,00E+00	NA	1,20E-01	0,00	0	3	0	0
NFU1 iron-sulfur cluster scaffold homolog, mitochondrial	NFU1_MOUSE	NO	1,00E+00	NA	3,70E-01	NA	3,70E-01	0,00	1,00E+00	NA	1	0	0	0
Na(+)/H(+) exchange regulatory cofactor NHE-RF1	NHRF1_MOUSE	YES	1,00E+00	NA	3,30E-01	0,78	3,20E-02	0,00	2,30E-05	0,00	5	6	0	0
Neuronal pentraxin-1	NPTX1_MOUSE	NO	1,00E+00	NA	2,50E-02	0,17	3,70E-01	0,00	5,00E-03	0,00	3	16	0	0
Diphosphoinositol polyphosphate phosphohydrolase 1	NUDT3_MOUSE	NO	1,00E+00	NA	8,50E-01	1,14	1,40E-01	0,00	1,30E-01	0,00	3	2	0	0
Ornithine aminotransferase, mitochondrial	OAT_MOUSE	NO	1,00E+00	NA	3,70E-01	0,00	1,00E+00	NA	3,70E-01	0,00	0	1	0	0
Plasminogen activator inhibitor 1 RNA-binding protein	PAIRB_MOUSE	NO	1,00E+00	NA	1,50E-01	2,40	1,60E-02	0,00	1,30E-01	0,00	4	2	0	0
Poly [ADP-ribose] polymerase 1	PARP1_MOUSE	NO	1,00E+00	NA	3,70E-01	0,00	1,00E+00	NA	3,70E-01	0,00	0	1	0	0
Programmed cell death protein 10	PDC10_MOUSE	YES	1,00E+00	NA	1,00E+00	1,00	3,70E-01	0,00	3,70E-01	0,00	1	1	0	0
Parkinson disease 7 domain-containing protein 1	PDDC1_MOUSE	YES	1,00E+00	NA	9,40E-01	1,00	1,20E-01	0,00	1,20E-01	0,00	2	2	0	0
Core-binding factor subunit beta	PEBB_MOUSE	NO	1,00E+00	NA	3,60E-01	0,74	2,40E-03	0,00	2,70E-02	0,00	5	6	0	0
Phosphoglucomutase-2	PGM2_MOUSE	NO	1,00E+00	NA	6,20E-01	1,60	1,20E-01	0,00	1,20E-01	0,00	3	2	0	0
Phosphatidylinositol-binding clathrin assembly protein	PICA_MOUSE	NO	1,00E+00	NA	1,60E-01	1,90	4,50E-04	0,00	1,20E-01	0,00	13	7	0	0
Peptidyl-prolyl cis-trans isomerase NIMA-interacting 4	PIN4_MOUSE	NO	1,00E+00	NA	8,30E-01	0,83	3,70E-01	0,00	3,70E-01	0,00	2	2	0	0
Pleckstrin homology domain-containing family O member 2	PKHO2_MOUSE	NO	1,00E+00	NA	1,90E-01	2,00	3,90E-03	0,00	1,40E-01	0,00	7	4	0	0
Phospholipase A-2-activating protein	PLAP_MOUSE	NO	1,00E+00	NA	3,70E-01	NA	3,70E-01	0,00	1,00E+00	NA	1	0	0	0
1-phosphatidylinositol-4,5-bisphosphate phosphodiesterase gamma-2	PLCG2_MOUSE	NO	1,00E+00	NA	9,10E-01	1,11	1,30E-01	0,00	5,10E-02	0,00	7	6	0	0
Phospholipase D3	PLD3_MOUSE	NO	1,00E+00	NA	1,00E+00	1,00	3,70E-01	0,00	3,70E-01	0,00	1	1	0	0
Perilipin-3	PLIN3_MOUSE	NO	1,00E+00	NA	7,70E-01	1,67	1,30E-01	0,00	3,70E-01	0,00	2	1	0	0

Phosphomannomutase 2	PMM2_MOUSE	NO	1,00E+00	NA	3,70E-01	0,00	1,00E+00	NA	3,70E-01	0,00	0	1	0	0
Lysosomal acid phosphatase	PPAL_MOUSE	NO	1,00E+00	NA	3,70E-01	NA	3,70E-01	0,00	1,00E+00	NA	1	0	0	0
40 kDa peptidyl-prolyl cis-trans isomerase	PPID_MOUSE	NO	1,00E+00	NA	3,70E-01	0,00	1,00E+00	NA	3,70E-01	0,00	0	1	0	0
Peptidyl-prolyl cis-trans isomerase-like 1	PPIL1_MOUSE	NO	1,00E+00	NA	8,40E-01	1,33	3,70E-01	0,00	3,70E-01	0,00	1	1	0	0
Ribose-phosphate pyrophosphokinase 2	PRPS2_MOUSE	NO	1,00E+00	NA	3,70E-01	NA	3,70E-01	0,00	1,00E+00	NA	2	0	0	0
26S protease regulatory subunit 4	PRS4_MOUSE	NO	1,00E+00	NA	8,50E-01	1,33	3,70E-01	0,00	3,70E-01	0,00	1	1	0	0
26S protease regulatory subunit 6A	PRS6A_MOUSE	NO	1,00E+00	NA	1,30E-01	NA	1,30E-01	0,00	1,00E+00	NA	2	0	0	0
26S protease regulatory subunit 7	PRS7_MOUSE	NO	1,00E+00	NA	3,20E-01	1,80	2,60E-02	0,00	1,20E-01	0,00	6	3	0	0
26S protease regulatory subunit 8	PRS8_MOUSE	NO	1,00E+00	NA	3,70E-01	NA	3,70E-01	0,00	1,00E+00	NA	1	0	0	0
26S proteasome non-ATPase regulatory subunit 12	PSD12_MOUSE	NO	1,00E+00	NA	3,70E-01	NA	3,70E-01	0,00	1,00E+00	NA	1	0	0	0
26S proteasome non-ATPase regulatory subunit 13	PSD13_MOUSE	NO	1,00E+00	NA	3,70E-01	NA	3,70E-01	0,00	1,00E+00	NA	1	0	0	0
DNA replication complex GINS protein PSF2	PSF2_MOUSE	NO	1,00E+00	NA	3,70E-01	0,00	1,00E+00	NA	3,70E-01	0,00	0	1	0	0
26S proteasome non-ATPase regulatory subunit 5	PSMD5_MOUSE	NO	1,00E+00	NA	7,50E-01	1,29	1,20E-01	0,00	1,20E-01	0,00	3	2	0	0
Trifunctional purine biosynthetic protein adenosine-3	PUR2_MOUSE	NO	1,00E+00	NA	9,00E-01	1,11	1,30E-01	0,00	1,60E-01	0,00	3	3	0	0
Phosphoribosylformylglycinamidine synthase	PUR4_MOUSE	NO	1,00E+00	NA	7,00E-01	0,87	1,20E-01	0,00	1,50E-03	0,00	7	8	0	0
Multifunctional protein ADE2	PUR6_MOUSE	NO	1,00E+00	NA	3,70E-01	0,00	1,00E+00	NA	3,70E-01	0,00	0	1	0	0
Adenylosuccinate lyase	PUR8_MOUSE	NO	1,00E+00	NA	3,70E-01	0,00	1,00E+00	NA	3,70E-01	0,00	0	1	0	0
Adenylosuccinate synthetase isozyme 1	PURA1_MOUSE	NO	1,00E+00	NA	3,70E-01	1,27	3,70E-03	0,00	7,00E-05	0,00	11	9	0	0
Adenylosuccinate synthetase isozyme 2	PURA2_MOUSE	NO	1,00E+00	NA	7,80E-01	0,91	3,30E-05	0,00	4,80E-02	0,00	11	12	0	0
CTP synthase 2	PYRG2_MOUSE	NO	1,00E+00	NA	3,70E-01	0,00	1,00E+00	NA	3,70E-01	0,00	0	1	0	0
Ras-related protein Rab-1B	RAB1B_MOUSE	NO	1,00E+00	NA	3,70E-01	NA	3,70E-01	0,00	1,00E+00	NA	1	0	0	0
GTPase NRas	RASN_MOUSE	YES	1,00E+00	NA	3,70E-01	NA	3,70E-01	0,00	1,00E+00	NA	1	0	0	0
Histone-binding protein RBBP7	RBBP7_MOUSE	NO	1,00E+00	NA	7,10E-01	1,20	1,90E-02	0,00	4,30E-03	0,00	8	7	0	0
RNA-binding protein 8A	RBM8A_MOUSE	NO	1,00E+00	NA	9,00E-01	0,80	3,70E-01	0,00	3,70E-01	0,00	1	2	0	0
Regulator of G-protein signaling 10	RGS10_MOUSE	NO	1,00E+00	NA	2,50E-01	1,73	2,30E-02	0,00	2,30E-03	0,00	6	4	0	0
GTP-binding protein Rheb	RHEB_MOUSE	YES	1,00E+00	NA	3,70E-01	NA	3,70E-01	0,00	1,00E+00	NA	1	0	0	0
Rho GTPase-activating protein 1	RHG01_MOUSE	YES	1,00E+00	NA	3,80E-02	1,75	3,80E-04	0,00	4,10E-03	0,00	12	7	0	0
Rho GTPase-activating protein 18	RHG18_MOUSE	NO	1,00E+00	NA	6,20E-01	0,40	3,70E-01	0,00	3,70E-01	0,00	1	2	0	0
Ribonucleoside-diphosphate reductase large subunit	RIR1_MOUSE	NO	1,00E+00	NA	3,70E-01	NA	3,70E-01	0,00	1,00E+00	NA	1	0	0	0
Ribonucleoside-diphosphate reductase subunit M2	RIR2_MOUSE	NO	1,00E+00	NA	3,70E-01	0,00	1,00E+00	NA	3,70E-01	0,00	0	1	0	0
39S ribosomal protein L12, mitochondrial	RM12_MOUSE	NO	1,00E+00	NA	3,70E-01	0,00	1,00E+00	NA	3,70E-01	0,00	0	1	0	0
Regulator of microtubule dynamics protein 1	RMD1_MOUSE	NO	1,00E+00	NA	1,20E-01	0,00	1,00E+00	NA	1,20E-01	0,00	0	3	0	0
Ribonuclease H2 subunit A	RNH2A_MOUSE	NO	1,00E+00	NA	4,20E-01	2,50	1,30E-01	0,00	3,70E-01	0,00	2	1	0	0
Regulation of nuclear pre-mRNA domain-containing protein 1B	RPR1B_MOUSE	NO	1,00E+00	NA	3,70E-01	NA	3,70E-01	0,00	1,00E+00	NA	1	0	0	0
40S ribosomal protein S28	RS28_MOUSE	NO	1,00E+00	NA	7,10E-02	0,36	2,30E-01	0,00	1,10E-03	0,00	3	8	0	0
Reticulon-3	RTN3_MOUSE	NO	1,00E+00	NA	3,70E-01	0,00	1,00E+00	NA	3,70E-01	0,00	0	1	0	0
Protein S100-A6	S10A6_MOUSE	YES	1,00E+00	NA	1,20E-01	0,00	1,00E+00	NA	1,20E-01	0,00	0	3	0	0
Protein S100-A11	S10AB_MOUSE	NO	1,00E+00	NA	2,30E-01	3,00	1,70E-03	0,00	3,70E-01	0,00	4	1	0	0
SUMO-activating enzyme subunit 1	SAE1_MOUSE	NO	1,00E+00	NA	3,70E-01	NA	3,70E-01	0,00	1,00E+00	NA	1	0	0	0
SUMO-activating enzyme subunit 2	SAE2_MOUSE	NO	1,00E+00	NA	3,90E-01	2,67	1,40E-01	0,00	3,70E-01	0,00	3	1	0	0
SAP domain-containing ribonucleoprotein	SARNP_MOUSE	NO	1,00E+00	NA	1,30E-02	NA	1,30E-02	0,00	1,00E+00	NA	4	0	0	0
SAM and SH3 domain-containing protein 3	SASH3_MOUSE	NO	1,00E+00	NA	6,70E-01	1,60	1,40E-01	0,00	3,70E-01	0,00	3	2	0	0
Protein transport protein Sec23A	SC23A_MOUSE	NO	1,00E+00	NA	2,10E-01	0,56	1,20E-01	0,00	2,60E-03	0,00	3	6	0	0
Sec1 family domain-containing protein 1	SCFD1_MOUSE	NO	1,00E+00	NA	4,20E-01	2,50	1,30E-01	0,00	3,70E-01	0,00	2	1	0	0
Stromal cell-derived factor 2-like protein 1	SDF2L_MOUSE	NO	1,00E+00	NA	1,20E-01	NA	1,20E-01	0,00	1,00E+00	NA	2	0	0	0
Splicing factor 3A subunit 3	SF3A3_MOUSE	NO	1,00E+00	NA	3,70E-01	NA	3,70E-01	0,00	1,00E+00	NA	1	0	0	0
Splicing factor 3B subunit 1	SF3B1_MOUSE	NO	1,00E+00	NA	3,70E-01	NA	3,70E-01	0,00	1,00E+00	NA	1	0	0	0
Splicing factor 3B subunit 3	SF3B3_MOUSE	NO	1,00E+00	NA	8,70E-01	0,75	3,70E-01	0,00	3,70E-01	0,00	1	1	0	0
Small glutamine-rich tetratricopeptide repeat-containing protein alpha	SGTA_MOUSE	NO	1,00E+00	NA	3,70E-01	NA	3,70E-01	0,00	1,00E+00	NA	1	0	0	0
SH3 domain-binding glutamic acid-rich-like protein 2	SH3L2_MOUSE	NO	1,00E+00	NA	3,70E-01	NA	3,70E-01	0,00	1,00E+00	NA	1	0	0	0
Phosphatidylinositol-3,4,5-trisphosphate 5-phosphatase 1	SHIP1_MOUSE	YES	1,00E+00	NA	3,70E-01	NA	3,70E-01	0,00	1,00E+00	NA	1	0	0	0
S-phase kinase-associated protein 1	SKP1_MOUSE	NO	1,00E+00	NA	6,60E-01	0,63	3,70E-01	0,00	1,40E-01	0,00	2	3	0	0
Small nuclear ribonucleoprotein Sm D1	SMD1_MOUSE	NO	1,00E+00	NA	3,70E-01	NA	3,70E-01	0,00	1,00E+00	NA	1	0	0	0
Small nuclear ribonucleoprotein Sm D2	SMD2_MOUSE	NO	1,00E+00	NA	2,50E-01	1,92	2,20E-03	0,00	1,20E-01	0,00	8	4	0	0
Sorting nexin-1	SNX1_MOUSE	NO	1,00E+00	NA	3,90E-01	1,60	1,40E-01	0,00	3,70E-01	0,00	3	2	0	0
Spectrin alpha chain, brain	SPTA2_MOUSE	YES	1,00E+00	NA	1,10E-01	2,00	3,80E-03	0,00	4,40E-02	0,00	11	5	0	0
Spectrin beta chain, brain 1	SPTB2_MOUSE	YES	1,00E+00	NA	5,90E-01	1,60	1,40E-01	0,00	1,30E-01	0,00	3	2	0	0
Serine/threonine-protein kinase 24	STK24_MOUSE	NO	1,00E+00	NA	8,50E-01	1,33	3,70E-01	0,00	3,70E-01	0,00	1	1	0	0
Syntaxin-12	STX12_MOUSE	NO	1,00E+00	NA	7,30E-01	0,95	2,10E-02	0,00	5,90E-04	0,00	6	7	0	0
Syntaxin-binding protein 2	STXB2_MOUSE	YES	1,00E+00	NA	3,70E-01	NA	3,70E-01	0,00	1,00E+00	NA	1	0	0	0
Alanyl-tRNA synthetase, cytoplasmic	SYAC_MOUSE	NO	1,00E+00	NA	1,00E+00	1,00	3,70E-01	0,00	3,70E-01	0,00	2	2	0	0
Phenylalanyl-tRNA synthetase beta chain	SYFB_MOUSE	NO	1,00E+00	NA	3,70E-01	0,00	1,00E+00	NA	3,70E-01	0,00	0	1	0	0
Lysyl-tRNA synthetase	SYK_MOUSE	NO	1,00E+00	NA	8,40E-01	0,78	3,70E-01	0,00	1,60E-01	0,00	2	3	0	0
Seryl-tRNA synthetase, cytoplasmic	SYSC_MOUSE	NO	1,00E+00	NA	7,90E-01	1,21	1,20E-01	0,00	1,20E-01	0,00	6	5	0	0
Tryptophanyl-tRNA synthetase, cytoplasmic	SYWC_MOUSE	NO	1,00E+00	NA	7,10E-01	1,50	1,60E-01	0,00	3,70E-01	0,00	2	1	0	0
Tyrosyl-tRNA synthetase, cytoplasmic	SYYC_MOUSE	NO	1,00E+00	NA	1,00E+00	1,00	3,30E-02	0,00	1,20E-01	0,00	4	4	0	0
Tubulin beta-2A chain	TBB2A_MOUSE	NO	1,00E+00	NA	1,20E-01	1,13	2,20E-04	0,00	1,60E-04	0,00	6	5	0	0
Tubulin-specific chaperone C	TBCC_MOUSE	NO	1,00E+00	NA	1,30E-01	NA	1,30E-01	0,00	1,00E+00	NA	2	0	0	0
F-box-like/WD repeat-containing protein TBL1XR1	TBL1R_MOUSE	NO	1,00E+00	NA	3,70E-01	NA	3,70E-01	0,00	1,00E+00	NA	1	0	0	0
Tumor necrosis factor, alpha-induced protein 8	TFIP8_MOUSE	NO	1,00E+00	NA	3,70E-01	NA	3,70E-01	0,00	1,00E+00	NA	1	0	0	0
THO complex subunit 4	THOC4_MOUSE	NO	1,00E+00	NA	4,60E-01	2,80	1,50E-01	0,00	3,70E-01	0,00	5	2	0	0
THUMP domain-containing protein 1	THUM1_MOUSE	NO	1,00E+00	NA	1,00E+00	1,04	1,00E-02	0,00	3,00E-03	0,00	9	9	0	0
Transcription intermediary factor 1-beta	TIF1B_MOUSE	NO	1,00E+00	NA	3,00E-01	NA	3,00E-01	0,00	1,00E+00	NA	6	0	0	0
Mitochondrial import inner membrane translocase subunit Tim8 A	TIM8A_MOUSE	NO	1,00E+00	NA	1,20E-01	0,00	1,00E+00	NA	1,20E-01	0,00	0	2	0	0
Transportin-1	TNPO1_MOUSE	NO	1,00E+00	NA	1,20E-01	NA	1,20E-01	0,00	1,00E+00	NA	1	0	0	0
DNA topoisomerase 2-alpha	TOP2A_MOUSE	NO	1,00E+00	NA	3,70E-01	NA	3,70E-01	0,00	1,00E+00	NA	1	0	0	0
Tumor necrosis factor, alpha-induced protein 8-like protein 2	TP8L2_MOUSE	NO	1,00E+00	NA	3,70E-01	NA	3,70E-01	0,00	1,00E+00	NA	1	0	0	0
Tumor protein D54	TPD54_MOUSE	NO	1,00E+00	NA	3,50E-01	1,71	2,20E-03	0,00	1,20E-01	0,00	4	2	0	0
Thiamin pyrophosphokinase 1	TPK1_MOUSE	NO	1,00E+00	NA	1,40E-01	0,00	1,00E+00	NA	1,40E-01	0,00	0	3	0	0
Tropomyosin alpha-1 chain	TPM1_MOUSE	NO	1,00E+00	NA	1,90E-01	0,78	1,20E-01	0,00	5,10E-03	0,00	2	3	0	0
Tripeptidyl-peptidase 2	TPP2_MOUSE	NO	1,00E+00	NA	9,40E-01	1,09	6,90E-02	0,00	7,40E-05	0,00	8	7	0	0
tRNA-nucleotidyltransferase 1, mitochondrial	TRNT1_MOUSE	NO	1,00E+00	NA	1,40E-01	0,53	1,20E-01	0,00	6,70E-04	0,00	3	6	0	0
Splicing factor U2AF 65 kDa subunit	U2AF2_MOUSE	NO	1,00E+00	NA	5,00E-02	0,17	3,70E-01	0,00	1,80E-02	0,00	1	4	0	0
Ubiquitin-like modifier-activating enzyme 6	UBA6_MOUSE	NO	1,00E+00	NA	3,70E-01	NA	3,70E-01	0,00	1,00E+00	NA	1	0	0	0
Ubiquilin-1	UBQL1_MOUSE	NO	1,00E+00	NA	4,10E-01	0,43	3,70E-01	0,00	1,40E-01	0,00	1	2	0	0
Ubiquitin carboxyl-terminal hydrolase isozyme L5	UCHL5_MOUSE	NO	1,00E+00	NA	1,30E-01	NA	1,30E-01	0,00	1,00E+00	NA	2	0	0	0
Ufm1-conjugating enzyme 1	UFC1_MOUSE	NO	1,00E+00	NA	6,20E-01	1,22	3,90E-03	0,00	7,20E-03	0,00	4	3	0	0
UDP-glucose:glycoprotein glucosyltransferase 1	UGGG1_MOUSE	NO	1,00E+00	NA	1,60E-01	NA	1,60E-01	0,00	1,00E+00	NA	2	0	0	0
UTP--glucose-1-phosphate uridylyltransferase	UGPA_MOUSE	NO	1,00E+00	NA	9,70E-02	4,25	1,90E-02	0,00	3,70E-01	0,00	6	1	0	0
General vesicular transport factor p115	USO1_MOUSE	NO	1,00E+00	NA	8,00E-01	1,50	3,70E-01	0,00	3,70E-01	0,00	1	1	0	0
Vacuolar protein-sorting-associated protein 25	VPS25_MOUSE	NO	1,00E+00	NA	3,70E-01	NA	3,70E-01	0,00	1,00E+00	NA	2	0	0	0
Vesicle transport through interaction with t-SNAREs homolog 1B	VTI1B_MOUSE	NO	1,00E+00	NA	3,70E-01	NA	3,70E-01	0,00	1,00E+00	NA	1	0	0	0
Wiskott-Aldrich syndrome protein homolog	WASP_MOUSE	NO	1,00E+00	NA	6,20E-01	0,82	1,20E-01	0,00	3,50E-03	0,00	3	4	0	0
WAS/WASL-interacting protein family member 1	WIPF1_MOUSE	NO	1,00E+00	NA	7,30E-01	0,70	1,90E-01	0,00	3,70E-01	0,00	2	3	0	0
Zinc finger protein ZPR1	ZPR1_MOUSE	NO	1,00E+00	NA	9,80E-01	1,00	3,70E-01	0,00	3,70E-01	0,00	1	1	0	0

Table S3. Fluorescence-activated cell sorting in sham- and AngII-treated *miR-155* WT and KO mice

Blood				**% of life**			
	Marker			WT sham	WT Ang	KO sham	KO Ang
Monocyte	CD11b+ Ly6G-			**11.9±0.8**	**18.7±2.3$^{\$}$**	**11.3±1.8**	**11.4±1.0***
		Ly6C-[3]		69.7±3.0	55.8±2.0$^{\$\$}$	73.7±5.4	65.2±4.5
		Ly6C+[3]		31.2±2.9	45.0±2.2$^{\$\$}$	27.1±5.4	35.6±4.6
Granulocyte	CD11b+Ly6G+			**18.6±2.8**	**29.7±2.0$^{\$}$**	**19.1±2.1**	**29.2±3.4$^{\$}$**
T-cell	CD3+			**26.4±1.6**	**24.8±2.8**	**27.0±1.5**	**25.8±1.3**
		CD4+[1]		62.0±0.4	54.3±0.7$^{\$\$\$\$}$	57.8±0.9***	55.7±1.0
			CD25+ Foxp3+[2]	8.2±0.3	10.2±0.4$^{\$\$\$}$	4.9±0.4****	5.5±0.3****
		CD8+[1]		35.2±0.4	42.7±0.6$^{\$\$\$\$}$	39.1±0.8***	41.0±0.8
B-cell	B220+			**30.7±4.2**	**20.7±2.2**	**36.9±3.8**	**27.4±3.9**
NK	NK1-1+			**6.3±0.6**	**6.8±1.4**	**6.4±0.8**	**5.4±0.3**

[1] % of CD3+; [2] % of CD4+; [3] % of CD11b+Ly6G-

Blood			**True counts**			
	Marker		WT sham	WT Ang	KO sham	KO Ang
Leukocyte	CD45+		**2418±185**	**4010±540$^{\$}$**	**4427±145******	**3486±297$^{\$}$**
Monocyte	CD11b+ Ly6G-		**93±5**	**218±12$^{\$\$\$}$**	**160±22***	**178±35**
		Ly6C-	56±6	100±9$^{\$}$	73±13	55±1**
		Ly6C+	38±1	120±13$^{\$\$}$	88±11*	124±34
Granulocyte	CD11b+Ly6G+		**177±38**	**656±149$^{\$}$**	**326±53**	**558±44$^{\$}$**
T-cell	CD3+		**626±39**	**951±190**	**1030±87***	**825±61**
		CD4+	367±27	519±119	572±45*	439±32
		CD8+	244±10	409±69	435±40*	365±29
B-cell	B220+		**1348±135**	**1871±425**	**2624±35******	**1685±170$^{\$\$\$}$**
NK	NK1-1+		**9±0**	**15±2$^{\$}$**	**15±3**	**16±0**

Heart (per 100 milligram)			**True counts**			
	Marker		WT sham	WT Ang	KO sham	KO Ang
Leukocyte	CD45+		**12163±1514**	**34119±3360$^{\$\$\$}$**	**13466±3098**	**22654±5049**
Macrophage	CD11b+ F4/80+		**4096±1152**	**21480±3559$^{\$\$}$**	**4945±1557**	**11744±3354**
Monocyte	CD11b+ Ly6G-		**656±36**	**2216±114$^{\$\$\$\$}$**	**752±111**	**2536±718$^{\$\$}$**
		Ly6C-	496±23	1754±135$^{\$\$\$}$	574±87	1825±491$^{\$\$}$
		Ly6C+	164±15	478±38$^{\$}$	183±41	731±215$^{\$}$
Granulocyte	CD11b+Ly6G+		**64±28**	**113±20**	**33±13**	**67±18**
T-cell	CD3+		**466±78**	**1497±203$^{\$\$\$}$**	**447±95**	**760±130**
		CD4+	187±44	601±117$^{\$}$	128±32	201±43
		CD8+	118±16	368±70$^{\$\$}$	115±30	117±33
B-cell	B220+		**3612±504**	**3731±870**	**4159±1155**	**2424±361**

*P<0.05, **P<0.01, ***P<0.005, ****P<0.001 versus WT

$^{\$}$P<0.05, $^{\$\$}$P<0.01, $^{\$\$\$}$P<0.005, $^{\$\$\$\$}$P<0.001 versus sham

Table S4. Primers for quantitative real-time PCR

Name	Primer sequence
Mouse Acta1-F	TGAGACCACCTACAACAGCA
Mouse Acta1-R	CCAGAGCTGTGATCTCCTTC
Mouse Nppa-F	ATTGACAGGATTGGAGCCCAGAGT
Mouse Nppa-R	TGACACACCACAAGGGCTTAGGAT
Mouse Nppb-F	GTTTGGGCTGTAACGCACTGA
Mouse Nppb-R	GAAAGAGACCCAGGCAGAGTCA
Mouse Gapdh-F	GGTGGACCTCATGGCCTACA
Mouse Gapdh-R	CTCTCTTGCTCAGTGTCCTTGCT Product size: 82 nt
Mouse-Socs1-F	CCTCCTCGTCCTCGTCTTC
Mouse-Socs1-R	AAGGTGCGGAAGTGAGTGTC Product size: 103 nt
Mouse-Il6-F	CAAAGCCAGAGTCCTTCAGAG
Mouse-Il6-R	GCCACTCCTTCTGTGACTCC
Mouse-Icam1-F	TGGAGACGCAGAGGACCTTA
Mouse-Icam1-R	CGCTCAGAAGAACCACCTTC
Mouse-Tnfa-F	CCACCACGCTCTTCTGTCTA
Mouse-Tnfa-R	AGGGTCTGGGCCATAGAACT
Mouse-Il1b-F	GTAATGAAAGACGGCACACC
Mouse-Il1b-R	TACCAGTTGGGGAACTCTGC
Mouse-LFA1-F	AGGTTGACCTGATCCACGAG
Mouse-LFA1-R	CAGGTTCCGTTTGAAGAAGC
Mouse-VLA4a-F	CCATCAGCTTGCTACTTGGA
Mouse-VLA4a-R	CATCATTGCTTTTGCTGTTGA
Mouse-inos-F	GCAGCGGCTCCATGACTCCC
Mouse-inos-R	AGGTGGTCCTCCTCCGGGTG
Mouse-Arg1-F	CAAGACAGGGCTCCTTTCAG
Mouse-Arg1-R	GCTTATGGTTACCCTCCCGT
Rat Acta1-F	TCGCTGACCGCATGCA
Rat Acta1-R	CCGCCGATCCACACTGA
Rat Nppa-F	ATCACCAAGGGCTTCTTCCT
Rat Nppa-R	TGTTGGACACCGCACTGTAT
Rat Nppb-F	GCTGCTTTGGGCAGAAGATAGA
Rat Nppb-R	GCCAGGAGGTCTTCCTAAAACA

Rat Gapdh-F	GGTGGACCTCATGGCCTACA
Rat Gapdh-R	CTCTCTTGCTCTCAGTATCCTTGCT

Table S5. Comparison of demographic and echocardiographic parameters of AOS and CABG patients.

	CABG control	AOS
n	11	15
Male, % (n)	100 (11)	60 (9)
Age, y	65±2	70±2
Ejection fraction, %	61.7±1.3	54.8±2.4*
End diastolic Dimensions, mm	49±1	50±2
Averaged wall thickness in diastole, mm	8.6±0.2	11.5±0.4***

Supplemental Figures

Figure S1

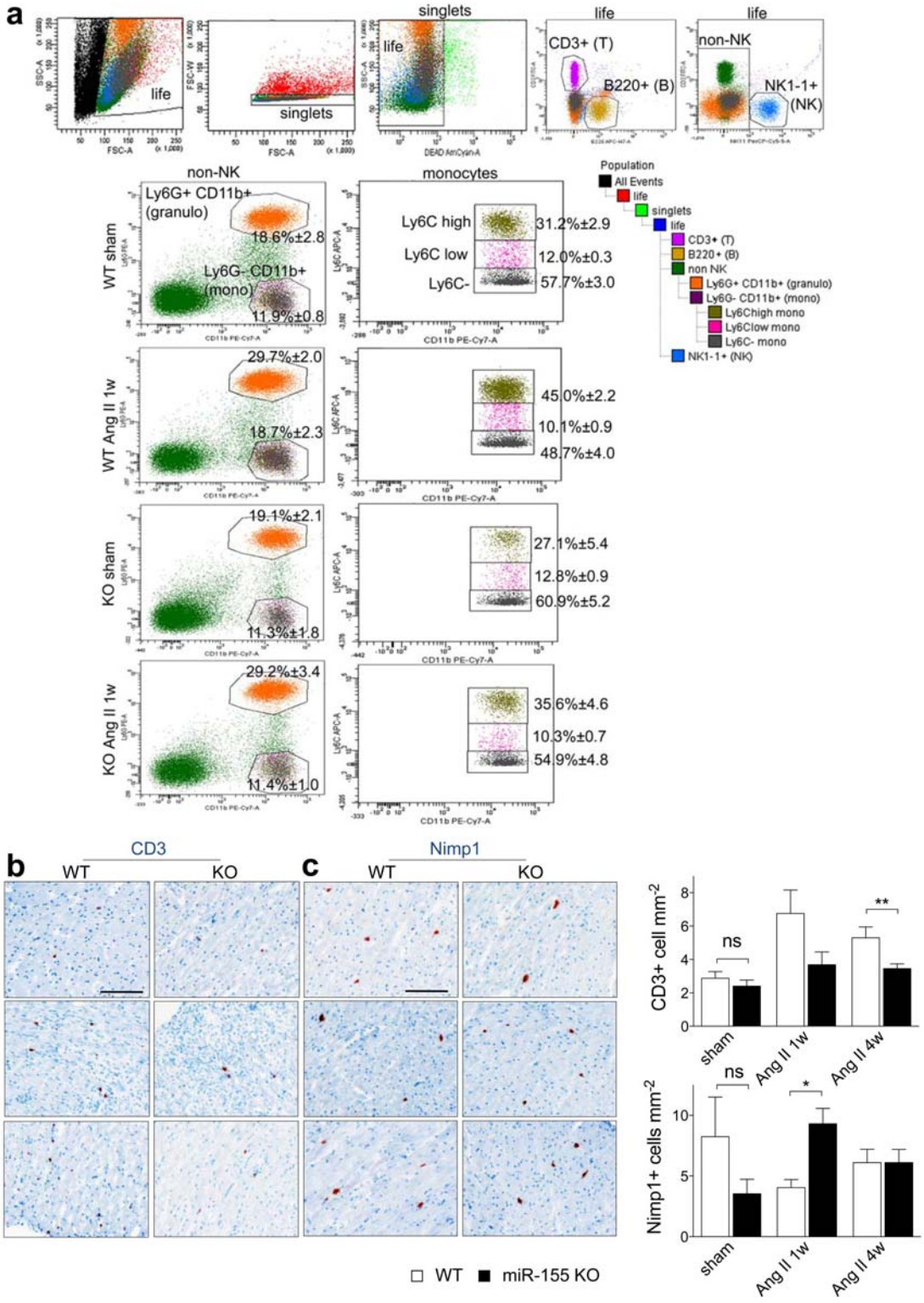

Figure S2

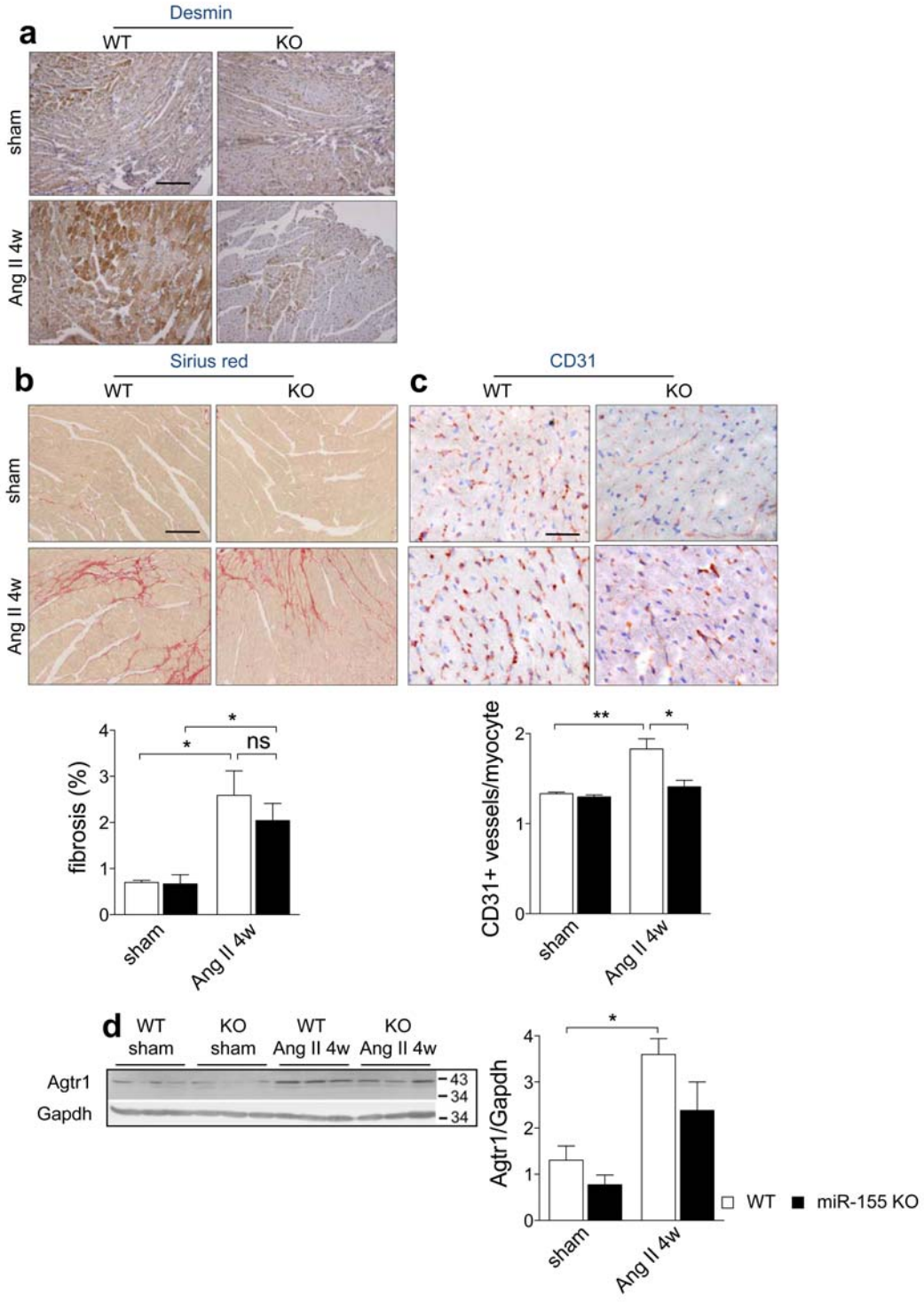

Figure S3

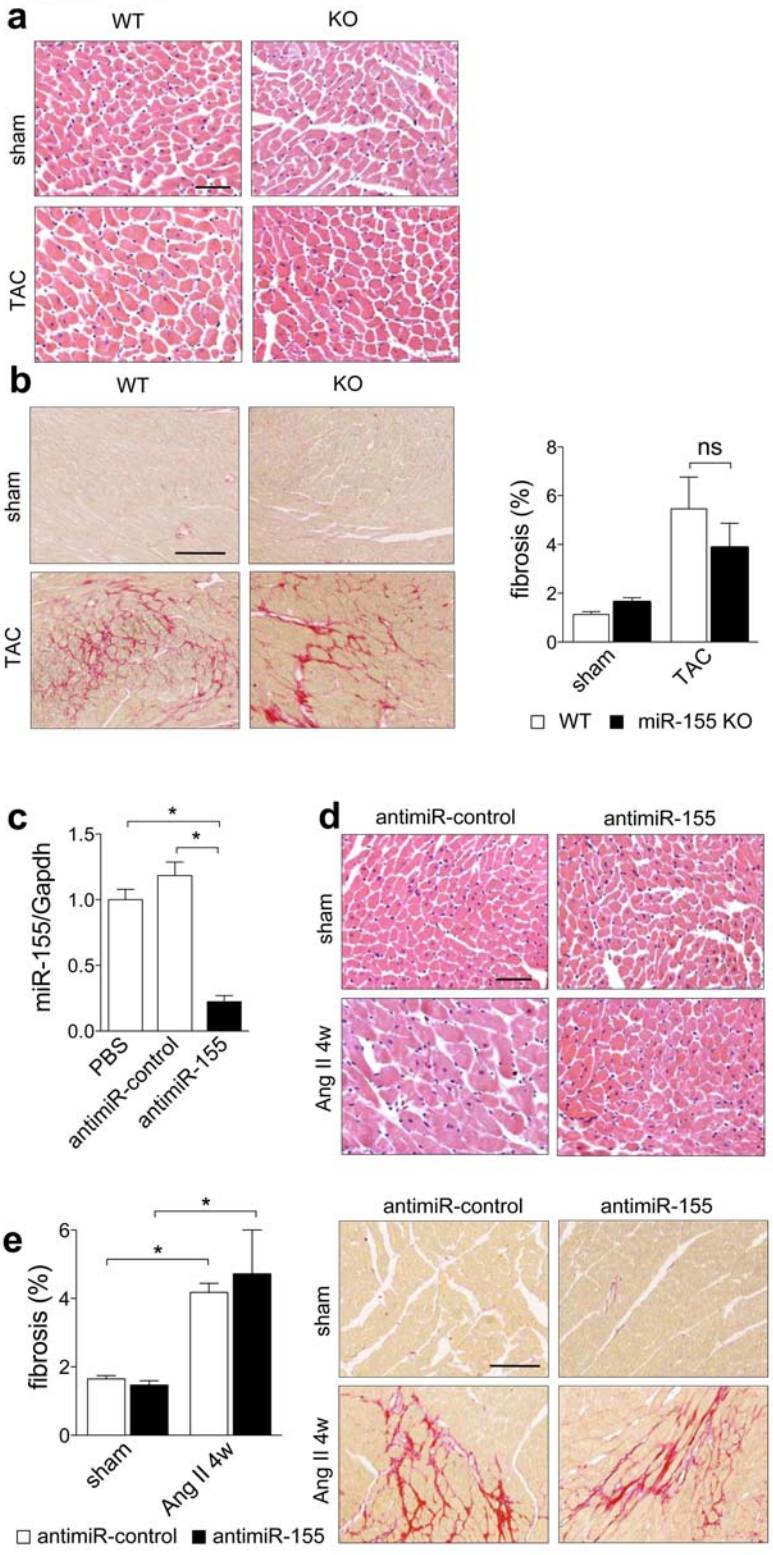

Figure S4

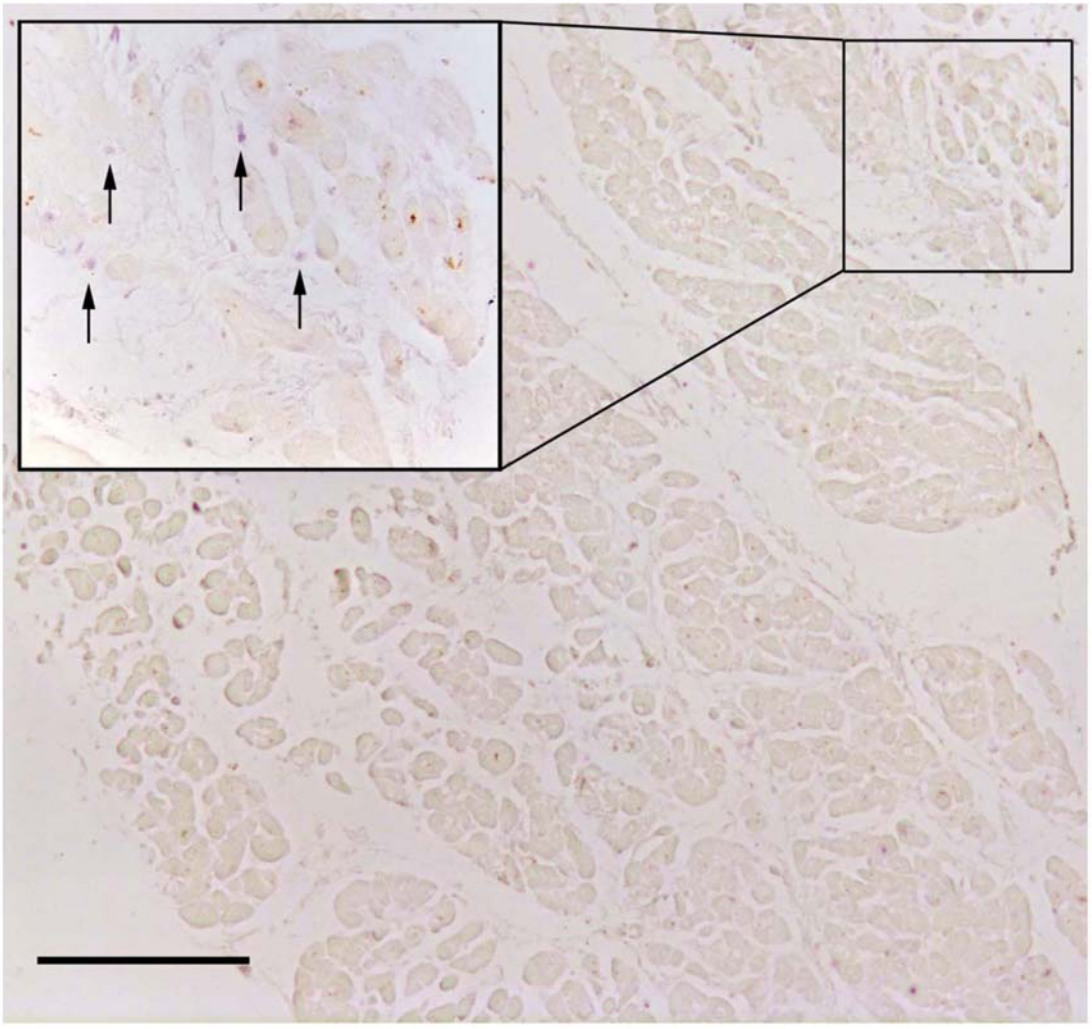

Figure S5

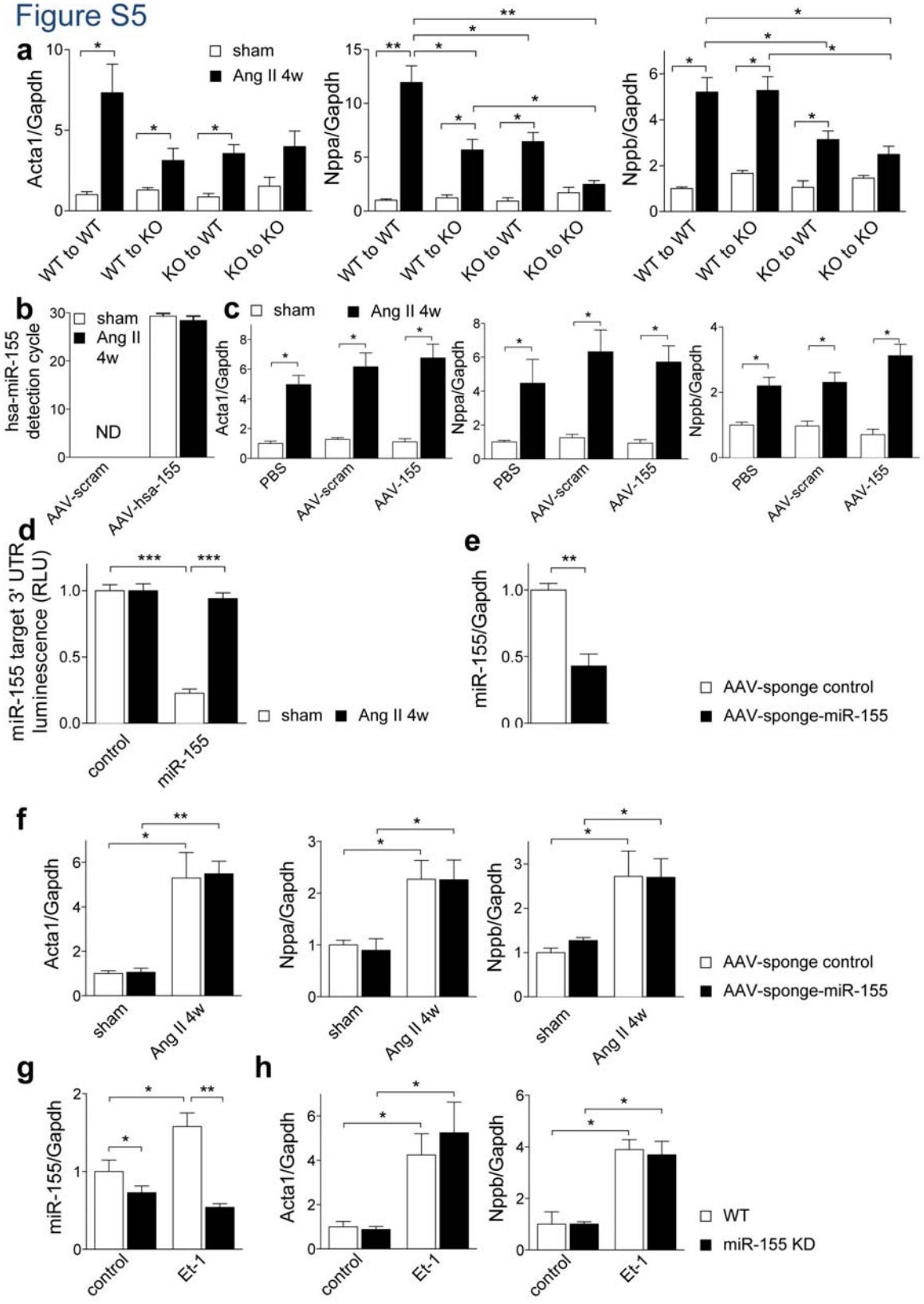

Supplemental Figure legends

Fig. S1: *MiR-155* is required for pressure overload-induced monocyte mobilization, but plays no major role in pressure overload-induced cardiac T-cell and neutrophil infiltration. (**a**) Gating strategy and representative flow cytometry pictures with averages and standard errors of counted immune cell subpopulations, as also described in **Figure 2a** and in **Supplementary Table 3**. Though only WT AngII mice show increased mobilization of Ly6C-high monocytes, there is no significant difference between WT and KO monocyte subtypes based on Ly6C-positivity. (**b**, **c**) Quantification of immunoreactive cells using antibodies against CD3 (T-cells; **b**) and NIMP-1 (neutrophils; **c**). Infiltration of T-cells – though substantially lower in number as compared to macrophages - is significantly reduced in *miR-155* KO versus WT hearts after 4 weeks, while numbers of NIMP-1-positive neutrophils are not different at baseline and 4 weeks of AngII and show higher numbers of infiltrating cells in KO hearts after 1 week. Data are represented by mean +/- SEM. Scale bars: 100μm. n=4/group; **P* < 0.05, ***P* < 0.01, ****P* < 0.005.

Fig. S2: Protection from cardiac hypertrophy in the absence of *miR-155* is reflected by reduced desmin, but is independent of fibrosis, vascularization and Agtr1 expression. (**a**) Desmin staining as a marker of cardiac stress shows a marked increase in WT hearts but not KO hearts subjected to AngII (scale bar: 100μm). (**b**) Quantification and representative images of Sirius red staining show comparable fibrosis in response to AngII-induced pressure overload in both genotypes (scale bar: 100μm). (**c**) The number of CD31-positive vessels per myocyte is similar between *miR-155* WT and KO hearts at baseline, but increases only in WT hearts in response to AngII (representative images are shown). (**d**) Protein levels of the Agtr1 are not significantly different between the hearts of WT and KO mice both at baseline and in response to AngII infusion (representative western blot images are shown). Data are represented by

mean +/- SEM. WT sham, n=13; WT AngII 4w, n=11; KO sham, n=11; KO AngII 4w, n=14; *$P < 0.05$, **$P < 0.01$.

Fig. S3: Absence of *miR-155* protects against TAC- and AngII-induced cardiac inflammation, hypertrophy and failure. (**a**) Both WT and KO mice develop cardiac hypertrophy following TAC, but this response is significantly blunted in KO mice. Panels show representative images of H&E-stained sections of the left ventricles of *miR-155* WT and KO mice at baseline and after 4 weeks of TAC (scale bar: 50μm). (**b**) Quantification of Sirius red staining shows comparable fibrosis in response to TAC-induced pressure overload in both genotypes (scale bar: 100μm). (**c**) qRT-PCR analysis of *miR-155* levels in mouse hearts 4 weeks after treatment with antimiRs shows significant knockdown by antimiRs against *miR-155*. (**d**) Representative images of H&E-stained sections of the left ventricles of *miR-155* WT and KO mice at baseline and after 4 weeks of AngII infusion (scale bar: 50μm). (**e**) Quantification and representative images of Sirius red staining show comparable fibrosis in response to AngII-induced pressure overload after control and anti-*miR-155* antagomirs (scale bar: 100μm). Data are represented by mean +/- SEM. WT sham, n=5; WT TAC, n=6; KO sham, n=11; KO TAC, n=11; WT scrambled sham, n=6; WT scrambled AngII, n=8; antimiR-155 sham, n=6; antimiR-155 AngII, n=6; *$P < 0.05$, **$P < 0.01$, ***$P < 0.005$.

Fig. S4: *miR-155* is expressed in interstitial cells in a human hypertrophied heart. *In situ* hybridization of *miR-155* in a cardiac section of a patient with idiopathic cardiomyopathy and hypertrophy. While *miR-155* expression is hardly detected in myocytes, *miR-155* signal (in blue) can be observed in interstitial cells.

Fig. S5: Macrophages influence hypertrophic growth of cardiomyocytes via *miR-155*. (**a**) Cardiac *Acta1*, *Nppa* and *Nppb* expression in AngII- or sham-treated mice following adoptive bone marrow transfer between *miR-155* WT and KO mice shows partial rescue of the hypertrophic response of KO mice reconstituted with WT bone marrow as well as blunting of the hypertrophic response in WT mice reconstituted with KO bone marrow. (**b**) qRT-PCR analysis of human *miR-155* levels in mouse hearts 7 weeks after infection with AAV9. Human *miR-155* was detected only in AAV9-hsa-miR-155-treated mouse groups. Note that human and mouse *miR-155* differ by one nucleotide outside the seed region, enabling human-specific *miR-155* detection. (**c**) *In vivo* cardiac myocyte *miR-155* overexpression using AAV9-hsa-*miR-155* leads to similar induction of the fetal genes *Acta1*, *Nppa* and *Nppb* as compared to both PBS and AAV9-scrambled treatment following AngII. (**d**-**f**) Vice versa, *in vivo* cardiac myocyte *miR-155* inhibition using AAV9-sponge-*miR-155* also induces similar levels of hypertrophic gene expression following AngII (**f**). *In vitro* luciferase validation of sponge efficiency shows that the knockdown of the luciferase target to 23%±3 upon addition of miR-155 is rescued by the co-expression of sponge-*miR-155* to >90% (**d**). Expression of a control sponge containing 4 mutated binding sites had no influence (not shown). *In vivo*, AAV9-sponge-*miR-155* reduced cardiac *miR-155* expression by 57%±7 (**e**). (**g**, **h**) Knockdown of *miR-155* in RCMs with antagomiRs (**g**) does not influence induction of the fetal genes *Acta1* and *Nppb* (**h**). Data are represented by mean +/- SEM. All quantitative *in vitro* data were generated from a minimum of three replicates. WT>WT sham, n=7; WT>WT AngII, n=13; KO>KO sham, n=7; KO>KO AngII, n=7; WT>KO sham, n=7; WT>KO AngII, n=11; KO>WT sham, n=5; KO>WT AngII, n=12; PBS sham, n=8; PBS AngII, n=8; AAV-scram sham, n=8; AAV-scram AngII, n=12; AAV-155 sham, n=6; AAV-155 AngII, n=8; AAV-sponge control sham, n=5; AAV-sponge control AngII, n=10; AAV-sponge-miR-155

sham, n=5; AAV-sponge-miR-155 AngII, n=10; *P < 0.05, **P < 0.01, ***P < 0.005; ND, not detected.

Supplemental references

1. Rodriguez A, Vigorito E, Clare S, Warren MV, Couttet P, Soond DR, van Dongen S, Grocock RJ, Das PP, Miska EA, Vetrie D, Okkenhaug K, Enright AJ, Dougan G, Turner M, Bradley A. Requirement of bic/microRNA-155 for normal immune function. *Science.* 2007;316:608-611.
2. Bai L, Beckers L, Wijnands E, Lutgens SP, Herias MV, Saftig P, Daemen MJ, Cleutjens K, Lutgens E, Biessen EA, Heeneman S. Cathepsin K gene disruption does not affect murine aneurysm formation. *Atherosclerosis.* 2010;209:96-103.
3. da Costa Martins PA, Salic K, Gladka MM, Armand AS, Leptidis S, el Azzouzi H, Hansen A, Coenen-de Roo CJ, Bierhuizen MF, van der Nagel R, van Kuik J, de Weger R, de Bruin A, Condorelli G, Arbones ML, Eschenhagen T, De Windt LJ. MicroRNA-199b targets the nuclear kinase Dyrk1a in an auto-amplification loop promoting calcineurin/NFAT signalling. *Nat Cell Biol.* 2010;12:1220-1227.
4. Rockman HA, Ross RS, Harris AN, Knowlton KU, Steinhelper ME, Field LJ, Ross J, Jr., Chien KR. Segregation of atrial-specific and inducible expression of an atrial natriuretic factor transgene in an in vivo murine model of cardiac hypertrophy. *Proc Natl Acad Sci U S A.* 1991;88:8277-8281.
5. Goossens P, Gijbels MJ, Zernecke A, Eijgelaar W, Vergouwe MN, van der Made I, Vanderlocht J, Beckers L, Buurman WA, Daemen MJ, Kalinke U, Weber C, Lutgens E, de Winther MP. Myeloid type I interferon signaling promotes atherosclerosis by stimulating macrophage recruitment to lesions. *Cell Metab.* 2010;12:142-153.
6. Vandendriessche T, Thorrez L, Acosta-Sanchez A, Petrus I, Wang L, Ma L, L DEW, Iwasaki Y, Gillijns V, Wilson JM, Collen D, Chuah MK. Efficacy and safety of adeno-associated viral vectors based on serotype 8 and 9 vs. lentiviral vectors for hemophilia B gene therapy. *J Thromb Haemost.* 2007;5:16-24.
7. Swinnen M, Vanhoutte D, Van Almen GC, Hamdani N, Schellings MW, D'Hooge J, Van der Velden J, Weaver MS, Sage EH, Bornstein P, Verheyen FK, VandenDriessche T, Chuah MK, Westermann D, Paulus WJ, Van de Werf F, Schroen B, Carmeliet P, Pinto YM, Heymans S. Absence of thrombospondin-2 causes age-related dilated cardiomyopathy. *Circulation.* 2009;120:1585-1597.
8. Junqueira LC, Bignolas G, Brentani RR. Picrosirius staining plus polarization microscopy, a specific method for collagen detection in tissue sections. *Histochem J.* 1979;11:447-455.
9. Jorgensen S, Baker A, Moller S, Nielsen BS. Robust one-day in situ hybridization protocol for detection of microRNAs in paraffin samples using LNA probes. *Methods.* 2010;52:375-381.
10. Nuovo GJ. In situ detection of microRNAs in paraffin embedded, formalin fixed tissues and the co-localization of their putative targets. *Methods.* 2010;52:307-315.
11. Corsten MF, Papageorgiou A, Verhesen W, Carai P, Lindow M, Obad S, Summer G, Coort SL, Hazebroek M, van Leeuwen R, Gijbels MJ, Wijnands E, Biessen EA, De Winther MP, Stassen FR, Carmeliet P, Kauppinen S, Schroen B, Heymans S. MicroRNA profiling identifies microRNA-155 as an adverse mediator of cardiac injury and dysfunction during acute viral myocarditis. *Circ Res.* 2012;111:415-425.
12. De Windt LJ, Willemsen PH, Popping S, Van der Vusse GJ, Reneman RS, Van Bilsen M. Cloning and cellular distribution of a group II phospholipase A2 expressed in the heart. *J Mol Cell Cardiol.* 1997;29:2095-2106.
13. Peiser L, Gough PJ, Kodama T, Gordon S. Macrophage class A scavenger receptor-mediated phagocytosis of Escherichia coli: role of cell heterogeneity,

microbial strain, and culture conditions in vitro. *Infect Immun.* 2000;68:1953-1963.

14. Hume DA, Gordon S. Optimal conditions for proliferation of bone marrow-derived mouse macrophages in culture: the roles of CSF-1, serum, Ca2+, and adherence. *J Cell Physiol.* 1983;117:189-194.

15. Wiese M, Castiglione K, Hensel M, Schleicher U, Bogdan C, Jantsch J. Small interfering RNA (siRNA) delivery into murine bone marrow-derived macrophages by electroporation. *J Immunol Methods.* 2010;353:102-110.

16. Yin X, Cuello F, Mayr U, Hao Z, Hornshaw M, Ehler E, Avkiran M, Mayr M. Proteomics analysis of the cardiac myofilament subproteome reveals dynamic alterations in phosphatase subunit distribution. *Mol Cell Proteomics.* 2010;9:497-509.